Thermax 1 2 3 Excel

Research

Design

Fundamentals

3

Multi-Objective Optimisation and Exergoeconomic Analyses of Energy-Conversion Systems using Excel

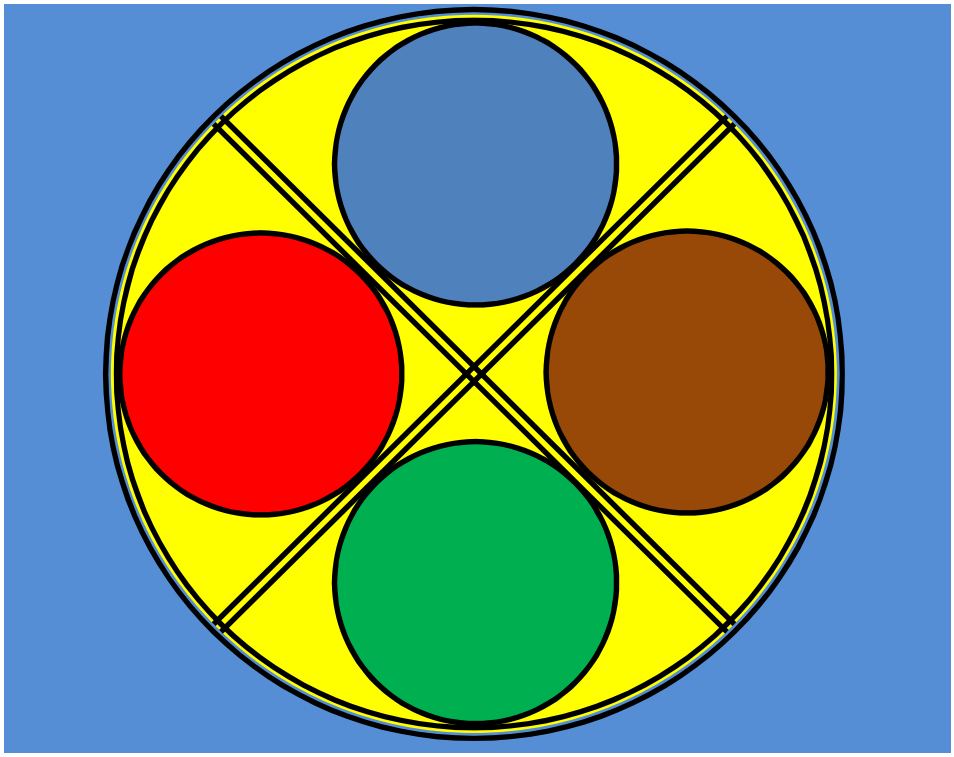

Mohamed M. El-Awad

Multi-Objective Optimisation and Exergoeconomic Analyses of Energy-Conversion Systems using Excel

Multi-Objective Optimisation and Exergo-economic Analyses of Energy-Conversion Systems using Excel

Mohamed M. El-Awad

April, 2026

Thermax (GAS and AIR groups) can be downloaded from:

https://docs.google.com/document/d/15mOzV33K3S8_VJjnVQVN9-ND0mO5VYYqxbV9If3ot8A/edit?usp=drive_link

Preface

In the past, the pressures on the world's natural resources and the environment were not as high as they are today. Therefore, the designers of energy-conversion systems strived to satisfy two conflicting objectives of their designs; (a) maximising the performance efficiency of the systems and (b) minimising their owning costs. By assessing both objectives in terms of monetary measures, the design optimisation problem could be solved by minimising a "total annualised cost rate" that accounts for the two factors. However, design optimisation of present-day energy systems is more challenging due to the additional constraints that have to be met, including the effect on the environment, and the increasing complexity of the systems themselves. Solving optimisation problems of present-day energy-conversion systems would not have been possible without taking advantage of the recently developed computer-aided techniques for multi-objective optimisation (MOO) and exergoeconomic analyses. This book aims to give senior engineering students and young researchers in the field a gentle introduction to these two modern tools and show how they can be used to complement one another for design optimisation analyses of energy conversion systems.

MOO and exergoeconomics are two different optimisation methodologies. MOO applies iterative search methods to optimise the system with predefined objectives and provides the engineer with a small set of solutions to select from. Exergoeconomics uses thermodynamics and economics to associate costs to exergy flows and exergy destructions in the system and defines a number of exergoeconomic parameters to assess the economic performance of the system. Unlike MOO, the result of an exrgogoeconomic analysis is not an optimised system, but a set of indicators for setting-up optimisation strategies and, therefore, the optimised system depends on the engineer's interpretation of the exergoeconomic results. To improve the accuracy of the method, an advanced exergoeconomic method has been developed that splits the rates of exergy destructions and associated costs into avoidable and unavoidable and self-generated (endogenous) and imported (exogenous) parts and redefines the exergoeconomic parameters accordingly. The application of the two methods for design optimisation may pose more questions than the answers it gives. Since the two methods are still under development, it is hoped that this book provides understandable and applicable answers to these questions if not comprehensive and conclusive ones.

This book is the third in a set of three books that adopt the widely available and easy-to-use spreadsheet application Microsoft Excel as modelling platform. Although the use of Excel for thermal-fluid analyses in general and the analyses of energy-conversion systems in particular is not a new idea, the present set of books are intended to present a comprehensive approach for applying computer-aided methods at all levels of thermo-fluid analyses including those related to the fundamental courses, design-based courses, and research-oriented assignments. To enhance the learning process, the books adopt a Learn-By-Examples (LBE) approach that suits the modern learning/teaching techniques better than the traditional approach. Many of the examples and cases given in these books

are obtained from relevant popular textbooks or based on published research work available in the open literature so that reference can be made to these sources for additional information if necessary.

The Excel-based modelling platform adopted in the book has four elements; (i) Excel with its user-interface and built-in functions, (ii) the Solver add-in that comes with Excel, (iii) the integrated Visual Basic for Applications (VBA) programming language, and (iv) a multi-substance add-in for fluid properties called Thermax. The first book of this set describes the Excel-based modelling platform in more details and applies it for various types of basic computer-aided analyses and optimisation of thermal-fluid systems using conventional methods. The second book focusses on Thermax and uses it for conducting thermodynamic analyses of various types of energy-conversion systems. This third book extends the application area of the Excel-based platform by illustrating its adequacy for both MOO and exergoeconomic analyses of energy-conversion systems. In this regards, the book describes a technique that uses Excel's Solver with the TOPSIS decision-making method for conducting MOO analyses.

The first chapter of the book reviews the basic principles of thermoeconomic analyses and single-objective optimisation. Chapter 2 and Chapter 3 focus on exergoeconomic analysis and MOO methods respectively, and show how they can be applied with the Excel-based platform. Chapter 4 deals with exergoeconomic analyses of a two-stage air compressor. Chapter 5 and Chapter 6 use Excel-aided models for conducting objective-guided exergoeconomic analyses and advanced exergo-economic analyses of the simple gas-turbine, respectively. Chapter 7 and Chapter 8 deal with MOO analyses of multi-stage and cascade vapour compression systems, respectively. Chapters 9 introduces the Solver-TOPSIS technique and validates its results with those obtained by the MIDACO solver. Chapters 10 and 11 extend the treatment of Chapter 9 by applying the technique for MOO analyses of the regenerative gas turbine and the air-bottoming cycle, respectively. Chapter 12 concludes the book by presenting an Excel-aided procedure for MOO and exergoeconomic analysis of a gas-turbine cogeneration system. Although the book is primarily written for educational purposes, it is hoped that it is equally useful for practicing engineers with interest in thermal and energy-conversion systems.

Acknowledgements
The development of Thermax and the writing of this set of books would not have been possible without benefitting from the efforts of many academics and researchers who have made their publications, data, and software available in the open literature or on their websites. I am also indebted to Universiti Putra Malaysia and Universiti Tenaga Nasional (Malaysia), the University of Khartoum (Sudan), and the University of Technology and Applied Sciences (Oman) for their generous support at different periods of my academic career and hope that they find this effort a worthy token of appreciation and gratitude.

CONTENTS

1

Introduction

The design and operation of modern energy supply and conversion systems is becoming increasingly challenging because of the complexity of the energy systems themselves as well as the complexity of their design and operation requirements. The complexity of the systems is due to the use of combined power-generation cycles and multi-stage pressure and cascade refrigeration systems instead of the simple systems and the use of cogeneration and tri-generation systems and integrated and hybrid systems. The large number of components in these systems make the location and evaluation of the system losses, which is crucial for minimising the cost of the system's product(s), more difficult [1]. The complexity of the design and operation requirements is due to the fact that fossil-fuels, which still provide most of the energy needed for meeting the energy demands of our industries and transportation systems and our commercial and residential sectors, are also the main cause of global warming, air-pollution, acid precipitation, ozone depletion, and emission of radioactive substances. In a world evolving with increasing concerns for environmental issues the designers and operators of energy systems cannot be satisfied with only the technical and economic merits of their systems, but have to consider the environmental impact, as well as the health, safety and societal acceptance, as equally important design objectives [2]. The difficulty is that not all these design objectives can be simultaneously met because some of them are in conflict with one another.

While the traditional optimisation methods that maximise or minimise a single objective function cannot adequately deal with multiple conflicting objectives, the traditional energy-based thermo-economic optimisation methods cannot locate and evaluate the monetary and environmental costs associated with mass and energy flows in a complex energy-conversion system. To be able to deal with these complexities, today's designers of energy-conversion and utilisation systems need to take advantage of two recently developed optimisation methods that provide them with the right tools; which are the multi-objective optimisation (MOO) methods and the exergoeconomic analysis methods. MOO methods enable the designers of energy-conversion systems to find acceptable trade-offs between the various conflicting optimisation objectives. The exergoeconomic analysis method, or exergoeconomics, combines thermodynamic (exergy) and economic principles at component level to provide the designers of complex energy-conversion systems with valuable information that cannot be obtained otherwise [3]. MOO and exergoeconomics, which are the two main topics of this book, are still subjects of intensive research. Before delving into detailed discussions of the two topics in the following chapters of the book, it is helpful to review the conventional thermo-economic method and the single-objective optimisation methods and give examples of the application of MOO and exergoeconomics for the design of energy systems and the anticipated benefits of using them. Chapters 2 and 3 show how the two optimisation methods can be implemented by using Microsoft Excel as a modelling platform.

1.1. Thermoeconomics

The design of energy-conversion systems involves the application of principles from thermo-fluids (thermodynamics, fluid mechanics, and heat transfer), material science, manufacturing, and mechanical design together with principles from engineering economics [4]. The term "thermoeconomics" is generally used to refer to this wide area of application although it is also used more narrowly to mean "exergoeconomics" [5, 6].

In this book, it is used in the general sense that also includes exergy-based economic analyses, while "exergoeconomics" is used to refer to the specific methodologies that combine second-law and economic concepts at the component level. Exergoeconomics, which itself has now developed from "conventional" to "advanced" [7], provides a powerful tool for design optimisation analyses of complex energy-conversion systems, while thermoeconomics provides overall measures of the systems' economic performance that can also be used for their optimisation. This section gives a brief account of the conventional thermoeconomics by illustrating its applications for product costing, design optimisation, and comparison of alternative designs.

1.1.1. Thermoeconomics for product costing

Estimating the cost of the product(s), which is an important consideration in design analyses of energy-conversion systems, can be significantly affected by the technology used in the energy-conversion system. For example, heat and electricity can be produced independently, or simultaneously via cogeneration or tri-generation. To illustrate the use of thermoeconomics for appropriately estimating the product cost of an energy-conversion system, consider the coal-fired power plant shown on Figure 1.1.

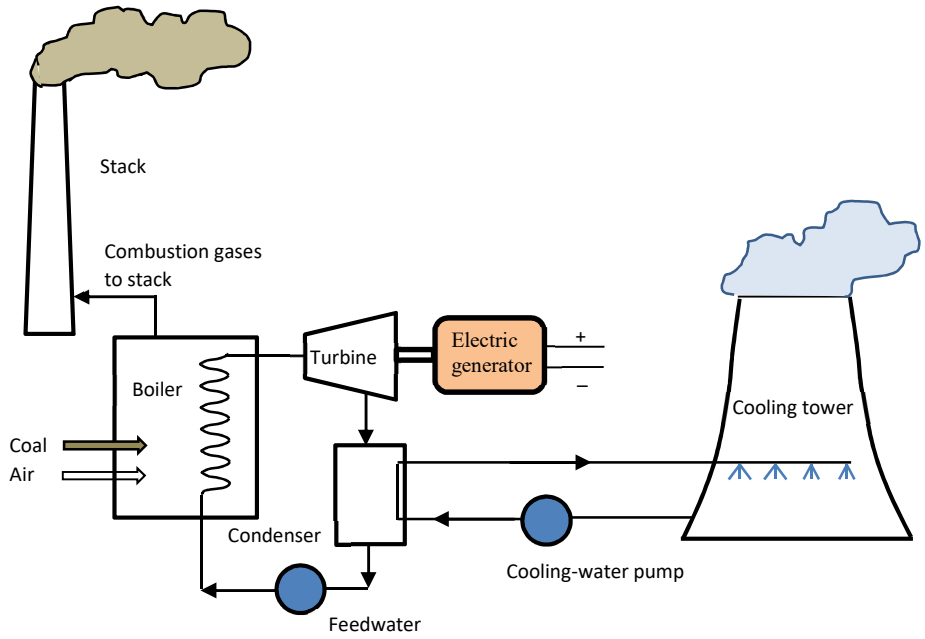

Figure 1.1. Schematic of a coal-fired steam-turbine power plant (adapted from [4])

The main components of the plant are the boiler, the turbine, the condenser, the feed-water pump, the stack, the natural-draft cooling tower, the cooling-water circulating pump, and the electric generator. The plant needs many other auxiliary components which are not shown on the figure. Obviously, assigning cost to the electricity produced

by the power plant should consider the cost of these equipment and the initial construction costs. It should also consider the cost of land and the running costs the main part of which is the cost of the fuel (coal). In addition to the above, the cost should also cover the various operation and maintenance costs that include the salaries, income taxes, etc.

Now consider the cogeneration system shown on Figure 1.2 that has two principal products: electricity and low-pressure steam for use in some process. Determining the cost that should be allocated to each product is important to the commercial success of cogeneration. If costs are not allocated appropriately for the two products, one product may be overpriced (and thus unlikely to be purchased) and the other under-priced (and thus unable to recover costs even if in great demand) [1]. Back in 1930s it was thought that the fuel cost should be allocated to the steam and the power in proportion to their *energy* content. However, the cogenerated electricity cost determined in this manner, was far less expensive than electricity produced in conventional power plants. It was Keenan [8] who pointed out that the value of the steam and the electricity rests in the "availability" not in their energy and, therefore, it should be used as the basis for appropriately apportioning cost associated with the cogeneration of electric power and steam for distribution [9].

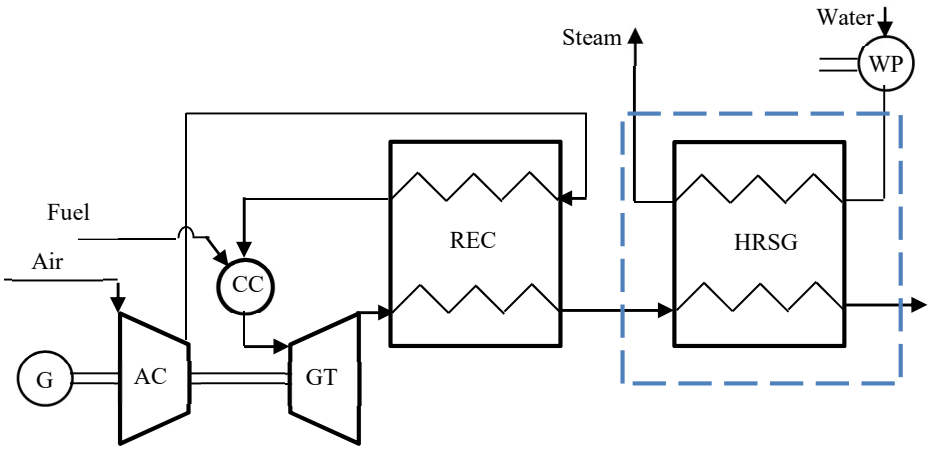

Figure 1.2. Schematic of a gas-turbine based cogeneration system (adapted from [10])

Since the cost of fuel is the main part of the running costs, the exergetic efficiency of the power plant should be taken into consideration because a more efficient plant consumes less fuel than another plant of a similar size but with less efficiency. For a plant that has a single fuel input and produces a single product in the form of electricity, Moran [11] introduced the following formula to estimate the unit cost of the product, c_w in \$/GJ:

$$c_w = \frac{c_f}{\eta_b}\left[1+\frac{\sum \dot{Z}_k}{c_f \dot{B}_f^{CHE}}\right] \tag{1.1}$$

Where, c_f is the unit cost of fuel based on exergy ($/GJ) and η_b is the second-law efficiency of the plant defined by:

$$\eta_b = \dot{W}_e / \dot{B}_f^{CHE} \tag{1.2}$$

Where, $\dot{B}^{CHE}$ is the chemical exergy flow rate of the fuel, in GJ/s, and $\dot{W}_e$ is the electrical power produced in the same unit as $\dot{B}^{CHE}$. $\dot{Z}_k$ in Equation (1.1) is the capital investment cost rate of component *k* ($/s) which is given by:

$$\dot{Z}_k = \frac{Z_k^0 \times CRF \times \phi}{3600 \times \tau} \tag{1.3}$$

Where, Z_k^0 is the initial capital cost of the component, *CRF* the capital recovery factor, ϕ the maintenance factor, and τ the annual operating hours. A typical value for $\phi$is 1.06 and the capital recovery factor is calculated from:

$$CRF(i,n) = i / \left[1 - (1+i)^{-n}\right] \tag{1.4}$$

Where *i* is the interest rate and *n* is the expected life of the plant in number of years. Gorji-Bandpy and Ebrahimian [12] compared the cost estimation by Equation (1.1) to those of the more involved SPECO and MOPSA exergoeconomic methods to be discussed in Chapter 2. In spite of its simplicity, they showed that the unit cost of electricity determined by Equation (1.1) is lower by 15% from that determined by SPECO, while that determined by MOPSA is higher by 12%.

1.1.2. Thermoeconomics for design optimisation

Thermoeconomics can also be used for design optimisation of a whole energy system or one of its components. For illustration, consider the heat-recovery steam generator (HRSG) of the cogeneration system shown on Figure 1.2. A key design parameter for the HRSG is the average temperature difference between the two streams passing through the heat exchanger, ΔT_{ave}, because the irreversibility in the heat-exchanger is directly related to this temperature difference. Increasing ΔT_{ave} increases the fuel cost, but decreasing it means a larger heat transfer area and a greater capital cost because there is an inverse relation between ΔT_{ave} and the surface area required for a specified heat transfer rate [4]. Figure 1.3 shows the variation of the fuel cost and the capital cost of the HRSG with ΔT_{ave}. As the figure shows, the value of ΔT_{ave} that gives the minimum fuel cost corresponds to the maximum capital cost and vice versa. Therefore, ΔT_{ave} should be selected such that it gives the required trade-off between these two conflicting design factors. This can be achieved by minimising the total cost of the HRSG, C_{Total}, which is the sum of the capital cost and the fuel cost.

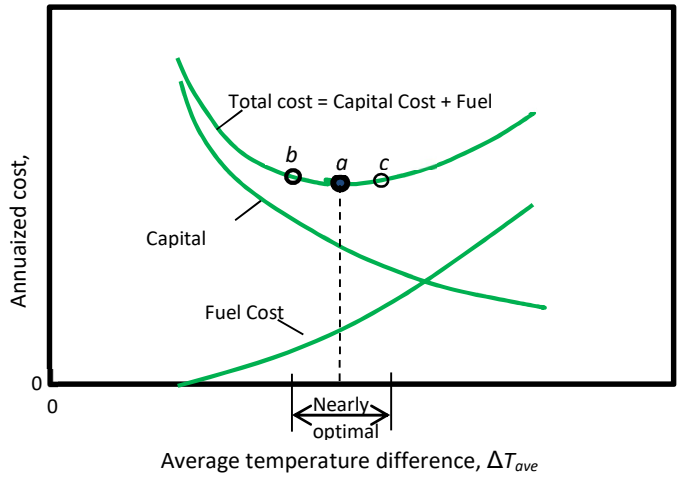

Figure 1.3. Cost curves for a single heat exchanger (adopted from [4])

Figure 1.3 shows that the total cost of the HRSG exhibits a minimum at the point labelled *a*, but the curve is relatively flat in the neighbourhood of the minimum. Therefore, there is a range of ΔT_{ave} values that could be considered nearly optimal from the standpoint of minimum total cost. If reducing the fuel cost were deemed more important than minimising the capital cost, we might choose a design that would operate at point *b*. Point *c* would be a more desirable operating point if capital cost were of greater concern. Such trade-offs are common in design situations [4].

An example of using thermoeconomics to optimise the whole energy-conversion system is given by Equation (1.1) which can be the objective function for minimising the unit cost of electricity of the coal-fired power plant by determining the initial capital costs of the various components from relevant formulae that involve the desired design variables of the system. In this case, the optimisation problem becomes:

$$\text{Minimise } c_w = f(x_1, x_2, x_3, ..., x_n) \tag{1.5}$$

Where x_1 to x_n are the relevant design variables like the boiler pressure, the inlet temperature and pressure ratio of the turbine, flow rate of the cooling water, etc. Saghafifar and Poullikkas [13] conducted a thermoeconomic optimisation of various air bottoming cycles by minimising their total operation costs. They used the graphical tools provided by MATLAB for optimising the different options, but the algorithms described in Section 1.2 for single-objective optimisation can also be used [14,15].

1.1.3. Thermoeconomics for comparing alternative designs

For comparing alternative designs of energy systems, thermoeconomic can utilise the familiar economic indicators such as the Net Present Value (NPV), the Life Cycle Cost (LCC), and the Discounted Payback (DPB) period [16]. Al-Falahi et al. [17] considered a solar-powered absorption cooling system and compared the economics of the system with two types of absorption cycles, water-lithium bromide (H_2O-LiBr) and ammonia-water (NH_3-H_2O), under the same operating conditions. They used the following formula to determine the cumulative thermo-economic cost based on the expenses and exergy flows for the two cycles:

$$c_p = 1000 \times \left(\frac{\left(\dot{W}_{tot} \times c_w\right) + \left(\dot{Z}_{tot} / 3600\right)}{\dot{E}_{fo}} \right) \tag{1.6}$$

where, c_p is the thermo-economic product cost (\$/GJ), c_w is the energy price (~0.065 \$/kWh), $\dot{W}_{tot}$ is the cycle power (kW), and $\dot{Z}_{tot}$ is the hourly cost (\$/h), while $\dot{E}_{fo}$ is the exergy stream outlet from the system to the user (kW). Their results for a case study of 200 TR total cooling load revealed that H_2O-LiBr gives lower thermo-economic product cost (0.14 \$/GJ) compared to the NH_3-H_2O (0.16 \$/GJ).

1.2. Single-objective optimisation

A broad definition of optimisation is: "a procedure of finding and comparing feasible solutions until no better solution can be found." [18]. With this broad definition, almost all engineering design is optimisation [19]. A definition that is more specific to the design of energy-conversion systems is given by Bejan et al. [20] which is "the modification of the structure *and* the design parameters of a system *to minimise the total levelized cost of the system products* under *boundary conditions* associated with available materials, financial resources, protection of the environment, and governmental regulations, together with the safety, operability, reliability, availability, and maintainability of the system". However, optimising an energy-conversion system that involves numerous design parameters is a formidable task that is "easy said than done". An important aspect of the optimisation process is the formulation of the design problem in a mathematical format which is acceptable to an optimisation algorithm [21]. There are many optimisation algorithms that suit different types of problems and, therefore, the selection of the suitable one is another important aspect of the process. These two aspects are discussed below. The discussion is limited to single-objective optimisation problems.

1.2.1. Mathematical formulation of the optimisation problem

Mathematically, the single-objective constrained optimisation problem of minimising an objective function f with respect to n design parameters x_i (also called optimisation variables and decision parameters) is expressed by the following equation [22]:

$$\begin{aligned} &\text{Minimise:} && f(x) && \\ &\text{Subject to:} && g_j(x) \le 0 && j = 1, m \end{aligned} \tag{1.7}$$

$$h_k(x) = 0 \qquad k = 1, p$$
$$x_i^{(L)} \le x_i \le x_i^{(U)} \qquad i = 1, n$$

In Equation (1.7), f(x) represents the objective (or goal) function, the functions $g_j(x)$ and $h_k(x)$ represent an inequality constraint function and an equality constraint function, respectively. The searchable design space is defined by the upper and lower bounds of the design variables, $x_i^{(L)}$ and $x_i^{(U)}$, which are referred to as the side constraints, and x is called a feasible point if it satisfies all the constraints and the feasible region is the set of all feasible x values. In the general case, the objective and constraint functions can be linear or non-linear and explicit or implicit functions of x. The function and constraints can also be continuous, discrete, or Boolean. Note that *maximising* $g(x)$ corresponds to *minimising* $f(x) = -g(x)$ by the *duality principle* [18]. Optimisation problems are classified as convex or *non-convex* problems as shown on Figure 1.4.a and 1.4.b, respectively. As shown on Figure 1.4.b, more than one optimum (referred to as local or relative optima) may exist for non-convex problems.

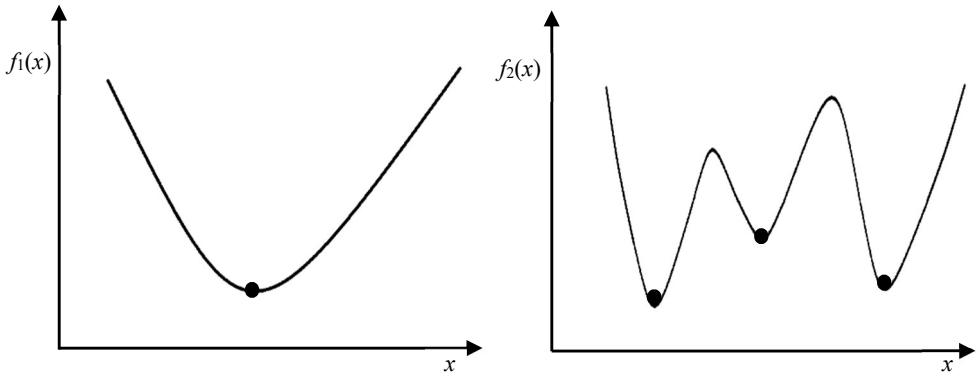

(a) *Convex* (b) *Non-convex*

Figure 1.4. Convex and non-convex optimisation objective functions (adapted from [22])

The solution to the optimisation problem specified in Equation (1.7) is to find the combination of design variables that results in the best value of the objective function while satisfying all the equality functions, inequality functions, and side constraints. With respect to an energy-conversion system, the formulation of the optimisation problem in a mathematical format involves the selection of objectives, design variables, constraints, and models of the system:

1. The objective function represents the performance indicator of the system that is to be minimised, e.g., the fuel consumption or the total annualized cost, or maximised, e.g., the exergetic efficiency or the annual revenue.

2. The design or decision variables are the set of unknown design parameters such the compression ratio of a compressor or a turbine, the inlet temperature of a gas-turbine, the effectiveness of a heat-exchanger, etc.
3. The constraints are the conditions that allow the unknown parameters to take on certain values but exclude others in order to make the design feasible. For example, the maximum pressure ratio of a gas-turbine can be required to be less than 16 or the its maximum inlet temperature to be less than 1600K.
4. The models of system are the thermodynamic model, economic model, exergoeconomic model, environmental model, etc.

Figure 1.5 shows the components of the optimisation problem and their alternative forms [18]. Different combinations of the optimisation components require different solution algorithms.

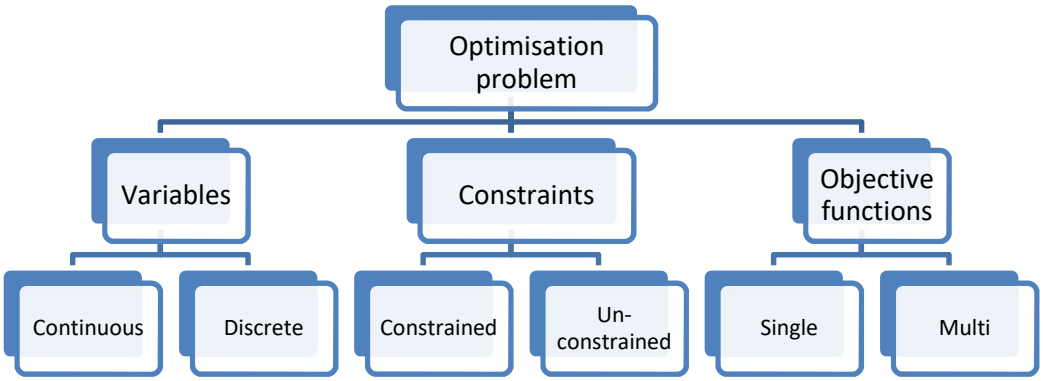

Figure 1.5. Components of an optimisation problem (adopted from [18])

1.2.2. Optimisation methods and algorithms

Optimisation methods, techniques, or algorithms can be classified in many ways depending on the following considerations [19]:

- Global or local optimisation
- Convex or non-convex optimisation
- Unconstrained or box-constrained optimisation, and other special-case constraints
- Special classes of functions (linear, etc.)
- Differentiable or non-differentiable functions
- Gradient-based or derivative-free algorithms
- Others.

Since it is not possible to provide a thorough description of the many optimisation techniques in the limited space available here, the following discussion focuses on the techniques that are commonly used in engineering applications. Following Venter [22],

the methods are divided into two main groups: local optimisation algorithms and global optimisation algorithms.

A. Local optimisation algorithms

The local algorithms will converge on any of the three optimum points shown on Figure 1.4.b depending on which one is encountered first. A simple approach for using local optimisation algorithms to find the global minima in the design space is to use a multi-start approach according to which multiple local searches are performed each starting from a different starting point. In general, these techniques follow one of the two basic ways for determining the optimum solution; (a) a gradient-based differential method or (b) a direct search method (non-gradient methods) [18].

Gradient-based methods

As their name indicates, these techniques use calculus to search for the optimum solution by calculating the derivatives of the objective function and constraints. Examples of these methods are: the steepest descent method, Newton's method, and the conjugate gradients method [19]. Most local optimisation algorithms are gradient-based and the techniques are widely used for solving a variety of optimisation problems in engineering because they are efficient (in terms of the number of function evaluations required to find the optimum), can solve problems with large numbers of design variables, and require little problem-specific parameter tuning [22]. However, apart from being only able to locate a local optimum, these algorithms also have several drawbacks that include their difficulty of solving discrete optimisation problems, their complex algorithms that are difficult to implement efficiently, and their susceptibility to numerical noise.

Direct (Non-gradient based) methods

These methods use only function values at different points to perform a search and do not use the derivatives of the function. Examples of these methods are: Hooke-Jeeves method and Powell's conjugate direction method [18]. However, these methods are most suitable for simple problems involving a relatively small number of variables.

B. Global optimisation algorithms

It is important to note that no algorithm can guarantee convergence on a global optimum in the general sense and most algorithms only guarantee a local optimum [19,22]. However, global optimisation algorithms have a much better chance of finding the global or near global optimum than the local optimisation algorithms. Global optimisation algorithms are classified as either evolutionary algorithms or deterministic algorithms. The following discussion focuses on the evolutionary optimisation algorithms which have become very popular in engineering analyses over the last two or three decades for both single-objective and multi-objective optimisation [23]. These methods are inspired by some phenomena in nature and, unlike the local techniques where a single design point is updated (typically using gradient information) from one iteration to the next, they do not require any gradient information. Instead, they make use of a set of design points (generally referred to as a population) to find the optimum design point. A number of evolutionary algorithms have been developed, but the two most popular and more

established algorithms are the Genetic Algorithm (GA) [24], which was inspired by Darwin's principle of survival of the fittest, and the Particle Swarm Optimisation (PSO) algorithm [25], which was based on a simplified social model. The following descriptions shed more light on these two algorithms.

Genetic algorithm

GAs are computerised search and optimisation algorithms based on the mechanics of natural selection and natural genetics [26]. They combine survival of the fittest among string structures and a systematic information exchange guided by random operators to form a sensible search procedure. Beginning with a randomly created population of string structures, each string is evaluated and a better population is created by operating on the current population using three operators: *reproduction*, *cross over* and *mutation*. The reproduction operator selects the good strings in the population and forms the mating pool. The cross over operator selects two strings from the mating pool at random and exchanges some portions of the strings. The mutation operator changes the string locally to create a better string with a small probability. The population is then evaluated and tested for termination. Successive populations are repeatedly operated by the three operators till the termination criteria are attained. The flowchart shown in Figure 1.6 presents the general overview of a genetic algorithm [27].

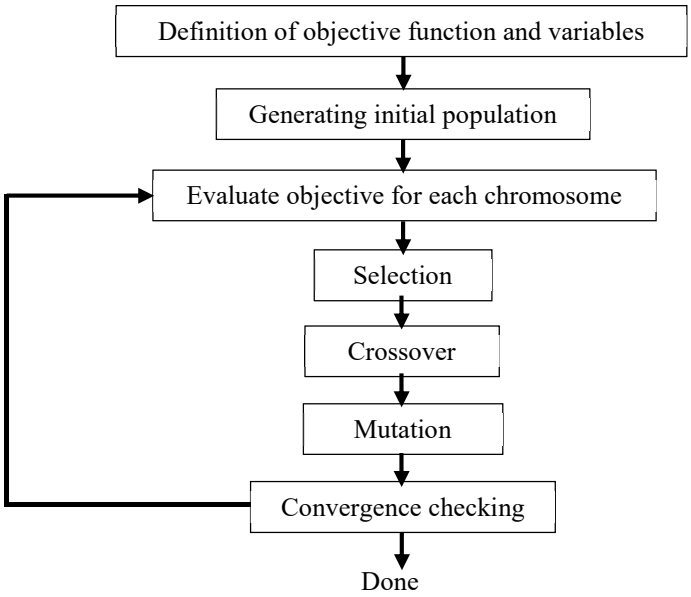

Figure 1.6. Flow chart of a genetic algorithm [27]

The main components of the genetic algorithm are defined below [27]:

Gene: Variables of optimisation

Chromosome:	An array of genes that is passed on the objective function
Individual:	A possible result, a single member of a population that consists of a chromosome and its objective function
Population:	A group of individuals
Generation:	One iteration of the genetic algorithm
GA operators:	Selection, crossover and mutation
Selection:	The process of choosing parents for reproduction (usually based on fitness)
Crossover:	An operator that forms a new chromosome from two parent chromosomes by combining part of the information from each
Mutation:	A reproduction operator that randomly alters the values of genes in a parent chromosome
Reproduction:	Generation with the GA operators or the creation of offspring

Particle swarm optimisation

PSO is based on simulation of social behaviour of birds flocking or fish schooling [22,23]. It is a stochastic method that does not use operators inspired by natural evolution for creating a new population, but depends on the exchange of information between the individuals, called *particles*, in the population, called *swarm*. Each particle of the swarm is treated as a point in a hyper space through which the particles fly with two essential capabilities: their memory of their own best position (local best) and knowledge of their global or their neighbourhood's best (global best). The basic concept of the algorithm lies in accelerating each particle toward its local best and global best. The performance of each particle is measured by a fitness function. The convergence is influenced by the inertia weight which is used to control the impact of previous velocity on current velocity. A suitable value of the inertia weight is to be used for creating a balance between the local and global exploration ability of the swarm thereby providing the best solution.

Advantages and drawbacks of evolutionary algorithms

Evolutionary GA and PSO algorithms are well suited for discrete optimisation problems and have the advantage of being extremely robust, have an increased chance of finding a global or near global optimum, and they are easy to implement. The big drawbacks associated with these algorithms are their high computational cost, poor constraint-handling abilities, problem-specific parameter tuning and limited problem size.

1.3. Exergoeconomics and MOO applied to energy-conversion systems

A large number of research papers have been published in recent years relevant to the application of exergoeconomics and MOO for energy-conversion systems. Since a comprehensive review of all these efforts is not possible here, the following short review aims to give examples that demonstrate the applications of the two methodologies for energy-conversion systems and their anticipated benefits. Most of the papers cited below have been obtained from open online journals, research-exchange platforms (Academia [28], Researchgate [29], Engineering archive [30] and Elsevier SSRN preprint services [31]) or from conference proceedings that are available at the internet, e.g. [32]. The given examples relate to the following five types of energy-conversion systems:

- Conventional power plants
- Cogeneration and tri-generation systems
- Integrated and hybridised systems
- Low-grade waste heat recovery
- Industrial refrigeration systems and processes

Conventional power plants

In their analysis to optimise the operating parameters of a gas turbine power plant that produces 140 MW of electricity, Gorji-Bandpy and Goodarzian [33] used a genetic algorithm. They defined their objective functions for optimisation so as to minimise a total cost function and maximise an exergetic efficiency and the decision variables were the compressor pressure ratio, compressor isentropic efficiency, turbine isentropic efficiency, combustion products temperature, air mass flow rate, and fuel mass flow rate. The results of their thermoeconomic analysis showed the deep relation of the unit cost on the change of the operating parameters of the gas turbine power plant. They showed that the cost of the final product was 9.78% lower compared to the base case and this was achieved with 8.77% increase in the total capital investment.

Shamoushaki et. al. [34] performed exergy and exergoeconomic analysis and optimisation of a gas turbine cycle by using three algorithms: NSGA-II, MOPSO and MOEA-D. Two objective functions were considered: the total cost rate and the exergy efficiency. The optimal solution obtained by NSGA-II, which was the lowest total cost rate (1.922 US$/s) was 30% less than MOPSO algorithm and 6.2% less than MOEA-D algorithm. Also, the exergy efficiency obtained by the NSGA-II algorithm was about 55.1% which was 12% greater than MOPSO algorithm and 10% greater than MOEA-D algorithm. After overall comparison of the performance of these algorithms, the results showed that the performance of the NSGA-II algorithm was better than those of the two other algorithms. Shamoushaki and Ehyaei [35] performed exergy, economic and environmental analysis as well as multi-objective optimisation of Aliabad Katoul power plant by using the NSGA-II algorithm. Two objective functions were considered which were the total cost rate and the environmental impact cost. Optimisation of the objective functions was done in two modes of the cycle; with and without an air preheater. The results showed that the existence of air preheater reduces both objective functions. For the optimised cycle without air preheater, the amount of total cost rate and environmental cost rate were about 30% and 33%, respectively, higher than those of the cycle with air preheater. Also, exergy losses of the various components illustrated that the combustion chamber has the maximum rate of exergy destruction (about 73%).

Cogeneration and tri-generation systems

Ghaebi et al. [3] conducted exergoeconomic optimisation of a tri-generation system for cooling, heating and power purposes which was made up of an air compressor, combustion chamber, gas turbine, dual pressure heat recovery steam generator and absorption chiller. The design parameters they selected for their study were the air

compressor pressure ratio, gas turbine inlet temperature, pinch point temperature in the dual pressure heat recovery steam generator, pressure of steam that enters the generator of the absorption chiller, process steam pressure, and evaporator of the absorption chiller chilled water outlet temperature. For the economic model, they adopted the total revenue requirement (TRR) method and defined the cost of the total system product as the single objective function. For the optimisation method they used a GA technique. Compared to the base design, their results show that the total product cost was reduced by about 15 percent after the exergoeconomic optimisation.

Baghernejad et al. [36] also developed a model for analysing a solar tri-generation system that produces electricity, heating and cooling according to the exergetic, economic and environmental targets. They used the GA optimisation toolbox of MATLAB for multi-objective optimisation of the tri-generation system with the two objectives of maximising the exergetic efficiency of the system while minimising its unit costs of productions. The optimisation process led to 26.34% increase in the exergetic efficiency and 11.5% decrease of the unit cost of products compared to the base design. The application of optimisation process shows that exergoeconomic analysis improved significantly the total performance of the tri-generation system in a way that fuel cost, exergy destruction cost and environmental impacts (CO_2 emissions cost) are reduced by 24.17%, 38.87% and 24.17%, respectively.

In a more recent study, Nondy and Gogoi [37] comprehensively assessed two gas turbine-based combined cooling, heating, and power (CCHP) systems taking the system cost rate and normalised CO_2 emissions as objective functions. They used the NSGA-II algorithm to perform MOO of both systems by considering six decision variables which were the air-compressor pressure ratio, the isentropic efficiencies of the air-compressor and gas-turbine, the air-preheater outlet temperature, the steam-turbine inlet pressure, and the pinch point temperature difference. Their study demonstrated the significant improvements in system performance and environmental impact achieved through MOO since both systems achieved around 8–9 % reduction in system cost rates and around 1.5–2 % reduction in the normalised CO_2 emissions. Their study, which also highlights the need for trade-offs amongst the key design variables particularly the pressure ratio and isentropic efficiency of the air compressor, offers valuable insights into the performance, efficiency, and optimisation potential of CCHP systems.

Integrated and hybridised systems

Babaelahi and Lotfalipour [38] presented an innovative solar-geothermal integrated system for power generation and water desalination. By harnessing renewable solar and geothermal energy, their system offers a sustainable solution for energy, water, and environmental challenges. Their study incorporated exergy-based economic and environmental assessments and the emergy concept [39,40] to quantify the total available energy required, enabling a comprehensive sustainability evaluation. Through multi-objective optimisation using genetic algorithms, the system's design and operational parameters were optimised to enhance exergy efficiency, economic emergy performance,

and environmental emergy performance simultaneously. To identify optimal operating points balancing energy efficiency, economic feasibility, and environmental impact, the optimisation framework considered turbine inlet conditions, pressures, and desalination configurations. The results demonstrated significant improvements of up to 23.49% in exergy efficiency, 25.97% in economic emergy performance, and 16.04% in environmental emergy performance compared to the baseline system.

Benet et al. [26] studied the application of GA techniques to the design of hybridised marine power plants aiming to find compromised solutions between the hybridisation of emerging technologies and the use of alternative fuels. According to them, the combination of new technologies such as fuel cells with the conventional internal combustion engines, gas turbines and/or batteries can enhance the efficiency of the resulting hybridised power plants compared to the conventional engines installed on-board ships while the use of alternative fuels, such as hydrogen, methanol or ammonia, to power the ships can reduce the carbon footprint of the vessels. However, hybridisation and the use of alternative fuels require several variables to be taken into account concurrently such as efficiency, reliability, flexibility, space requirements, mass, and investment and maintenance costs. According to them, multi-objective optimisation helps the decision-maker to select the most suitable components for the power plant and determine their capacities according to the set of requirements that must be met.

Low-grade waste heat recovery

Recovery of low-grade waste heat in industrial processes is an essential energy management topic. The organic Rankine cycle (ORC), which has the benefits of being energy-efficient, enabling investment savings, and being ecologically friendly, is crucial in recycling energy from low-temperature waste heat. Both the application of the optimum cycle design and the provision of optimum working conditions are the issues that need to be focused on efficiently using energy. Küçük and Kılıç [41] performed energy, exergy, and exergoeconomic analysis of four different ORC configurations operating with renewable or low grade waste heat. The solution of the multi-objective optimisation problem was realised with the Taguchi-Grey Relational Analysis (TGRA) method. The best thermodynamic and exergoeconomic performance result was calculated for the configuration of ORC with Feed Fluid Heater-Internal Heat Exchanger (IHE–FFH–ORC). As a result of the optimisation process, the thermal and exergy efficiencies, the total system cost and the unit cost of produced electricity for the IHE–FFH–ORC power system were calculated as 22.6% and 73.5%, 1.06 $/h, 0.039 $/kWh, respectively. The payback period was 2.9 years.

Behzadi et al [42] performed energy, exergy, and exergoeconomic analysis of an integrated system for Tehran's waste-to-energy (WtE) power plant coupled with an ORC. By conducting a parametric thermodynamic study of the essential parameters (moisture content, pinch point temperature differences of the heat-recovery of gasifiers (HROG), steam generator's superheat temperature difference, and steam turbine inlet pressure), they identified R123 as working fluid that gives the best system performance for the

ORC. By implementing the waste-heat-recovery system into the WtE plant with R123, the energy and exergy efficiencies would increase from 17.27% to 19.51% and 14.49%–16.36%, respectively. Their exergy analysis revealed that the gasifier and steam generator were the main source of exergy destruction in the overall system. They also conducted a multi-objective optimisation based on genetic algorithm using MATLAB software to find the optimum point with respect to exergy efficiency and total product unit cost as the objective functions. The analysis showed that the exergy efficiency and total product unit cost at the optimum point were 19.61% and 24.65 $/GJ, respectively.

Keyvan Bahlouli [43] conducted a parametric study for a combined cycle that combines a gas turbine-modular helium reactor (GT-MHR) and two organic Rankine cycles operated from the GT-MHR waste heat. The aim of their study was to reveal the influences of decision parameters on the performance and total cost of the cycle. In order to optimise the system from both thermodynamic and economic aspects, they applied a multi-objective optimisation strategy the purpose of which was to maximise the exergy efficiency and to minimise the total cost rate of the system. The decision variables in the optimisation process they selected were the compressor pressure ratio, temperatures of inlet turbine and evaporators, temperature difference in the evaporator and degree of superheat at the inlet of the ORC turbines. After optimisation, they found that the exergy efficiency reached 50.20% compared to 49.84% of the base case and the capital expense was approximately reduced by 2.4%.

Industrial refrigeration systems and processes

Keshtkar and Talebizadeh [44] conducted optimisation analyses of a two stage-cascade refrigeration system based on exergetic, economic, and environmental considerations. In their analyses, they considered R134a and R744 as the refrigerants in the high and the low temperature circuits, respectively. Initially, they used single-objective exergetic and economic strategies to evaluate the system's performance with different effective parameters so as to indicate the optimum operation conditions. As would be expected, the exergetic and economic single-optimisation analyses lead to higher exergetic efficiency and lower cost, respectively, compared to the base design. Then, they conducted a multi-objective exergetic and economic optimisation analysis by using the genetic algorithm with a decision-making strategy based on the Pareto frontier using TOPSIS method. Compared to the base design, the MOO analysis increased the total system cost and the exergetic efficiency by 28.6% and 99.5%, respectively, and reduced the compressors work by 46.6%.

Cooling towers are needed for refrigeration systems in power plants and large commercial buildings for removing the heat emitted by these systems to the environment. The world-wide concerns regarding the environmental wear and water scarcity calls for mitigating the impact of the systems in which the cooling towers are coupled with compression chillers. According to Nedjah et al. [45], one way for doing so is to maximise the energy efficiency of the industrial processes. Therefore, they proposed the application of MOO algorithms to find out the optimal operational set-points of the

refrigeration system. To find the best trade-offs that simultaneously maximise the cooling tower's effectiveness and minimise the global power requirement of the system while respecting operational constraints for the safe operation of the equipment, they applied two algorithms; PSO and TRIBES. They also compared two different models of the refrigeration system so that the best algorithm and the best equipment model for the refrigeration system could be selected. One of the configurations they studied achieved an energy efficiency factor of 1.78, which yields a power savings of 9.48%, with a reduction of tower effectiveness by only 5.32%.

To address the problem of global climate change, Mei et. al. [46] developed a novel configuration of H_2S concentrator adopting pressure drop method and self-stripping method in dual-stage Selexol process of integrated gasification combined cycle. By using exergoeconomic analysis they found that the total product specific cost and total exergoeconomic factor of the process were 48.54 $/hr and 7.84%. They also carried out a multi-objective optimisation of the model by using the NSGA-II algorithm in conjunction with Aspen Plus to get the optimal operating conditions according to three targets for actual operation. The multi-objective optimisation results revealed that the optimal point between CO_2 capture efficiency and total exergy efficiency was such that CO_2 capture efficiency was 93.13% and the total exergy efficiency was 26.09%. Jovijari et al. [47] conducted exergy, exergoeconomic, and exergoenvironmental analysis of a natural gas liquid recovery process and Amid et al. [48] conducted exergetic, exergoeconomic, and exergoenvironmental aspects of an industrial-scale molasses-based ethanol production plant.

1.4. Closure

This chapter reviews the conventional methodologies of thermoeconomic analysis and single-objective optimisation as a background for discussing exergooeconomic analysis and multi-objective optimisation in the following chapters of the book. To relate to the discussions of the two newly-developed methods, the chapter focusses on exergy-based costing instead of the traditional energy-based one and on the evolutionary optimisation methods instead of the traditional deterministic ones. The chapter also gives examples of applying the two methods in various types of energy-conversion systems. Chapter 2 and Chapter 3 discuss the exergoeconomic analysis method and multi-objective optimisation in more details and give simple examples that show how the tools provided by the Excel-based modelling platform can be used for conducting them. Since the two methods are still subjects of intensive research and it is not possible to describe all the methods and techniques with each main methodology, the two chapters focus on the techniques that are mostly used in optimisation analyses of energy-conversion systems; which are the SPECO (Specific exergy costing) method and the genetic algorithms.

Chapters 4 through 6 deal with exergoeconomic analyses of energy-conversion systems. Chapter 4 applies the method for assessing the economic benefit of utilising the hot water that exits the intercooler of a two-stage intercooled air compressor. The method is applied for the system by considering two options. In the first option the system has one product,

which is the compressed air, while in the second option the hot water generated by the intercooler is considered as a second product. Chapter 5 illustrates the use of mathematical optimisation methods for conducting objective-guided exergoeconomic analyses by considering the simple gas turbine, while Chapter 6 illustrates the use of advanced exergoeconomic analysis method and discusses the difficulties associated with applying the method.

Both Chapter 7 and Chapter 8 deal with multi-objective optimisation analyses of vapour-compression refrigeration systems. Chapter 7 presents an Excel-aided model for MOO analyses of an innovative two-stage compression VCR system that incorporates an intercooler after the first-stage compressor. A tri-objective optimisation analysis of the system is conducted with R152a and R717 to maximise its exergetic efficiency and minimise its capital investment and the total equivalent warming index (TEWI). Chapter 8 deals with the selection of a suitable refrigerant pair for an improved cascade VCR system that incorporates a flash-tank in the low-temperature circuit and an intercooler in the high-temperature circuit. The performance of the system is compared with twelve pairs of eight refrigerants of low global-warming potentials (GWP) and four-objective optimisation analyses are conducted for the four pairs with best performance to maximise the COP and exergetic efficiency and minimise the total annualised cost and TEWI.

All the MOO analyses presented in Chapters 3 through 8 involve a maximum of four design variables and, therefore, could be conducted by using the free version of the MIDACO solver [49] that limits the number of changing variables to four. In order to conduct MOO analyses with more changing variables, Chapter 9 presents a technique for using Excel's Solver with the TOPSIS method for MOO analyses with a priori preference of the objectives without limiting the number of design variables. The applicability of the Solver-TOPSIS technique is demonstrated in this chapter by applying it to the same systems considered in Chapters 3, 4, 7, and 8. Chapters 10 and 11 illustrate the generality of the technique by applying it for conducting dual-objective optimisation analyses of the regenerative gas-turbine and the air-bottoming cycle, respectively. Chapter 10 also shows that the technique can be applied by both solution methods offered by Solver. Chapter 12 concludes the book by describing an Excel-aided model for MOO and exergoeconomic analyses of the CGAM gas-turbine co-generation system [51].

References

[1] M.A. Rosen, A Concise Review of Exergy-Based Economic Methods, 3rd IASME/WSEAS Int. Conf. on Energy & Environment, University of Cambridge, UK, February 23-25, 2008.

[2] I. Dincer, Renewable energy and sustainable development: a crucial review, Renewable and Sustainable Energy Reviews, Volume 4, Issue 2, June 2000, Pages 157-175

[3] H. Ghaebi, M.H. Saidi, P. Ahmadi, Exergoeconomic optimization of a trigeneration system for heating, cooling and power production purpose based on

TRR method and using evolutionary algorithm, Applied Thermal Engineering 36 (2012) 113e125.

[4] M.J. Moran and H.N. Shapiro, Fundamentals of Engineering Thermodynamics, 5th edition, John Wiley, & Sons. Inc. 2006.

[5] A. Picallo-Perez, J.M. Sala, L.D. Portillo and R. Vidal, Delving Into Thermoeconomics: A Brief Theoretical Comparison of Thermoeconomic Approaches for Simple Cooling Systems. Front. Sustain. (2021) 2:656818. doi: 10.3389/frsus.2021.656818

[6] G. Tsatsaronis, Definitions and nomenclature in exergy analysis and exergoeconomics, Energy 32 (2007) 249–253

[7] G. Tsatsaronis, On the Future of Exergy-based Methods, Proceedings of ECOS 2023 - the 36th international conference on efficiency, cost, optimization, simulation and environmental impact of energy systems, 25-30 June 2023, Las Palmas de Gran Canaria, Spain

[8] J.H. Keenan. A Steam Chart for Second Law Analysis. Mechanical Engineering 1932, 54, 195–204.

[9] A. Valero and C. T. Cuadra, Exergy, energy system analysis and optimization – Vol. II - Thermoeconomic Analysis, ©Encyclopedia of Life Support Systems (EOLSS)

[10] H. Aras and O. Balli. Exergoeconomic analysis of a combined heat and power system with the micro gas turbine (MGTCHP), Energy Exploration & Exploitation · Volume 26 · Number 1 · 2008 pp. 53–70

[11] J. Moran, Availability analysis: a guide to efficient energy use, Prentice Hall, pp. 199-215, (1982)

[12] M. Gorji-Bandpy and V. Ebrahimian, Exergoeconomic analysis of gas turbine power plants, International Energy Journal, Vol. 7. No. 1, (2006)

[13] M. Saghafifar, A. Poullikkas, Thermo–economic optimization of air bottoming cycles, Journal of Power Technologies 95 (3) (2015) 211–220

[14] L. Pierobon, & F. Haglind, Design and optimization of air bottoming cycles for waste heat recovery in off-shore platforms. Applied Energy (2014), 118, 156–165. DOI: 10.1016/j.apenergy.2013.12.0

[15] C. Yilmaz, Thermoeconomic cost analysis and comparison of methodologies for Dora II binary geothermal power plant, Geothermics 75 (2018) 48–57

[16] I. G. Kerdan , R. Raslan , P. Ruyssevelt, D. M. Gálvez, A comparison of an energy/economic-based against an exergoeconomic-based multi-objective optimisation for low carbon building energy design, Energy, Volume 128, 1June 2017, Pages 244-263

[17] A. Al-Falahi, F. Alobaid, B. Epple, Thermo-Economic Comparisons of Environmentally Friendly Solar Assisted Absorption Air Conditioning Systems. Appl. Sci. 2021, 11, 2442. https://doi.org/ 10.3390/app11052442

[18] K. Deb, Multi-Objective Optimization using Evolutionary Algorithms, JOHN WILEY & SONS, LTD, 2001

[19] S.G. Johnson, A Brief Overview of Optimization Problems, MIT course 18.335, Fall 2008.

[20] A. Bejan, G. Tsatsaronis, and M. Moran. *Thermal Design and Optimization*. New York: Wiley,. 1996.
[21] J. Renuka Kumari, Optimization Techniques – A Review, Int. Journal of Engineering Research and Application, Vol. 6, Issue 11, (Part -4) November 2016, pp.01-05.
[22] G. Venter: Review of Optimization Techniques, Encyclopedia of Aerospace Engineering. Edited by Richard Blockley and Wei Shyy, 2010 John Wiley & Sons, Ltd.
[23] I. Fister Jr., X.S. Yang, I. Fister, J. Brest, D. Fister, A Brief Review of Nature-Inspired Algorithms for Optimization, Elektrotehni˘ski Vestnik 80(3): 1–7, 2013 (English Edition)
[24] J.H. Holland, Adaptation in Natural and Artificial Systems, Ann Arbor, MI: MIT Press., 1975.
[25] J. Kennedy and R.C. Eberhart. Particle swarm optimization. In Proceedings of the 1995 IEEE International Conference on Neural Networks, Perth, Australia, 1995; 1942–1948.
[26] Á. Benet, A. Villalba-Herreros, Ó. Santiago and T.J. Leo Application of genetic algorithms to the design and dimensioning of maritime hybridpower plants fueled by alternative fuels, Proceedings of ECOS 2023 - the 36th International Conference on Efficiency, Cost, Optimization, Simulation and Environmental Impact of Energy Systems 25-30 June, 2023, Las Palmas de Gran Canaria, Spain
[27] A. R. Navaie, Thermal Design and Optimization of Heat Recovery Steam Generators and Waste Heat Boilers, Dissertation, Technische Universität Berlin, Institut für Energietechnik Berlin 2017.
[28] Academia, https://www.academia.edu/
[29] ResearchGate, https://www.researchgate.net/
[30] Engineering Archive, https://engrxiv.org/index
[31] Elsevier SSRN preprint services, https://www.elsevier.com/products/ssrn-preprint-services
[32] Proceedings of ECOS 2023 - the 36th International Conference on Efficiency, Cost, Optimization, Simulation and Environmental Impact of Energy Systems 25-30 June, 2023, Las palmas de Gran Canaria, Spain, https://www.proceedings.com/69564.html
[33] M. Gorji-Bandpy and H. Goodarzian, Exergoeconomic optimization of gas turbine power plants operating parameters using genetic algorithms: A case study, Thermal Science, Year 2011, Vol. 15, No. 1, pp. 43-54
[34] M. Shamoushaki, F. Ghanatir, M.A. Ehyaei, A. Ahmadi, Exergy and exergoeconomic analysis and multi-objective optimisation of gas turbine power plant by evolutionary algorithms. Case study: Aliabad Katoul power plant, Int. J. Exergy, Vol. 22, No. 3, 2017, 279-307.
[35] M. Shamoushaki, M.A. Ehyaei, Optimization of gas turbine power plant by evoloutionary algorithm; considering exergy, economic and environmental aspects, Journal of Thermal Engineering, Vol. 6, No. 2, Special Issue 11, pp. 180-200, March, 2020, Yildiz Technical University Press, Istanbul, Turkey

[36] A. Baghernejad, M. Yaghoubi, K. Jafarpur, Exergoeconomic optimization and environmental analysis of a novel solar-trigeneration system for heating, cooling and power production purpose, Solar Energy 134 (2016) 165–179

[37] J. Nondy, T.K. Gogoi, Exergoeconomic and environmental optimization of gas turbine-based CCHP systems: A comprehensive study with multi-objective optimization and decision making, International Journal of Thermofluids 23 (2024) 100821

[38] M. Babaelahi, M. Lotfalipour, Multi-objective optimization and comprehensive Thermodynamic, economic, and environmental analysis ofan innovative solar-geothermal integrated system forsynergistic power generation and water desalination, Energy Sources, Part A: Recovery, Utilization, and Environmental Effects, Volume 46, 2024 - Issue 1

[39] M. Aghbashlo and M.A. Rosen, Consolidating exergoeconomic and exergoenvironmental analyses using the emergy concept for better understanding energy conversion systems. J Clean Prod 2018; 172: 696–708. https://doi.org/10.1016/j.jclepro.2017.10.205

[40] S.K. Effatpanah, M.H. Ahmadi, S.H. Delbari, G. Lorenzini, Energy, Exergy, Exergoeconomic and Emergy-Based Exergoeconomic (Emergoeconomic) Analyses of a Biomass Combustion Waste Heat Recovery Organic Rankine Cycle. Entropy 2022, 24, 209. https://doi.org/10.3390/e24020209

[41] E. ¨O. Küçük, M. Kılıç Exergoeconomic analysis and multi-objective optimization of ORC configurations via Taguchi-Grey Relational Methods, Heliyon 9 (2023) e15007

[42] A. Behzadi, E. Gholamian, E. Houshfar, A. Habibollahzade, Multi-objective optimization and exergoeconomic analysis ofwaste heat recovery from Tehran's waste-to-energy plantintegrated with an ORC unit, Energy, Volume 160, 1, October 2018, Pages 1055 – 1068

[43] K. Bahlouli, Multi-objective optimization of a combined cycle using exergetic and exergoeconomic approaches, Energy Conversion and Management, Volume 171, 1 September 2018, Pages 1761 - 1772

[44] M.M. Keshtkar, P. Talebizadeh, Multi-objective optimization of a R744/R134a cascade refrigeration system: exergetic, economic, environmental, and sensitive analysis (3ES), Journal of Thermal Engineering, Vol. 5, No. 4, pp. 237-250, Jue, 2019, Yildiz Technical University Press, Istanbul, Turkey.

[45] N. Nedjah, L.D.M. Mourelle, M.S.D. Lizarazu. Swarm Intelligence-Based Multi-Objective Optimization Applied to Industrial Cooling Towers for Energy Efficiency. Sustainability 2022, 14, 11881. https://doi.org/10.3390/su141911881

[46] W. Mei, R. Zhai, Y. Zhao, Z. Yao, N. Ma, Exergoeconomic analysis and multi-objective optimization using NSGA-II in a novel dual-stage Selexol process of integrated gasification combined cycle, Energy, Volume 286, 1, January 2024, 129663

[47] F. Jovijari, A. Kosarineia, M. Mehrpooya, N.Nabhani, Exergy, Exergoeconomic, and Exergoenvironmental Analysis in Natural Gas Liquid Recovery Process, Iran. J. Chem. Chem. Eng. Research Article Vol. 42, No. 1, 2023

[48] S. Amid, M. Aghbashlo, M. Tabatabaei, K. Karimi, A. Nizami, M. Rehan, H. Hosseinzadeh-Bandbafha, M.M. Soufiyan, W. Peng, S.S. Lam, Exergetic, exergoeconomic, and exergoenvironmental aspects of an industrial-scale molasses-based ethanol production plant, Energy Conversion and Management 227 (2021) 113637
[49] MIDACO-Solver, http://www.midaco-solver.com/

2

Exergoeconomics

Exergoeconomics appropriately combines thermodynamic evaluations based on an exergy analysis with economic principles at the level of system components to provide the designer of an energy system with information that is not obtainable by regular energy or exergy analysis and economic analysis [1,2]. By measuring exergy destruction in the components of an energy system, the exergy analysis identifies the causes, locations and magnitudes of the inefficiencies [3,4] and by applying the concept of cost to exergy and exergy losses the economic principles allow the costs of the flows and equipment of any plant and, therefore, the cost of the final product to be calculated [5]. Since exergo-economics associates costs to internal exergy flows, it can be applied to evaluate the impact of thermodynamic inefficiencies on the cost formation process and the final products' costs and can be used for optimising variables of specific components as well as optimising the system as a whole [6]. The method is continuously improved so as to maximise its accuracy and expand its area of applicability. This chapter introduces the basic method and shows how it can be applied with the Excel-based modelling platform in design analyses of energy-conversion systems by considering simple cogeneration systems. Falling short of providing a more comprehensive and up-to-date discussion, the chapter gives a brief account of applying the method to more complex systems and outlines two of its recent developments which are the advanced exergoeconomic and exergo-environmental analyses methods.

2.1. A historical note

Recalling the history of exergy-based thermoeconomics helps us to understand how the current state of the art has been reached and anticipate future developments of the method. An important step in this respect is the acceptance of using exergy-based costing instead of energy-based costing. According to dos Santos et al. [7], the idea of associating the exergy (availability) of the final products of an energy system with their respective costs is due to Keenan [8] who developed a steam chart for second law analysis back in 1932. However, the use of second-law concepts in industry was initially resisted and the early studies on the second law analysis methodologies and exergy costing started in both Europe and America independently only in the late 1950s. According to Sciubba [5], the first association of economic value to exergy is due to Rant who, in 1955, stated that "Exergy is the part of energy having value" and that "energy without exergy is valueless".

In the 1960s and 1970s, a great number of publications by various scientists established the theoretical foundations of the exergy-based methodology. In the US, Tribus and Evans [9] studied desalination processes by exergy analysis, for which they coined the word ''thermoeconomics''. Their work marked the beginning of a concrete formulation of the methodology. The book published by Georgescu-Roegen [10] in 1971 is often cited as the pioneering reference in the field of thermoeconomics. In Europe, Bergmann and Schmidt [11] assigned costs to the exergy destruction in each component of a steam power plant and optimised feed water heaters in 1965. Szargut [12] analysed a simple cogeneration plant by using an exergy costing procedure and introduced an ecological cost coefficient (ECC) into the literature in 1967.

The 1980s witnessed a rapid expansion of the methodology and its applications in design and optimisation analyses of thermal systems. Two research trends in exergoeconomic analyses were followed during this decade one of which is the exergoeconomic accounting approach, which is a continuation of the work by Obert and Gaggioli [13], and the other is the Lagrangian-based approach first introduced by Evans and Tribus [14]. The weakness of the calculus methods has limited the application of the Lagrangian-based method to complex systems. Therefore, there have been no new progresses or interesting applications of these methods in recent years compared to the accounting methods that do not have these limitations. The term ‘‘exergoeconomics’’ itself was first proposed in 1984 by Tsatsaronis [1] as an unambiguous characterisation of the combination of economics and exergy concepts that enables not only the inefficiencies to be evaluated, but also the costs associated with them and the investment expenditures required to reduce them. Tsatsaronis also introduced other fundamental exergoeconomic terms such as “Fuel” and “Product” and the rules associated with them.

The most important contributions to exergoeconomic analysis were done in the 1990s during which a number of methods were proposed. Frangopoulos proposed the Thermoeconomic Functional Analysis (TFA), Von Spakovsky proposed the Engineering Functional Analysis (EFA), Lozano and Valero proposed the Theory of Exergy Cost (TEC), while Tsatsaronis and co-workers proposed the methods that finally became the specific exergy costing (SPECO) method. In 1994, the CGAM problem was defined to compare the results of these four methodologies [15]. In 1998, Kim et al. [16] introduced the Modified Productive Structure Analysis (MOPSA) method which was subsequently developed by Kwon et al. [17] and Kwak et al. [18]. The exergoeconomic methods that have been developed since the late 1980s can be ordered as follows:

(a) Thermoeconomic functional analysis (TFA)
(b) Last-in-first-out principle (LIFO)
(c) Engineering functional analysis (EFA)
(d) Theory of exergy cost (TEC)
(e) Exergy economic approach (EEA)
(f) Specific exergy costing (SPECO)
(g) Modified productive structure analysis (MOPSA)
(h) Structural theory of thermoeconomics (STT)
(i) Exergy-cost-energy-mass analysis (EXCEM)

The late 1990s also witnessed the use of fuzzy logic and genetic algorithm methods in optimisation analyses of energy systems. Since the beginning of this century exergoeconomic analyses have been widely applied to many energy systems such as power plants, combined heat and power production or cogeneration facilities and there have been further developments in the field such as the development of advanced exergoeconomics [19] and emergy-based exergoeconomics [20]. More detailed relevant historical accounts can be found in [5,7,21-24]. A review of the current state and future developments of exergoeconomics is given by Valero-Delgado and Torres [25].

2.2. The specific exergy costing (SPECO) method

The main hypothesis of exergoeconomics is that costs are transported with the exergy carriers in a thermal system, which can be physical and/or productive. All the exergo-economic methodologies are built from this hypothesis with the following objectives [6]:

(a) To identify the location, magnitude and real sources of thermodynamic losses (destroyed exergy and exergetic losses) in the thermal system;
(b) To calculate the cost associated to exergetic losses and destroyed exergy in any plant component; and
(c) To analyse the cost formation of each product separately in those thermal systems which produce more than one product.

The various exergoeconomic methodologies differ in the way they deal with the three above objectives. The following discussion focusses on the most widely applied method in the recent literature, which is the SPECO method.

2.2.1. A general description of the method

The SPECO method was initially developed by Tsatsaronis and Winhold [26], but Lazzaretto and Tsatsaronis [27] later proposed a simpler, more systematic and more general method that establishes a direct link between the fuel and product definitions for a component and the corresponding costing equations. Figure 2.1 shows a schematic of this method [20,28].

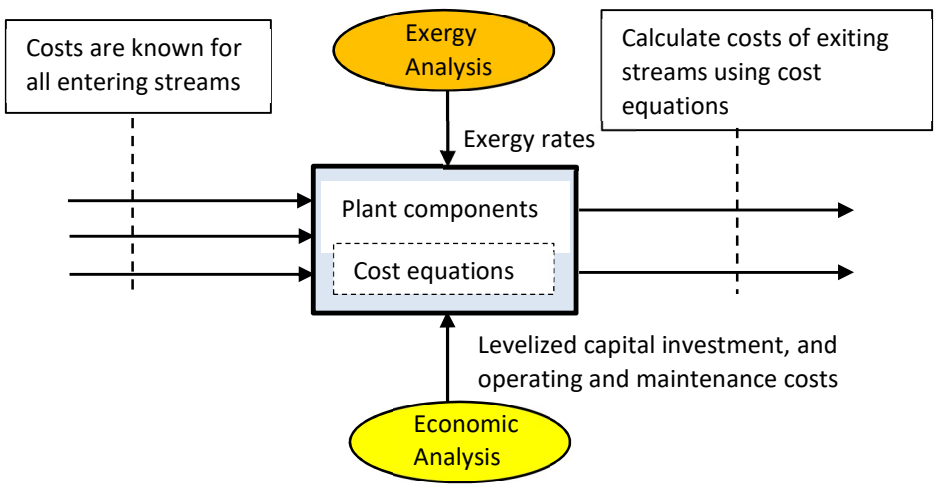

Figure 2.1. Schematic of the SPECO method (adopted from [20])

The method follows the four main steps described below [1,27,28]:

1- Identification of exergy streams: Refers to the application of the mass and energy conservation expressions as well as the exergy balance, respectively, to each

component of the system. In this step, all the entering and exiting exergy streams of each component are identified and calculated in the power unit; kW, MW, etc.

2- Definition of fuel and product for each component. The product is what we desire from a component, in terms of exergy, and the fuel is the required exergy to generate the product. Exergy differences (exergy additions to or removals from a stream) should be applied to all exergy streams associated with a change of physical exergy and to some exergy streams associated with the conversion of chemical exergy.

3- Identification of cost rate balance equations. Exergy costing involves cost balance usually formulated for each component separately. A cost balance applied to the k^{th} system component shows that the sum of cost rates associated with all existing exergy stream equals the sum of cost rates of all entering exergy streams, plus the appropriate charges due to capital investment and operating and maintenance expenses (all having the same unitary exergy cost).

4- Evaluation of the exergoeconomic variables and product cost. The exergoeconomic variables are used to assess the performance of the various components and identify the components where improvement is worthy.

2.2.2. Formulation of the cost-balance equations

The cost balance for a thermal system is usually performed at a steady state for each of the system components as a control volume [2,28]. For component k of the system that receives a heat transfer (q) and generates power (w) the equation is written as follows:

$$\sum_{e} \dot{C}_{e,k} + \dot{C}_{w,k} = \sum_{i} \dot{C}_{i,k} + \dot{C}_{q,k} + \dot{Z}_k \tag{2.1}$$

where the suffices i and e refer to the feed (input) and product (output) streams, respectively, $\dot{C}$ refers to an exergy stream cost rate (in \$ per hour), and $\dot{Z}_k$ represents non-exergy-related costs (in \$ per hour), which is mainly the rate of the component's initial cost. The meaning of each exergy stream cost in Equation (2.1) is as follows:

$\dot{C}_{i,k}$ = Input exergy stream

$\dot{C}_{e,k}$ = Output exergy stream

$\dot{C}_{w,k}$ = Work exergy stream

$\dot{C}_{q,k}$ = Heat exergy stream

In Equation (2.1), the work cost is treated as an output cost while the heat stream cost is treated as an input cost. Cost balances are generally written such that all terms are positive. $\dot{C}$ is related to the corresponding exergy flow $\dot{E}$ by:

$$\dot{C}_i = c_i \dot{E}_i \tag{2.2}$$

where c_i denotes the average cost of stream i per unit of exergy, e.g., \$/kJ. Note that the input exergy cost of each component is equal to the output rate of previous component. Therefore, the unknown quantity in the component equation is the product's exergy cost.

2.2.3. The auxiliary equations and the fuel/product rules

The number of streams entering and exiting the system components are usually more than the number of components in the system and, therefore, additional auxiliary relations are needed. These relations are obtained by using the *F*(fuel) and *P*(product) rules. Figure 2.2 shows the fuel and product exergy streams for three common components of energy-conversion systems, which are the compressor, turbine, and heat-exchanger.

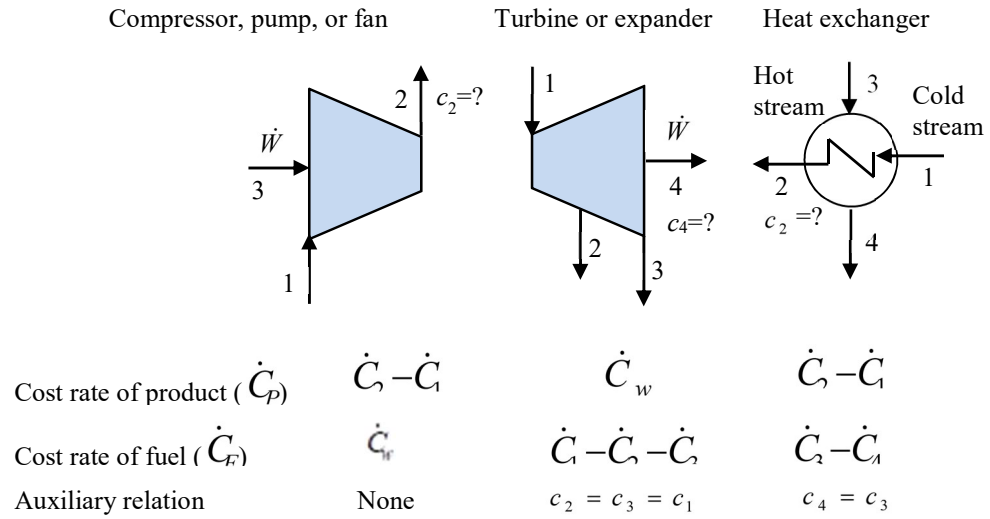

Figure 2.2. Cost rates associated with fuel and product and auxiliary thermoeconomic relations for compressor, turbines and heat-exchangers (adopted from [2])

Since the compressor has only one exit exergy stream, it does not require any auxiliary equation. However, both the turbine and heat-exchanger can have more than one exiting stream and, therefore, need auxiliary equations as shown on the figure. As a rule, n - 1 auxiliary relations are required for components with n exiting exergy streams. Solution of the resulting cost rate balance equations formulated for all the system components simultaneously yields the unknown cost rates from which the associated unit costs of the exiting exergy streams can be calculated. These are then used to determine the fuel and product costs of all the system components and the cost of exergy destruction in each component. In order to utilise this data for optimising specific components as well as optimising the system as a whole, the method defines a number of exergoeconomic variables as discussed in the following subsection.

2.2.4. The exergoeconomic variables

A number of exergoeconomic variables are defined by the exergoeconomic method to measure the cost effectiveness of exergy utilisation by the components of the thermal system being considered or find a trade-off between the investment cost and the component's efficiency [2,5]. The most commonly used variables are [2]:

The unit costs of the input (fuel): $$c_{F,k} = \dot{C}_{F,k} / \dot{E}_{F,k} \quad (2.3.a)$$

The unit costs of the output (product): $$c_{P,k} = \dot{C}_{P,k} / \dot{E}_{P,k} \quad (2.3.b)$$

The cost rate of exergy destruction: $$\dot{C}_{D,k} = c_{F,k} \dot{E}_{D,k} \quad (2.3.c)$$

The exergoeconomic factor: $$f_k = \frac{\dot{Z}_k}{\dot{Z}_k + \dot{C}_{D,k}} \quad (2.3.d)$$

The relative cost difference: $$r_k = \frac{c_{P,k} - c_{F,k}}{c_{F,k}} \quad (2.3.e)$$

2.2.5. Components aggregation and other considerations

The application of the SPECO method outlined in the above discussion omits a number of other considerations. In some cases, the available data might not be sufficient to treat each component of the system individually and components aggregation becomes necessary. However, the level at which the cost balances are formulated affects the results of the analysis. The accuracy of the results is also affected by separating the costing of chemical exergy and physical exergy or treating the four components of the physical exergy (mechanical, thermal, potential and kinetic) separately. Yet another consideration is the costing associated with the rejection of exergy (exergy loss) from a system to its surroundings. Bejan et al. [2] give a more detailed description of the method and its application to the CGAM benchmark cogeneration system. Applications of the method for the analysis and optimisation of complex cogeneration and tri-generation plants are described by, e.g., Mohammed [20], Zhao [21], Al-Sulaiman [28], and Çolpan [29].

2.3. Application of SPECO to a simple cogeneration system

To illustrate the application of the SPECO method by using Excel, consider the simple cogeneration system given in [2] that consists of a boiler and a steam turbine as shown on Figure 2.3. The feed water enters the boiler at 52 bars and 25°C to be heated to 466.1°C, but the pressure drops to 50 bars. The mass flow rate of the steam is 26.151 kg/s. To simplify the analysis, the rate of exergy input ($\dot{E}_{in}$) is fixed at 100 MW, exergy destruction in the boiler ($\dot{E}_{D,b}$) at 60 MW, exergy of the effluents ($\dot{E}_{out}$) at 5 MW, and exergy flow rate of the superheated steam entering the turbine ($\dot{E}_2$) at 35 MW.

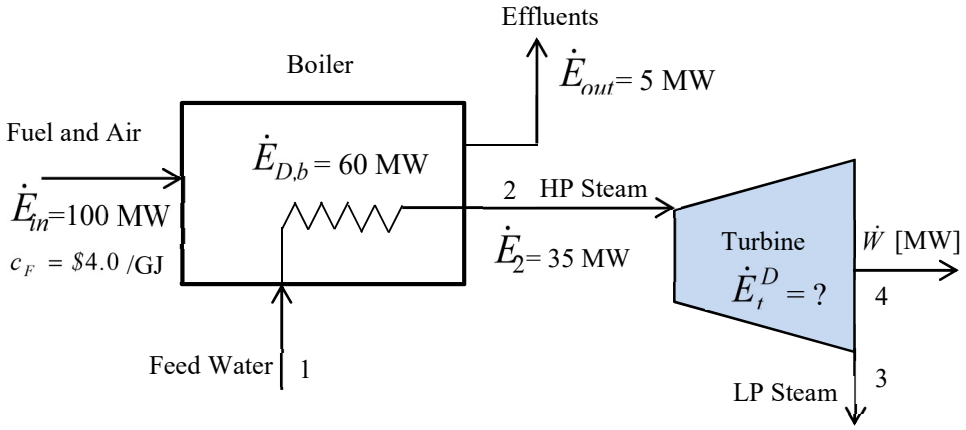

Figure 2.3. Schematic of a simple cogeneration system (adapted from Bejan et al. [2])

The polytropic efficiency of the turbine is 80% and the cost of fuel c_F = \$4.0/GJ. The cost rate of the boiler ($\dot{Z}_b$) is taken as \$0.3/s and the cost rate of the turbine ($\dot{Z}_t$) is given by:

$$\dot{Z}_t = 0.02\frac{\dot{W}}{10} \quad [\$/s] \tag{2.4}$$

where $\dot{W}$ is the power produced by the turbine in MW at the specified back pressure. An Excel-based model of the system will be developed to determine the power produced and the unit exergy costs of the power and steam and the results will be compared with those given by Bejan et al. [2] at various values of the back pressure.

2.3.1. The analytical model

The enthalpy of the low-pressure steam exiting the turbine is determined from:

$$h_3 = h_2 - (h_2 - h_{3s}) \times \eta_t \tag{2.5}$$

Where h_{3s} is the enthalpy after an assumed isentropic expansion in the turbine and η_t is the isentropic efficiency of the turbine. The turbine's power ($\dot{W}_e$), in MW, is given by:

$$\dot{W}_e = \dot{m}_s(h_2 - h_3)/1000 \tag{2.6}$$

The rate of exergy destruction in the turbine ($\dot{E}_{D,t}$), in MW, is given by:

$$\dot{E}_{D,t} = T_0\dot{m}_s(s_3 - s_2)/1000 \tag{2.7}$$

Applying Equation (2.1), the cost rate balance equations for the two components of the system, the boiler and turbine, are given by Equations (2.8) and (2.9), respectively:

$$\dot{C}_{in} + \dot{C}_1 + \dot{Z}_b = \dot{C}_2 + \dot{C}_{out} \tag{2.8}$$

$$\dot{C}_2 + \dot{Z}_t = \dot{C}_3 + \dot{C}_w \tag{2.9}$$

Given the cost of fuel c_F, the cost rate $\dot{C}_{in}$ is determined from:

$$\dot{C}_{in} = c_F \times \dot{E}_{in} \tag{2.10}$$

Since the cost of feed water and that of the combustion products are both zero,

$$\dot{C}_1 = 0 \tag{2.11}$$

$$\dot{C}_{out} = 0 \tag{2.12}$$

Substituting from Equations (2.11) and (2.12) and rearranging, Equation (2.8) becomes:

$$\dot{C}_2 = \dot{C}_{in} + \dot{Z}_b \tag{A}$$

Rearranging Equation (2.9), it becomes:

$$\dot{C}_w = \dot{C}_2 - \dot{C}_3 + \dot{Z}_t \tag{B}$$

There are three unknown cost rates, $\dot{C}_2$, $\dot{C}_3$, and $\dot{C}_w$, but only two equations and, therefore, one auxiliary equation is needed. By applying the rule $c_3 = c_2$ to the turbine, the following auxiliary equation is obtained:

$$\dot{C}_3 / \dot{E}_3 = \dot{C}_2 / \dot{E}_2 \tag{2.13}$$

Rearranging the equation:

$$\dot{C}_3 = \dot{E}_3 / \dot{E}_2 \times \dot{C}_2 \tag{C}$$

The solution of Equations (A), (B), and (C) determines the three unknown exergy cost rates. The application of the exergoeconomic method for this simple case is rather

straightforward, but the accuracy of the results depends on the model's estimation of the turbine's power ($\dot{W}_e$) and rate of exergy destruction in the turbine ($\dot{E}_{D,t}$).

2.3.2. Excel implementation and validation of the model

Figure 2.4 shows the Excel sheet developed for the cogeneration system. The left side of the sheet stores the given data, the middle part performs the thermodynamic calculations, and the part on the right side deals with the exergoeconomic calculations. The formula bar reveals the formula that calculates the cost rate $\dot{C}_2$ based on Equation (A). By using Thermax functions for the properties of water to determine the enthalpy and entropy values h_2, s_2, h_3, and s_3, the sheet calculates the power produced "We" from Equation (2.6) and the rate of exergy destruction in the turbine "ED_t" from Equation (2.7). The values of the four cost rates $\dot{C}_F$, $\dot{C}_2$, $\dot{C}_3$ and $\dot{C}_w$ are determined by direct substitution in Equations (2.10), (A), (B, and (C). The unit costs are then obtained by dividing the product cost rate with corresponding exergy flow rate ($/GJ) or mass flow rate ($/kg).

C_2 | =C_F+Z_b

	A	B	C	D	E	F	G	H	I	J	K
1	Data			Thermodynamic calculations			Exergoeconomic calculations				
2	P_2	50	bar	h_2	3359.452		Z_t	0.036	$/s		
3	T_2	466	oC	s_2	6.900563						
4							C_2	0.7		20	
5	P_3	1	bar	s_3s	6.900563		C_3	0.271123		1.037	$/kg
6	η_t	0.8		h_3s	2504.146		C_F	0.4		4	
7							C_e	0.464663		25.969	$/GJ
8	mw	26.15	kg/s	h_3	2675.207	oC					
9				s_3	7.356						
10	E_F	100	MW	T_3	99.73485	oC					
11	Ef_2	35	MW								
12				Ef_3	13.55615						
13	Z_b	0.3	$/s								
14				We	17.89299	MW					
15	T0	298.15	K								
16	P0	1.013	bar	ED_t	3.550867						
17											

Figure 2.4. The Excel sheet for thermodynamic and exergoeconomic analyses of the simple cogeneration system

Figures 2.5 to 2.9 compare the results obtained by the present model at values of the back pressure between 40 bar to 1 bar with those given by Bejan et al. [2]. Figure 2.5 that shows the model's estimations (Model) for T_3 shows that the temperature agrees well with the reference data (Ref [2]) at high values of the pressure, but the model's estimations slightly deviate from the reference values as the back pressure decreases. Figure 2.4 shows that the present model estimated the steam at the back pressure of 1 bar to leave at 99.7°C, which is slightly superheated, whereas Ref. [2] estimated it to leave at 99.61°C; which is the saturation temperature at 1 bar.

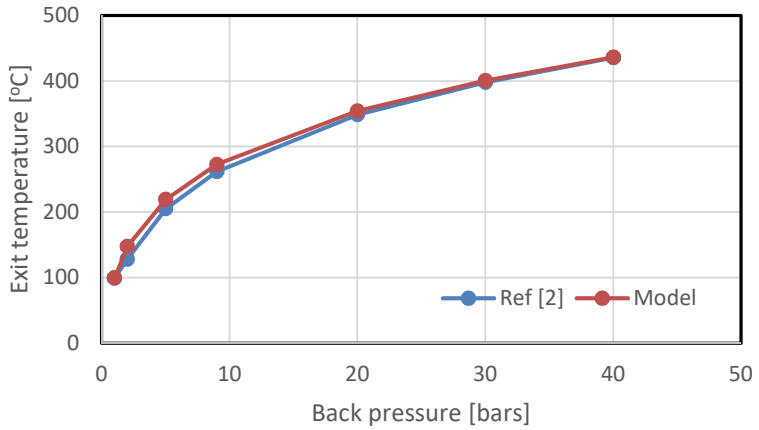

Figure 2.5. Variation of the LP steam exit temperature (T_3) with the back pressure

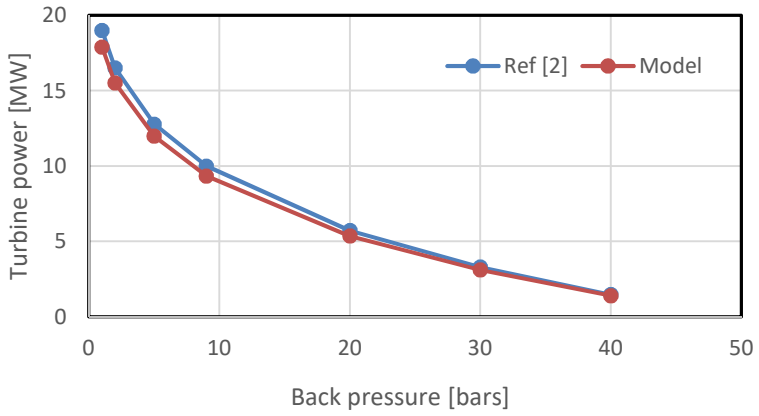

Figure 2.6. Variation of the turbine power with the back pressure, P_3

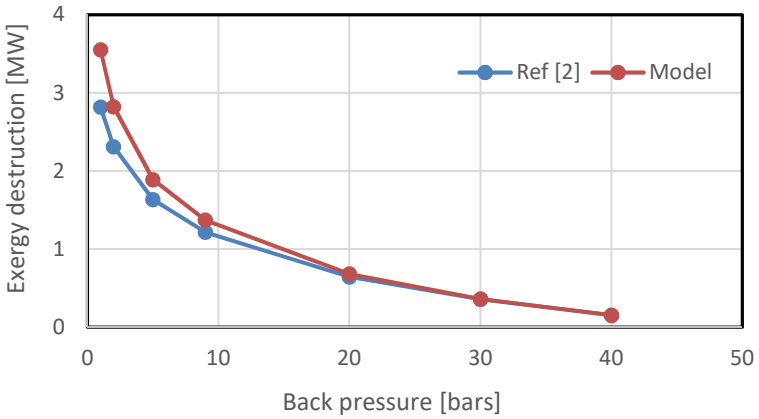

Figure 2.7. Variation of the rate of exergy destruction in the turbine with P_3

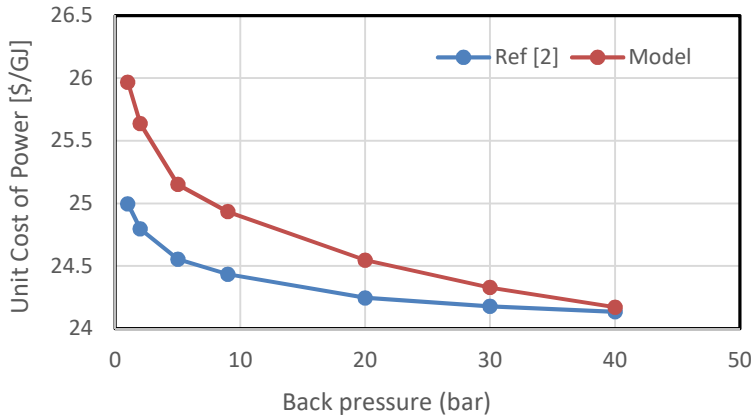

Figure 2.8. Variation of the unit exergy cost of the power produced with P_3

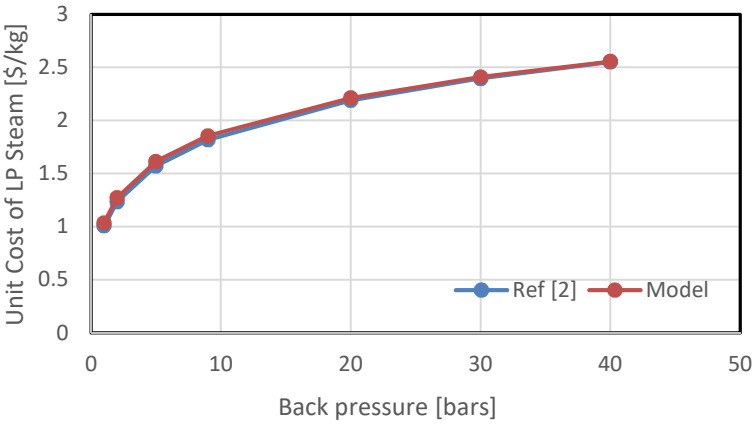

Figure 2.9. Variation of the unit exergy cost of low-pressure steam with P_3

Figures 2.6 and 2.7 show that both the turbine's power and rate of exergy destruction decrease as the back pressures is increased. Comparing the model's estimations to those of Ref. [2], the two figures also show close agreements with the corresponding reference values at high values of P_3, but the accuracy deteriorates as the back pressure decreases specially for the rate of exergy destruction. Figures 2.8 and 2.9 show the variation of the unit exergy cost of the power produced and that of the low-pressure steam with the back pressure. While unit exergy cost of the power produced decreases by increasing the back pressure, that of the steam increases. Compared to the values given by Ref. [2], the cost of steam is predicted well by the present model for all values of the back pressure, but the model considerably overestimates the cost of power at the low pack-pressure values because of its overestimation of the turbine's rate of exergy destruction.

To improve the model's accuracy, a user-defined function was written with VBA that divides the expansion process in the steam turbine into five consecutive stages instead of

a single stage. The VBA function, which is listed in Appendix B, is called "Expansion" and can be used to return the value of either T_3, h_3, s_3, or x_3. Figure 2.10 shows the modified sheet that uses the UDF with the back pressure specified as 1 bar and the formula bar in the figure reveals the formula in cell **E5** that calls the function to determine the value of the temperature T_3.

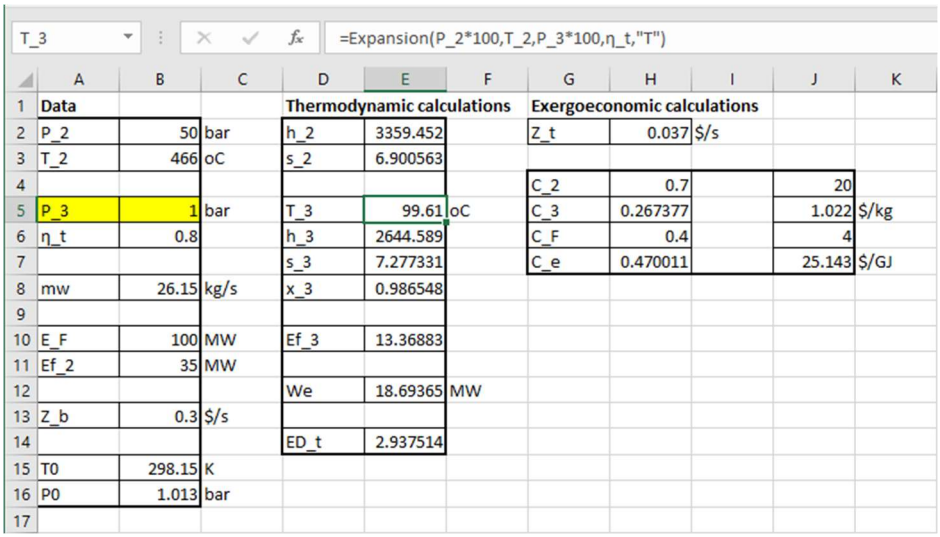

T_3 =Expansion(P_2*100,T_2,P_3*100,η_t,"T")

	A	B	C	D	E	F	G	H	I	J	K
1	**Data**			**Thermodynamic calculations**			**Exergoeconomic calculations**				
2	P_2	50	bar	h_2	3359.452		Z_t	0.037	$/s		
3	T_2	466	oC	s_2	6.900563						
4							C_2	0.7		20	
5	P_3	1	bar	T_3	99.61	oC	C_3	0.267377		1.022	$/kg
6	η_t	0.8		h_3	2644.589		C_F	0.4		4	
7				s_3	7.277331		C_e	0.470011		25.143	$/GJ
8	mw	26.15	kg/s	x_3	0.986548						
9											
10	E_F	100	MW	Ef_3	13.36883						
11	Ef_2	35	MW								
12				We	18.69365	MW					
13	Z_b	0.3	$/s								
14				ED_t	2.937514						
15	T0	298.15	K								
16	P0	1.013	bar								
17											

Figure 2.10. The improved Excel sheet of the simple cogeneration system

As the formula bar in Figure 2.10 shows, the VBA function requires five input parameters, which are the values of the inlet pressure P_2 in kPa, the inlet temperature T_2 in ^{o}C, the back pressure P_3 in kPa, the isentropic efficiency of the turbine η_t as a fraction, and a string variable that indicates the required property, i.e., "T" for T_3, "h" for h_3, "s" for s_3, or "x" for x_3. As Figure 2.10 shows, the model now estimates the steam at the back pressure of 1 bar to leave at 99.61^{o}C, which is the saturation temperature at 1 bar. Figures 2.11 and 2.12 compare the estimations of the modified model (Model2) with those of the original model (Model1) and those of Bejan et al. (Ref [2]) for the rate of exergy destruction in the turbine and the unit exergy cost of the power produced, respectively. The figures show that the UDF has considerably improved the model's estimation of the two parameters. Therefore, it is reasonable to assume that the model's accuracy can be improved further by dividing the expansion process into more than five stages, but the task of making the required modification to the UDF is left as an exercise (Exercise 2.1).

The simplified case considered in this section allowed the basic calculations of the SPECO method to be performed with Excel by avoiding the complexities of the system and the analytical model. However, the method is usually applied to systems with numerous elements while determining the exergy values as well. The following section presents a more realistic application of the method by adding an air-preheater to the simple cogeneration system.

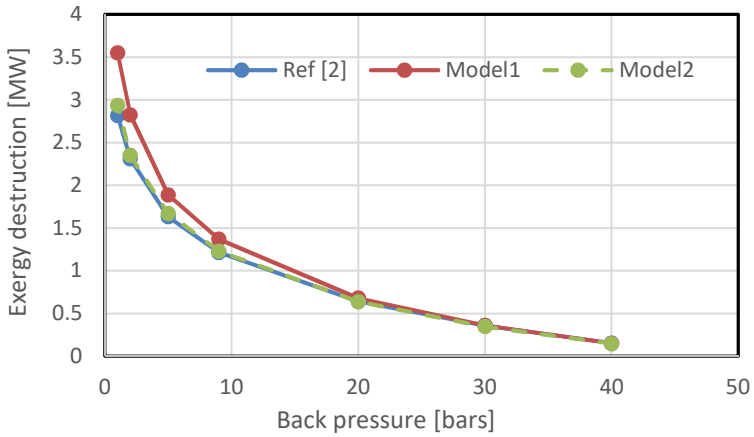

Figure 2.11. Variation of the rate of exergy destruction in the turbine with P_3

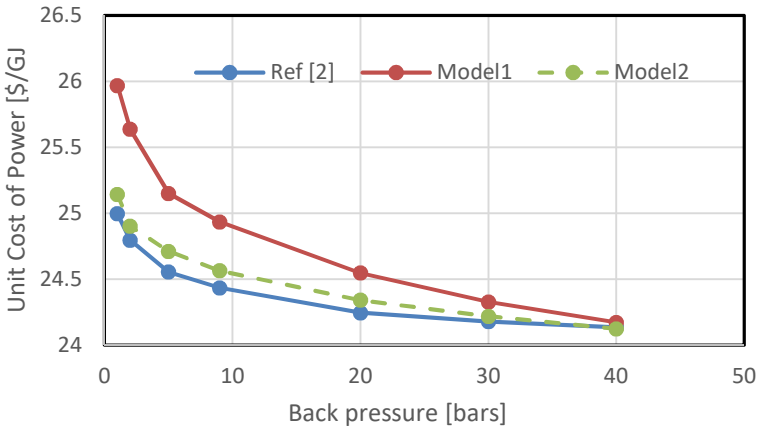

Figure 2.12. Variation of the unit exergy cost of the power produced with P_3

2.4. Exergoeconomic analysis of a cogeneration system with an air preheater

Figure 2.13 shows a co-generation system that adds an air-preheater to the simple system considered in the previous section. As for the simple system, the feed water enters the boiler at 52 bars and 25°C to be heated to 50 bars and 466.1°C and the mass flow rate of the steam is 26.151 kg/s. The air at the atmospheric condition enters the preheater before going to the boiler that burns coal. The mass flow rate of air is 60,000 kg/s. The polytropic efficiency of the turbine, η_t, is 80%, the effectiveness of the air preheater, ε, is 75%, the combustion efficiency, η_{cc}, is 94%, and pressure losses in the two sides of the air preheater are 4% of the corresponding inlet pressure. The cost rate of purchasing the boiler ($\dot{Z}_b$) is \$0.3/s and that of the turbine ($\dot{Z}_t$) is given by Equation (2.4). Based on typical costs of cogeneration systems [2], the cost rate of the air preheater is taken as \$0.004/s. Table 2.1 gives additional data needed for analysing the system. Note that T_7 is specified at 765K, which is higher than the temperature of the superheated steam by 25K.

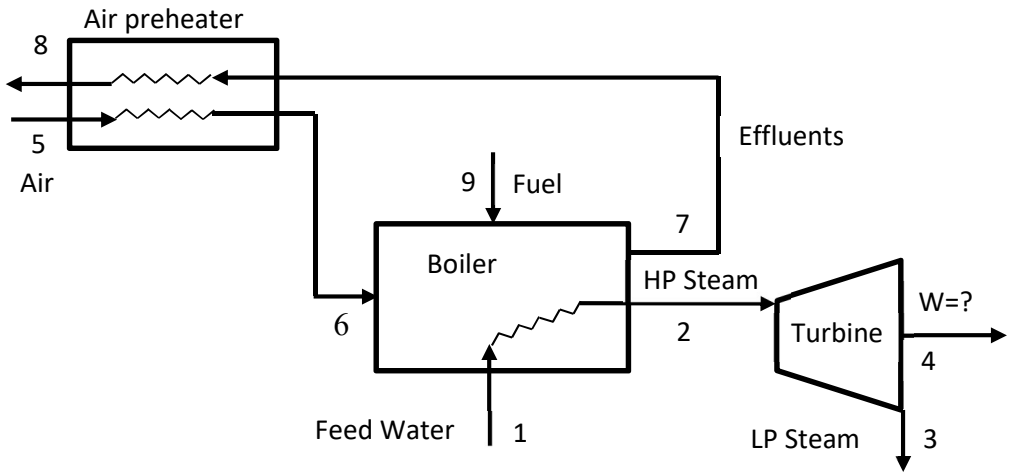

Figure 2.13. Schematic of the co-generation system with an air preheater

Table 2.1. The physical data of the improved cogeneration system

Parameter	Value
T_5 [K]	298.15
P_5 [bar]	1.15
T_7 [K]	765
Cost of coal (c_F) [$/GJ]	4.0
LHV of coal (graphite) [kJ/kg]	32,770
Exergy of coal (graphite) [kJ/kmol]	404,589

It is required to determine the power produced by the system at a back pressure of 9 bars and the corresponding unit exergy costs for the power and the steam and to determine which of the three system components deserves further investment so as to improve its performance and minimise the products' costs.

2.4.1. The analytical model

In general, the analysis follows the procedure described in the previous section, but the rate of exergy input, exergy of the effluents, and the rates of exergy destruction in the boiler and the air preheater are not predetermined but calculated by the model itself. The basic assumptions in the model's formulation are:

1. The system operates at steady state.
2. The kinetic and potential energy effects are negligible.
3. The feedwater and air enter the system with negligible exergy costs, i.e., $c_1 = c_5 = 0$.
4. The environment is at $T_0 = 298$ K and $P_0 = 101.3$ kPa

As for the simple cogeneration system, the enthalpy at state 3 is determined from:

$$h_3 = h_2 - (h_2 - h_{3s}) \times \eta_t \tag{2.17}$$

Where h_{3s} is the enthalpy after an isentropic process to the back pressure and η_t is the isentropic efficiency of the turbine. The temperature at state 6 is determined as follows:

$$T_6 = T_5 + \varepsilon(T_7 - T_5) \tag{2.18}$$

The enthalpy at state 8 is determined from the following energy balance:

$$h_8 = h_7 - \dot{m}_a(h_6 - h_5)/(\dot{m}_a + \dot{m}_f) \tag{2.19}$$

Where $\dot{m}_a$ and $\dot{m}_f$ are the mass flow rates of the air and the fuel, respectively.

The power of the turbine, in MW, is then calculated from:

$$\dot{W} = \dot{m}_s(h_2 - h_3)/1000 \tag{2.20}$$

Where $\dot{m}_s$ is the mass flow rate of the steam.

The heat input, in MW, and the rate of fuel consumption, in kg/s, are calculated from:

$$\dot{Q}_{in} = [\dot{m}_s(h_2 - h_1) + \dot{m}_a(h_7 - h_6)]/1000 \tag{2.21.a}$$

$$\dot{m}_f = \dot{Q}_{in} \times 1000/LHV/\eta_{cc} \tag{2.21.b}$$

Where *LHV* is the lower heating value of the fuel (which is treated as pure graphite) and η_{cc} is the combustion efficiency. Note that the mass flow rate the combustion products has been ignored in Equation (2.21.a) so as to simplify the model.

The rates of exergy destruction in the boiler ($\dot{E}_{D,b}$), the turbine ($\dot{E}_{D,t}$), and the air preheater ($\dot{E}_{D,aph}$) are determined from:

$$\dot{E}_{D,b} = \dot{E}_1 + \dot{E}_6 + \dot{E}_9 - \dot{E}_2 - \dot{E}_7 \tag{2.22.a}$$

$$\dot{E}_{D,t} = \dot{E}_2 - \dot{E}_3 - \dot{E}_4 \tag{2.22.b}$$

$$\dot{E}_{D,aph} = \dot{E}_5 + \dot{E}_7 - \dot{E}_6 - \dot{E}_8 \tag{2.22.c}$$

The cost rate balance equations for the cogeneration system are as follows:

Boiler:

$$\dot{C}_1 + \dot{C}_6 + \dot{C}_9 + \dot{Z}_b = \dot{C}_2 + \dot{C}_7 \tag{2.23}$$

Turbine:

$$\dot{C}_2 + \dot{Z}_t = \dot{C}_3 + \dot{C}_4 \tag{2.24}$$

Air preheater:

$$\dot{C}_5 + \dot{C}_7 + \dot{Z}_{aph} = \dot{C}_6 + \dot{C}_8 \tag{2.25}$$

The above three equations can be rearranged as follows:

$$\dot{C}_2 = \dot{C}_1 + \dot{C}_6 + \dot{C}_9 + \dot{Z}_b - \dot{C}_7 \tag{E}$$

$$\dot{C}_3 = \dot{C}_2 + \dot{Z}_t - \dot{C}_4 \tag{F}$$

$$\dot{C}_7 = \dot{C}_5 + \dot{Z}_{aph} - \dot{C}_6 - \dot{C}_8 \tag{G}$$

Since the cost of coal (c_F) is known and the costs of the feed water and inlet air are assumed to be negligible ($c_1 = c_5 = 0$), the relevant cost rates of the exergy streams at states 9, 1, and 5 are calculated or specified as follows:

$$\dot{C}_9 = c_F \times \dot{E}_9 \tag{H}$$

$$\dot{C}_1 = 0 \tag{I}$$

$$\dot{C}_5 = 0 \tag{J}$$

Three auxiliary equations are needed which are obtained by applying the rules, $c_4 = c_2$, $c_7 = c_6$, and $c_8 = c_7$. These yield the following equations:

$$\dot{C}_4 = \left(\dot{E}_4 / \dot{E}_2\right)\dot{C}_2 \tag{K}$$

$$\dot{C}_6 = \left(\dot{E}_6 / \dot{E}_7\right)\dot{C}_7 \tag{L}$$

$$\dot{C}_8 = \left(\dot{E}_8 / \dot{E}_7\right)\dot{C}_7 \qquad \text{(M)}$$

2.4.2. Excel implementation and exergoeconomic analysis

The Excel-aided model of this cogeneration system has been developed as a workbook that consists of three sheets. Figure 2.14 shows the first sheet of the model that calculates the temperatures T_2, T_6, and T_8 and enthalpy values of the different streams by using Thermax property functions for air and water. The data part on the left side of the sheet stores the values of the specified pressures and temperatures, the mass flow rate of the air (ma) and that of the feed water (mw), and the turbine's isentropic efficiency (η_t). Other specified data (ε, η_{cc}, LHV, E_{fuel}) are stored in column E. The sheet calculates the heat input (Qin), rate of fuel consumption (mf), and power produced (W). As the figure shows, for the specified value of the back pressure (P_3) of 9 bars the power produced by the system is 9.592 MW, which is 2.7% more than the 9.34 MW produced by the simple system at the same back pressure. The bottom three cells of column K determine the rates of exergy destruction in the three system components.

T_3 =Expansion(50*100,466.1,P_3*100,0.8,"T")

	A	B	C	D	E	F	G	H	I	J	K	L
1												
2	T_1	25	oC	T_5	298.15	K	P_3	9	bar			
3	P_1	52	bar	P_5	1.15	bar						
4	T_2	466.1	oC	P_6	1.104	bar	h_1	104.830		Qin	92.66052	MW
5	P_2	50	bar	T_7	765	K	h_2	3359.679				
6				P_7	1.060	bar				mf	3.0081	kg/s
7	ma	60.000	kg/s	P_8	1.013	bar	T_3	268.6319	oC	AFR	19.9462	
8							h_3	2992.896				
9	mw	26.151	kg/s	ε	0.75		s_3	7.058677		W	9.592	MW
10				η_cc	0.94					ε	0.322762	
11	η_t	0.8					h_5	297.9887				
12				Fuel_LHV	32770	kJ/kg				Ed_t	1.2304	MW
13				Fuel_Exg	404589	kJ/kmol	T_6	648.2875		ED_b	62.8877	MW
14							h_6	659.7093		ED_aph	3.4370	MW
15							h_7	785.4253				
16							h_8	440.9738				
17							T_8	439.0753				
18												

Figure 2.14. The first sheet of the model for the co-generation system

The second sheet of the model shown on Figure 2.15 calculates the exergy of the nine streams and their cost rates. The data part of this sheet shows the equipment cost rates of the three components of the system (Z_b, Z_aph, and Z_t) and the values of the dead-state reference temperature (T0) and pressure (P0). The sheet calculates the physical and chemical exergy values of the various streams and the corresponding exergy flow rates in MW. Note that the exergy of the effluents has been reduced by the air preheater from 12.38 MW at state 7 to 1.57 MW at state 8. The sheet solves the cost rate equations (E) to (M) to determine the unknown cost rates by using the iterative solution option of Excel.

This option makes it unnecessary to assemble the equations in a matrix form. The formula bar shows the equation for $\dot{C}_7$, which is Equation (G).

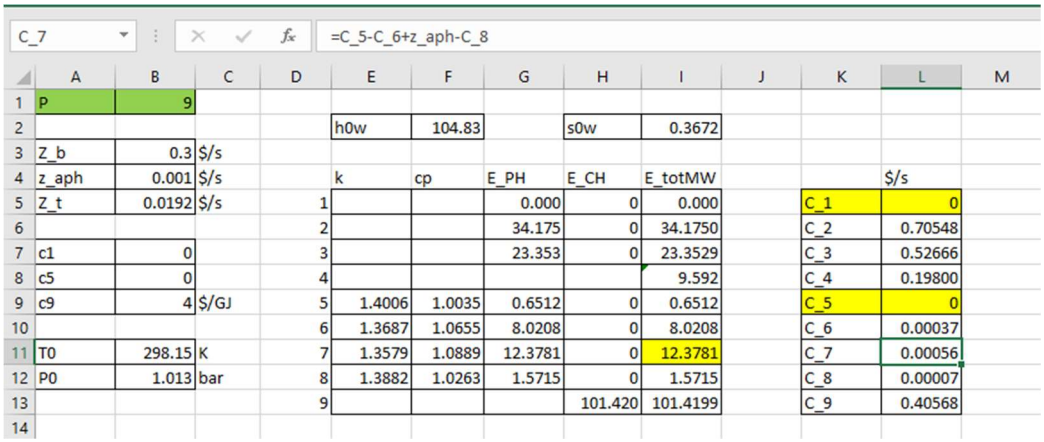

C_7 | =C_5-C_6+z_aph-C_8

	A	B	C	D	E	F	G	H	I	J	K	L	M
1	P	9											
2					h0w	104.83		s0w	0.3672				
3	Z_b	0.3	$/s										
4	z_aph	0.001	$/s		k	cp	E_PH	E_CH	E_totMW			$/s	
5	Z_t	0.0192	$/s	1			0.000	0	0.000		C_1	0	
6				2			34.175	0	34.1750		C_2	0.70548	
7	c1	0		3			23.353	0	23.3529		C_3	0.52666	
8	c5	0		4					9.592		C_4	0.19800	
9	c9	4	$/GJ	5	1.4006	1.0035	0.6512	0	0.6512		C_5	0	
10				6	1.3687	1.0655	8.0208	0	8.0208		C_6	0.00037	
11	T0	298.15	K	7	1.3579	1.0889	12.3781	0	12.3781		C_7	0.00056	
12	P0	1.013	bar	8	1.3882	1.0263	1.5715	0	1.5715		C_8	0.00007	
13				9				101.420	101.4199		C_9	0.40568	
14													

Figure 2.15. The second sheet of the model for the cogeneration system

The third sheet of the model shown on Figure 2.16 copies from Sheet 2 the values of the flow rates of exergy at the nine streams and the corresponding cost rates to calculate the values of their unit exergy costs which are then used to determine the product unit cost (c_P), the fuel cost (c_F), and the cost rate of exergy destruction ($\dot{C}_D$) for the three system components. The formula bar shows the calculation of c_F for the boiler. The sheet also copies from Sheet 2 the cost rates $\dot{Z}$ of the system components in its column K to calculate the values of the summation $\dot{C}_D + \dot{Z}$ and the exergoeconomic factor f.

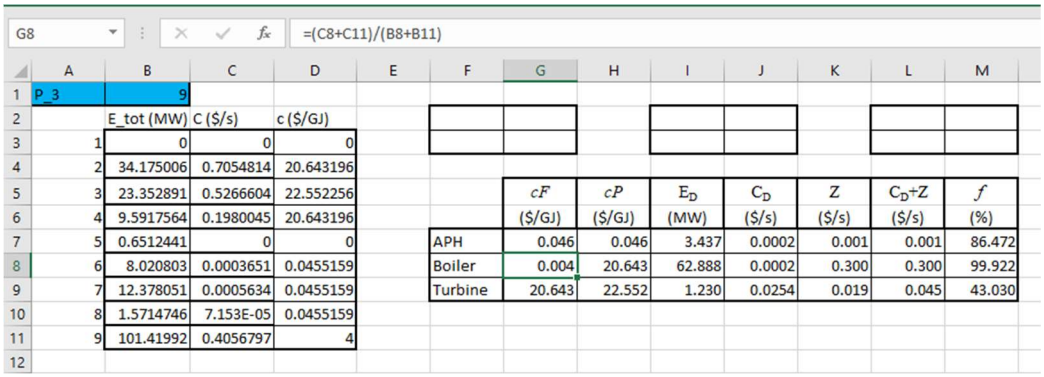

G8 | =(C8+C11)/(B8+B11)

	A	B	C	D	E	F	G	H	I	J	K	L	M
1	P_3	9											
2		E_tot (MW)	C ($/s)	c ($/GJ)									
3	1	0	0	0									
4	2	34.175006	0.7054814	20.643196									
5	3	23.352891	0.5266604	22.552256			cF	cP	E_D	C_D	Z	C_D+Z	f
6	4	9.5917564	0.1980045	20.643196			($/GJ)	($/GJ)	(MW)	($/s)	($/s)	($/s)	(%)
7	5	0.6512441	0	0		APH	0.046	0.046	3.437	0.0002	0.001	0.001	86.472
8	6	8.020803	0.0003651	0.0455159		Boiler	0.004	20.643	62.888	0.0002	0.300	0.300	99.922
9	7	12.378051	0.0005634	0.0455159		Turbine	20.643	22.552	1.230	0.0254	0.019	0.045	43.030
10	8	1.5714746	7.153E-05	0.0455159									
11	9	101.41992	0.4056797	4									
12													

Figure 2.16. Sheet 3 of the model for the cogeneration system

The exergoeconomic evaluation of the system is based on the values of the exergoeconomic factors obtained for its three components. From exergoeconomic consideration, the most important component is the one that has the highest value of the

variable $\dot{C}_D + \dot{Z}$. Table 2.2 ranks the three components of the cogeneration system according to their $\dot{C}_D + \dot{Z}$ values. Having a high value of $\dot{C}_D + \dot{Z}$, but a low value of f by a component means that the greater part of the product cost in the component is due to exergy destruction and loss. The table figures show that the boiler has the highest value of $\dot{C}_D + \dot{Z}$, but its exergetic factor is also the highest. The component with the lowest f is the turbine (typical values of f for turbines are up to 75% [2]). Although the highest rate of exergy destruction occurs in the boiler, it is the turbine that deserves more investment to improve its performance according to its value of f. Note that the value of f for the air preheater, which is 86.47%, is higher than usual (typical f values for air preheaters are less than 55%) and, therefore, the investment in this component can be reduced. However, this is unlikely to make a significant impact because of the low cost of the air preheater compared to the turbine and the boiler.

Table 2.2. Exergoeconomic performance of the cogeneration system components

	$\dot{C}_D$ ($/s)	$\dot{Z}$ ($/s)	$\dot{C}_D + \dot{Z}$ ($/s)	f (%)	*Typical f* (%) [2]
Boiler	0.0002	0.300	0.300	99.92	
Turbine	0.0254	0.019	0.045	43.03	35-75
Air preheater	0.0002	0.001	0.001	86.47	<55

2.5. Exergoeconomic analysis of more complex systems

The simplified cases considered in the two previous sections were intended to explain the methodology of exergoeconomic analysis and its application with Excel. Obviously, the method is more useful when the analysed system is more complex and includes more components. Figure 2.17 shows a schematic diagram of a combined cycle power plan (CCPP) that consists of a simple Brayton cycle and a simple Rankine cycle. Baghernejad and Anvari-Moghaddam [30] conducted exergoeconomic and environmental analyses of this system and two modified configurations of the CCPP. Table 2.3 shows their results for this system which they called Configuration 1. The table lists the system components in the order of their $\dot{C}_D + \dot{Z}$ values since the most important component from exergoeconomic consideration is the one that has the highest value of this variable. As can be seen from this table, the highest value of $\dot{C}_D + \dot{Z}$ belongs to the combustion chamber followed by the steam generator and steam turbine. The table shows that the combustion chamber also has the lowest exergoeconomic factor which means that its exergy destruction cost prevails over its initial cost. These results indicate that the combustion chamber is the component that deserves greater attention since improving its performance will improve that of the whole system. It is quite possible to enhance the performance of the combustion chamber by more investment and by adopting a more effective design. According to Baghsheikhi et al. [31], the factors that greatly affect the combustion process are the excess air ratio and the incoming air temperature. Reduction

of the air–fuel ratio and the use of preheated air improve the efficiency of the combustion process. More sophisticated methods, such as premixed combustion or staged combustion can also be used to reduce the thermodynamic irreversibilities in the process. It is also possible to optimise the thermal insulation so as to minimise heat losses, which subsequently minimises entropy generation and increases the overall efficiency. The table shows that the total exergoeconomic factors for the whole systems is only 7.53% which indicates that the total exergy destruction cost rate has a significantly higher share than the initial equipment cost rate. Therefore, the use of system components with higher initial cost that can improve the system's performance is justifiable since.

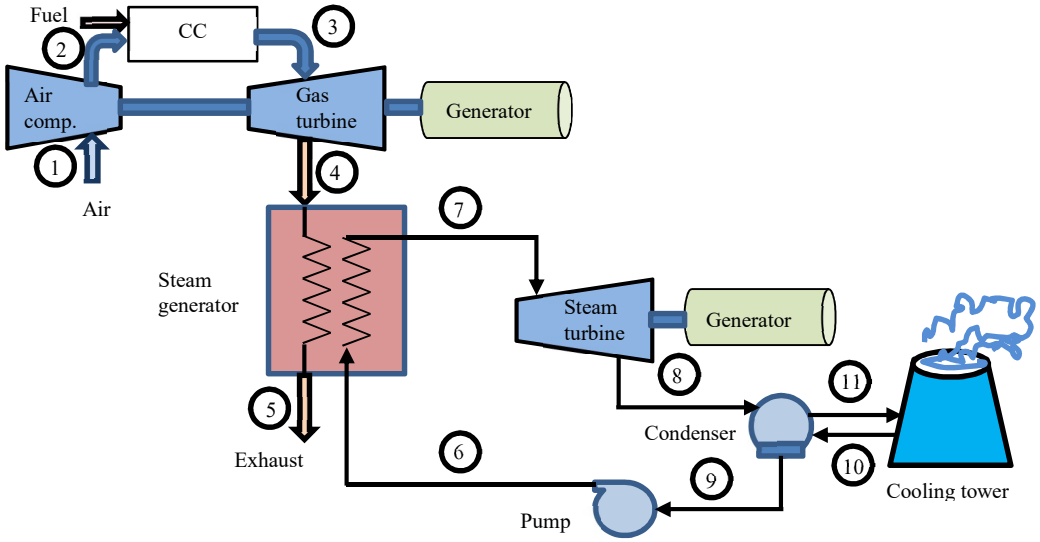

Figure 2.17. Schematic diagram of the simple CCPP (adopted from [30])

Table 2.3. Exergoeconomic analysis of the simple CCPP (Configuration 1) [30]

	$\dot{C}_D$ ($/h)	$\dot{Z}$ ($/h)	$\dot{C}_D + \dot{Z}$ ($/h)	f (%)
Combustion chamber	11,758	27.69	11,785.69	0.23
Steam generator	2174	240	2,414.00	9.94
Steam turbine	1641	340.6	1,981.60	17.19
Gas turbine	1175	275.3	1,450.30	18.98
Compressor	830.8	500.2	1,331.00	37.58
Condenser	916.5	121	1,037.50	11.66
Pump	18.52	4.38	22.90	19.15
Total system	18,513.82	1509.17	20,022.99	7.53

2.6. Advanced exergoeconomics and exergoenvironmental methods

The application of the exergoeconomic method for analysing and optimising various energy systems has revealed its strength and limitations and sparked the development of advanced exergoeconomic analyses methods and exergoenvironmental analyses methods. In what follows, brief overviews of these two methods are given.

2.6.1. Advanced exergoeconomics

One of the limitations of the conventional exergoeconomic method described above is that it do not reecognise that part of the exergy destruction in an energy-conversion system can be avoided by enhancement efforts, but part of it is unavoidable due to technological and economical limitations. The method also does not account for the interactions between the components toward contributing to the ineffciencies of thermal systems. Due to these limitations, the results of the conventional exergoeconomic analysis methods cannot reveal the real potential for improving effciency of the system components and can even be misleading [21,32-36]. Advanced exerogoeconomic methods address these limitations by splitting the exergy destruction in a component of a thermal system into avoidable and unavoidable and endogenous and exogenous-exergy portions. The avoidable and unavoidable portions can be combined with the endogenous and exogenous portions for further splitting as follows:

(a) avoidable endogenous-exergy destruction,
(b) unavoidable endogenous-exergy destruction,
(c) avoidable exogenous-exergy destruction and
(d) unavoidable exogenous-exergy destruction.

With the above categorisation of energy-destructions, advanced exergy and exergo-economic analyses have the ability of establishing interdependencies among the components of thermal systems and uncovering the real potential of improvement which is essential when a complex thermal system with many components is being analysed [33]. According to Zhao [23] and Fellah [34,35], the concept of the endogenous/ exogenous exergy destruction increases our understanding of the interaction between system components, and makes the optimisation strategy of the overall system, which may be misled by mutually affected components, more convenient. Therefore, the concept can help engineers to decide whether an alteration should be made to a particular component or to the other components of the system. Chapter 6 shows how the Excel-based modelling platform can be used for conducting the advanced exergoeconomic analysis method by considering the simple gas turbine.

2.6.2. Exergoenvironmental analyses

In addition to the depletion of energy other scarce natural resources, energy-related activities cause degradation of the environment. In order to take these effects into consideration, the scope of exergoeconomics had to broaden by the development of exergo-environmental analysis methods [37-40]. This subsection outlines two types of these methods, which are the conventional exergoenvironmental analysis method and the emergy-based exergoecono-environmental analysis method.

Conventional exergo-environmental analysis

This method combines exergy analyses with Life Cycle analysis (LCA) for evaluating the environmental impact of component's lifecycle on pollutant formation. The method defines the highest environmental impact caused by component inefficiencies and

lifetime pollutants and assesses the possible improvements of process's environmental impacts [41]. The structure of the method is analogous to that of the conventional exergoeconomic analysis as shown on Figure 2.18.

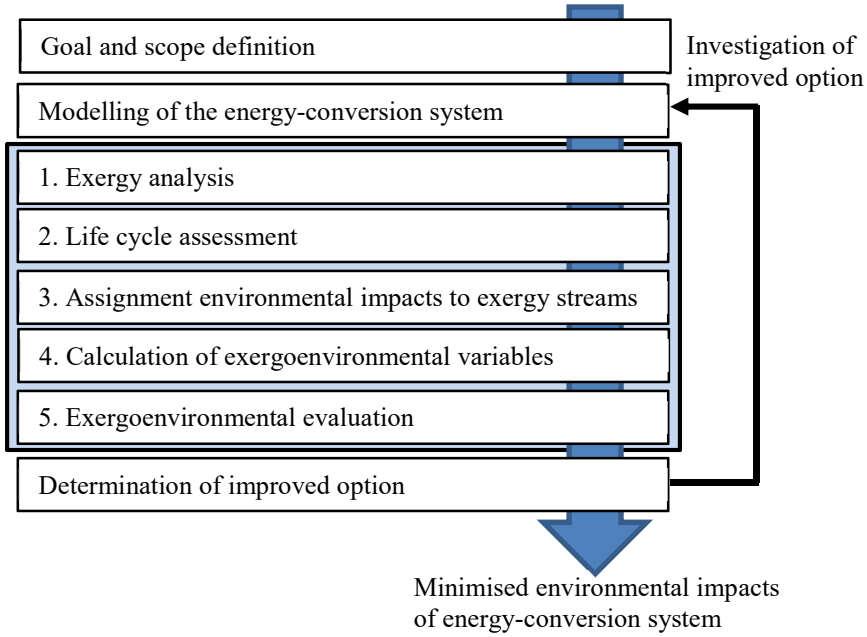

Figure 2.18. Structure of the exergoenvironmental analysis (adopted from [42])

The method consists of the following five main steps:

- After defining the goal and scope and modelling the energy conversion process starts the first major step which is the exergy analysis that determines all material and energy streams connecting the components and crossing the system boundaries as inputs and outputs.
- In the second step the environmental impact rate $\dot{B}_j$ of each material and fuel stream is determined by applying the method of life cycle assessment.
- In the third step the analysis assigns the results of the LCA to the corresponding exergy streams by relating the environmental impact rate $\dot{B}_j$ of each material and energy stream to its exergy content $\dot{E}_j$. The result is the specific environmental impact b_j (expressed in Eco-indicator points per exergy unit).
- On the basis of the exergy and environmental impact rates and the specific environmental impacts of every exergy stream in the process, the exergoenvironmental variables can be calculated for every process component. The variables are developed in analogy to the exergoeconomic variables defined in [2].
- Exergoenvironmental evaluation.

Emergy-based exergo-econoenvironmental analysis

Exergoeconomic and exergoenvironmental analyses sometimes lead to different dimensions/scales and different conclusions. In order to harmonise the dimensions/scales of these analyses, Aghbashlo and Rosen [43] suggested to translate the monetary terms of exergoeconomic analysis and environmental impact scores of exergoenvironmental analysis into emergy values. Emergy refers to the amount of available energy required, either directly or indirectly, to generate a given output flow or storage of energy or service, expressed as solar equivalent joules (sej) [42]. Aghbashlo and Rosen [20] also suggested expressing all energetic and non-energetic process inputs in terms of sej. Aghbashlo and Rosen [43] then introduced a new methodology based on the emergy concept according to which a new parameter called exergetic ecological emergy/financial emergy ratio is determined and used for deriving emergy-based exergo-econoenvironmental balances for an energy system by combining it with exergy cost concepts. The methodology is applied in four main steps:

- First, the energy system is formulated and analysed using the exergy method.
- Second, exergy cost theory is applied to determine unit exergy costs of all streams and unit exergy production costs of all components.
- Third, the exergetic ecological emergy/financial emergy ratio of all components and exogenous exergy streams are computed using data available in the literature.
- In the fourth step, the exergetic ecological emergy/financial emergy ratios of all streams are calculated using the SPECO approach [2,27].

Nourpour et al. [44] investigated an integrated solar combined cycle system (ISCCS) by applying conventional and advanced analysis of the system using exergy, exergo-economic, and exergoenvironmental analysis. Table 2.4, which is extracted from their data, shows the first and second components to be given priority of improvement based on each method of analysis. Among the six methods, the table shows that only the three advanced exergy-based analyses gave the priority to the same components and in the same order. Another interesting remark is that the first-priority component according to these methods is not the combustion chamber, as suggested by conventional exergetic and exergoenvironmental methods [2,28,30], but the low-pressure economiser.

Table 2.4. Outcomes of the eight analyses conducted by Nourpour et al. [44]

	First priority	Second priority
Exergetic analysis	CC	SF
Exergoeconomic analysis	SF	ST
Exergoenvironmental analysis	CC	ST
Advanced exergetic analysis	LPECO	SEVA
Advanced exergoeconomic analysis	LPECO	SEVA
Advanced Exergoenvironmental analysis	LPECO	SEVA

Abbreviation: CC: Combustion Chamber, LPECO: Low Pressure Economiser, SEVA: Solar Evaporator, SF: Solar Field, ST: steam turbine

2.7. Closure

This chapter introduces the exergoeconomic analysis method by focussing on the SPECO method that adopts the accounting approach to formulate a set of cost-rate equations associated with the exergy streams entering and exiting the components of a thermal system based on which a number of exergoeconomic variables can be formulated and used to analyse the cost formulation process in each component. The chapter illustrates the use of the Excel-based platform for conducting the SPECO method by considering two simplified cogeneration systems that highlight the basic concepts related to the method, but also shows how the method could be used to deal with a more complex system, which is a combined-cycle power plant, that involves a compressor and a condenser in addition to the turbine, combustion chamber, and heat-exchanger. Finally, the chapter gives brief accounts of the more advanced exergoeconomics and exergo-environmental methods.

It should be mentioned that the application of the SPECO method may involve a number of other considerations that have not been addressed adequately here such as the costing of exergy loss streams, treatment of dissipative elements, effect of aggregation level in applying exergy costing, and others. Some of these issues are considered in the following chapters, but more information is given in [1,2]. With respect to the tools provided by Excel for performing the exergoeconomic analysis method, the chapter illustrates the use of its iterative solution option for solving the algebraic system of equations generated by the method and the use of VBA to develop an additional user-defined function needed to improve the accuracy of the thermodynamic model.

References

[1] G. Tsatsaronis. Thermoeconomic analysis and optimization of energy systems. Prog Energy Combust Sci 1993;19:227-57.

[2] A. Bejan, G. Tsatsaronis, and M. Moran. Thermal Design and Optimization. New York: Wiley,. 1996.

[3] M.A. Rosen, A Concise Review of Exergy-Based Economic Methods, 3rd IASME/WSEAS Int. Conf. on Energy & Environment, University of Cambridge, UK, February 23-25, 2008

[4] C. Uysal, D. N. Ozen and H. Kurt, A comparative assessment of SPECO and MOPSA on costing of exergy destruction, Int. J. Exergy, Vol. 32, No. 1, 2020

[5] E. Sciubba, The Exergy Footprint and the resource cost of Externalities, Proceedings of ECOS 2023 - the 36th International Conference on Efficiency, Cost, Optimization, Simulation and Environmental Impact of Energy Systems 25-30 June, 2023, Las Palmas de Gran Canaria, Spain

[6] A. Picallo-Perez, J.M. Sala, L.D. Portillo and R. Vidal, Delving Into Thermoeconomics: A Brief Theoretical Comparison of Thermoeconomic Approaches for Simple Cooling Systems. Front. Sustain. (2021) 2:656818. doi: 10.3389/frsus.2021.656818

[7] R. G. dos Santos, M. Á. Lozano, L. M. Serra, A. B. Lourenço and J. J. C. S. Santos. Thermoeconomic Cost Allocation Approaches in a Simultaneous Heating and Cooling Heat Pump System, Proceedings of ECOS 2023 - the 36th International Conference on Efficiency, Cost, Optimization, Simulation and Environmental Impact of Energy Systems 25-30 June, 2023, Las Palmas de Gran Canaria, Spain

[8] J.H. Keenan. A Steam Chart for Second Law Analysis. Mechanical Engineering 1932, 54, 195–204.

[9] M. Tribus, R. Evans, A Contribution to the Theory of Thermoeconomics. University of California, Los Angeles (UCLA), Dept. of Engineering. Report 62-36, (1962) .

[10] N. Georgescu-Roegen. The Entropy Law and Economic Process. Cambridge: Harvard University Press, 1971.

[11] E. Bergmann, K.R. Schmidt. Zur kostenwirtschaflichten optimierung der wärmeaustauscher für die regenerative speisewaservorwärmung im dampfkraftwerkein störungsverfahren mit der exergie. Energie und Exergie Düsseldorf: VDI-Verlag; 1965. p. 63–89.

[12] J. Szargut. Grenzen für die anwendungsmöglichkeiten des Exergiebegriffs (Exergy for as system and for a flow process). Brenstof-Wärme-Kraft, 1967;19:309–13.

[13] E.F. Obert and R.A Gaggioli, Thermodynamics, McGraw-Hill, New York, (1963).

[14] R.B. Evans, and M. Tribus, Thermo-Economics of Saline Water Conversion, Industrial and Engineering Chemistry, Process Design and Development, 4 (2), (1965), 195-206.

[15] A. Valero, M.A. Lozano, L. Serra, G. Tsatsaronis, J. Pisa, C.A. Frangopoulos, M.R. von Spakovsky, CGAM Problem: Definition and Conventional Solution. Energy 1994, 19, 279–286, doi:10.1016/0360-5442(94)90112-0.

[16] S. Kim, S. Oh, Y. Kwon, H. Kwak, Exergoeconomic analysis of thermal system, Energy 23 (1998) 393–406.

[17] Y-H Kwon, H-Y Kwak, S-D Oh, Exergoeconomic analysis of gas turbine cogeneration systems, Exergy Int. J. 1(1) (2001) 31–40

[18] H. Kwak, D. Kim, J. Jeon, Exergetic and Thermoeconomic Analyses of Power Plants. Energy, 28 (2003), pp. 343-360.

[19] G. Tsatsaronis and M. H. Park, On avoidable and unavoidable exergy destructions and investment costs in thermal systems, Energy Convers. Manag., vol. 43, no. 9–12, pp. 1259–1270, 2002

[20] M. Aghbashlo and M.A. Rosen, Consolidating exergoeconomic and exergoenvironmental analyses using the emergy concept for better understanding energy conversion systems. J Clean Prod 2018; 172: 696–708. https://doi.org/10.1016/j.jclepro.2017.10.205

[21] A. Valero and C. T. Cuadra, Exergy, energy system analysis and optimization – Vol. II - Thermoeconomic Analysis, ©Encyclopedia of Life Support Systems (EOLSS)

[22] M. S. Muhammad, Exergoeconomic Analysis and Optimization of Combined Cycle Power Plants with Complex Configuration, Doctoral Dissertation, University of Belgrade, Faculty of Mechanical Engineering, 2015

[23] P. Zhao, A Computer Program for the Exergoeconomic Analysis of Energy Conversion Plants, Ph.D. Dissertation submitted to von der Fakultät III – Prozesswissenschaften der Technischen Universität Berlin zur Erlangung des akademischen Grades Doktor der Ingenieurwissenschaften -Dr.-Ing.-genehmigte Dissertation, 2015

[24] E. Sciubba, and G. Wall, A brief Commented History of Exergy From the Beginnings to 2004, International Journal of Thermodynamics, 2007, Vol. 10 (No. 1), pp. 1-26.

[25] A. Valero, A. Valero-Delgado, and C. Torres, The Future of Thermoeconomics after the School of Zaragoza, Proceedings of ECOS 2023 - the 36th international conference on efficiency, cost, optimization, simulation and environmental impact of energy systems, 25-30 June 2023, Las Palmas de Gran Canaria, Spain

[26] G. Tsatsaronis, M. Winhold, Exergoeconomic Analysis and Evaluation of Energy-Conversion Plants—I. A New General Methodology. Energy 1985, 10, 69–80, doi:10.1016/0360-5442(85)90020

[27] A. Lazzaretto and G. Tsatsaronis. SPECO: A systematic and general methodology for calculating efficiencies and costs in thermal systems. Energy, 31:1257–1289, 2006.

[28] F.A. Al-Sulaiman, Thermodynamic Modeling and Thermoeconomic Optimization of Integrated Trigeneration Plants Using Organic Rankine Cycles, A thesis presented to the University of Waterloo in fulfilment of the thesis requirement for the degree of Doctor of Philosophy in Mechanical Engineering, 2010.

[29] C. Ö. Çolpan, Exergy Analysis of Combined Cycle Cogeneration Systems. A thesis submitted in partial fulfillment of the requirements for the degree of Master of Science in Mechanical Engineering to the Graduate School of Natural and Applied Sciences of Middle East Technical University, May 2005.

[30] Baghernejad, A., Anvari-Moghaddam, A. Exergoeconomic and Environmental Analysis and Multi-Objective Optimization of a New Regenerative Gas Turbine Combined Cycle. Appl. Sci. 2021, 11, 11554. https://doi.org/10.3390/app112311554

[31] M. Baghsheikhi, P. Shafiei, M. Mohammadi, Energy, Exergy, and Exergoeconomic Analysis of a Combined Cycle Power Plant With Post-Combustion CO_2 Capture: A Case Study in Northern Iran, Energy Science & Engineering, 2025; 13:5075–5092

[32] S. Kelly, G. Tsatsaronis, T. Morosuk. Advanced exergetic analysis: Approaches for splitting the exergy destruction into endogenous and exogenous parts [J]. Energy, 2009, 34(3): 384-391.

[33] U. G. Azubuike, H. O. Njoku, O.V. Ekechukwu, Advanced Exergoeconomic Analysis of Thermal Systems: Concise Overview of Methodologies, Proceedings of the 2020 Sustainable Engineering and Industrial Technology Conference, Faculty of Engineering, University of Nigeria, Nsukka, 23rd to 26th March 2020

[34] G. Fellah, Avoidable And Unavoidable Exergy Destructions And The Associated Investment Cost For Evaluating The Performance of A Gas Turbine Cycle, J. Eng. Res. (University Tripoli), no. 32, pp. 1–14, 2021.

[35] G. Fellah, Endogenous and exogenous exergy destruction-a rational approach to evaluate the thermodynamic performance of a 285 MW gas turbine power plant, JER, Journal of Engineering Research (University of Tripoli) Issue (37) March 2024, 45-62

[36] T. Morosuk and G. Tsatsaronis, Advanced exergy analysis for chemically reacting systems - Application to a simple open gas-turbine system, Int. J. Thermodyn., vol. 12, no. 3, pp. 105–111, 2009

[37] D. Favrat, From thermoeconomics to environomics and beyond, Proceedings of ECOS 2023 - the 36th International Conference on Efficiency, Cost, Optimization, Simulation and Environmental Impact of Energy Systems 25-30 June, 2023, Las palmas de Gran Canaria, Spain

[38] C.A. Frangopoulos and G. Dimopoulos, A contribution to the discussion on the Future of Thermoeconomics, Proceedings of ECOS 2023 - the 36th International Conference on Efficiency, Cost, Optimization, Simulation and Environmental Impact of Energy Systems 25-30 June, 2023, Las palmas de Gran Canaria, Spain

[39] M. Aghbashlo, M.A. Rosen. Exergoeconoenvironmental analysis as a new concept for developing thermodynamically, economically, and environmentally sound energy conversion systems. J Cleaner Prod 2018;187:190–204. https://doi.org/10.1016/j.jclepro.2018.03.214.

[40] L. Meyer, R. Castillo, J. Buchgeister, G. Tsatsaronis, Application of Exergoeconomic and Exergoenvironmental Analysis to an SOFC System with an Allothermal Biomass Gasifier, Int. J. of Thermodynamics, Vol. 12 (No. 4), pp. 177-186, December 2009

[41] L. Meyer, J. Buchgeister, G. Tsatsaronis, L. Schebek, Formation of environmental impacts in energy conversion processes revealed by a novel exergoenvironmental analysis, Proceedings of IMECE2007 2007 ASME International Mechanical Engineering Congress and Exposition November 11-15, 2007, Seattle, Washington, USA, IMECE2007-42210

[42] H.T. Odum. 1996. Environmental Accounting, Emergy and Decision Making. John Wiley, NY,

[43] M. Aghbashlo, M.A. Rosen. Towards a better understanding of energy systems using emergy-based exergoeconoenvironmental analysis. IJEX 2019; 28(3): 209-208. https://doi.org/10.1504/IJEX.2019.098612

[44] M. Nourpour, M. H. Khoshgoftar Manesh, A. Pirozfar and M. Delpisheh, Exergy, Exergoeconomic, Exergoenvironmental, Emergybased Assessment and Advanced Exergy-based Analysis of an Integrated Solar Combined Cycle Power Plant, Energy & Environment, 2021, 1–28, DOI: 10.1177/0958305X211063558

3

Multi-objective optimisation

In the real-world, decisions need to be taken in the presence of trade-offs between two or more conflicting objectives. In engineering design, economics, finance, and logistics, for example, this is called *multi-objective optimisation* (MOO). MOO, in which a number of objective functions are to be minimised or maximised, is also referred to as *vector optimisation* because a vector of objectives is involved instead of a single objective [1]. In the past, MOO problems were usually cast and solved as *single-objective optimisation* (SOO) problems because of the lack of suitable solution methodologies. The limitation of this approach is that the optimisation objectives can be of different kinds or scales, which make it difficult to formulate the problem as a single objective function. Fortunately, the recent advances in the fields of applied mathematics, operational research, and digital computer technology have enabled the required solution methods to be developed [2]. This chapter discusses the scalarisation and the Pareto approaches to MOO and illustrates the application of the two approaches by using the Excel-based modelling platform, Excel's own solver, and the MIDACO solver [3].

3.1. The multi-objective optimisation problem

As an example multi-objective optimisation problem, consider the following problem that requires two simple functions f_1 and f_2 to be minimised simultaneously [3]:

$$f_1(x,y) = (x-0)^2 + (y-0)^2 \qquad 0 \le x \le 1;\ 0 \le y \le 1 \qquad (3.1.a)$$

$$f_2(x,y) = (x-1)^2 + (y-1)^2 \qquad 0 \le x \le 1;\ 0 \le y \le 1 \qquad (3.1.b)$$

The two functions f_1 and f_2 involve two variables, x and y, (called *decision variables*) the values of which are restricted to be between 0 to 1. Figure 3.1 shows Excel's surface plots of the two functions that shows their variation with x and y. The figure shows that the minimum value for f_1 is at (0,0), while that for f_2 is at (1,1). Therefore, the solution to this optimisation problem is not to find a single point at which the values of both functions are minimum, but to find a point, or points, that give the best trade-off between the two.

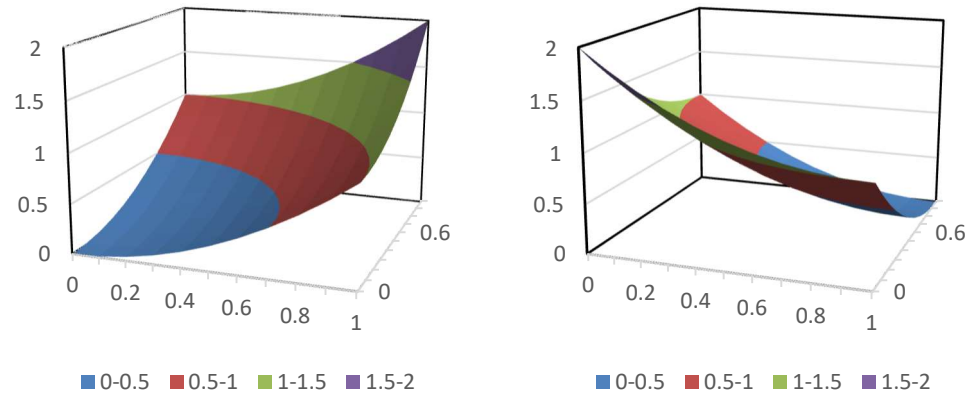

(a) f_1 (b) f_2

Figure 3.1. Surface plots of the two functions f_1 and f_2 in Equation (3.1)

The general multi-objective optimisation problem (MOOP) can be stated as follows [1]:

$$\left.\begin{array}{lll} \textit{Minimise / Maximise} & f_m(x), & m = 1,2,\ldots,M; \\ \textit{subject to} & g_i(x) \geq 0, & j = 1,2,\ldots,J; \\ & h_k(x) = 0, & k = 1,2,\ldots,K; \\ & x_i^{(L)} \leq x_i \leq x_i^{(U)}, & i = 1,2,\ldots,n \end{array}\right\} \tag{3.2}$$

There are M objective functions $f(x) = (f_1(x), f_2(x), \ldots, f_M(x))^T$ considered in the above formulation each of which can either be minimised or maximised. The terms $g_j(x)$ and $h_k(x)$ are called *constraint functions*. Associated with the problem are J inequality and K equality constraints. The inequality constraints are treated as 'greater-than-equal-to' types, but the above formulation also takes care of 'less-than-equal-to' type inequality constraint. The last set of constraints are called variable bounds, restricting each decision variable x_i to take a value within a lower bound, $x_i^{(L)}$, and an upper bound, $x_i^{(U)}$.

A solution $\boldsymbol{x}$ that does *not* satisfy all of the $(J + K)$ constraints and all of the $2N$ variable bounds stated above is called an *infeasible solution*, while any solution $\boldsymbol{x}$ that satisfies all constraints and variable bounds is called a *feasible solution*. Multi-objective optimisation problems have multiple feasible solutions because of the multiplicity of conflicting objectives, the complexity of the objective functions, and the constraints. The set of all feasible solutions is called the *feasible region*, S. An important difference between SOO problems and MOO problems is that the objective functions in a MOOP constitute a multi-dimensional space which is called *the objective space*, Z [1]. For each solution $\boldsymbol{x}$ in the usual decision variable space, there exists a point in the objective space denoted by $f(x) = \boldsymbol{z} = (z_1, z_2, \ldots, z_M)^T$. The mapping takes place between an n-dimensional solution vector and an M-dimensional objective vector. Figure 3.2 illustrates these two spaces for the bi-objective optimisation problem expressed by Equation (3.1).

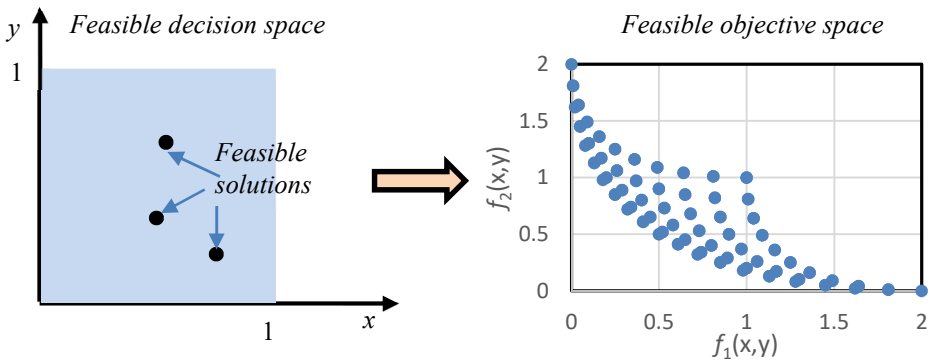

Figure 3.2. A graphical representation of the feasible decision space and objective space for Equation (3.1)

3.2. Multi-objective optimisation methods

There are two approaches for solving MOO problems [4,5]:

1. The scalarisation approach (the weighted sum method)
2. The Pareto approach

Considering the variety of the methods involved in the two approaches, only brief descriptions are given here. It is hoped that the discussion provides sufficient leading threads for the readers interested in a more in-depth study of this topic.

3.2.1. The Scalarisation approach

The scalarisation approach combines the multi-objective functions into a single function using weights before optimisation such that a weight for an objective is proportional to the preference factor assigned to that particular objective. Referring to Equation (3.1), the mathematical formulation of the scalarisation approach is as follows:

$$F(x,y) = w_1 \times f_1(x,y) + w_2 \times f_2(x,y) \tag{3.3}$$

Where, w_1 and w_2 are weights of the objective functions as defined by the user in proportion to the relative importance of the objective. Therefore, this approach is called a preference-based multi-objective optimisation. Let's apply this approach to solve the bi-objection problem given by Equation (3.1) by giving the two functions equal weights. With this preference choice, i.e., $w_1 = w_2 = 1$, Equation (3.3) takes the following form:

$$F(x,y) = f_1(x,y) + f_2(x,y) \tag{3.4}$$

Figure 3.3 shows an Excel sheet that calculates the values of F at the various values of x and y. The figure shows that the minimum value for F is 1, which occurs at (0.5,0.5). The corresponding values of both objective functions, f_1 and f_2, are equal to 0.5.

x/y	0	0.1	0.2	0.3	0.4	0.5	0.6	0.7	0.8	0.9	1
0	2	1.82	1.68	1.58	1.52	1.5	1.52	1.58	1.68	1.82	2
0.1	1.82	1.64	1.5	1.4	1.34	1.32	1.34	1.4	1.5	1.64	1.82
0.2	1.68	1.5	1.36	1.26	1.2	1.18	1.2	1.26	1.36	1.5	1.68
0.3	1.58	1.4	1.26	1.16	1.1	1.08	1.1	1.16	1.26	1.4	1.58
0.4	1.52	1.34	1.2	1.1	1.04	1.02	1.04	1.1	1.2	1.34	1.52
0.5	1.5	1.32	1.18	1.08	1.02	1	1.02	1.08	1.18	1.32	1.5
0.6	1.52	1.34	1.2	1.1	1.04	1.02	1.04	1.1	1.2	1.34	1.52
0.7	1.58	1.4	1.26	1.16	1.1	1.08	1.1	1.16	1.26	1.4	1.58
0.8	1.68	1.5	1.36	1.26	1.2	1.18	1.2	1.26	1.36	1.5	1.68
0.9	1.82	1.64	1.5	1.4	1.34	1.32	1.34	1.4	1.5	1.64	1.82
1	2	1.82	1.68	1.58	1.52	1.5	1.52	1.58	1.68	1.82	2

Figure 3.3. Values of the scaled function F at the various values of x and y

Scalarisation enables the problem to be solved by using a single-objective solver. Figure 3.4 shows an Excel sheet prepared for this purpose in which the first objective function,

f_1, is stored in cell **B3**, while the second function, f_2, is stored in cell **B4**. The function ribbon shows the first function stored in **B3**. The variables x and y are stored in cells **D3** and **D4**, respectively. Excel's Solver can now be used to minimise the function F, stored in cell **D6**, by changing the values of cells **D3** and D**4**. Figure 3.5 shows Solver's set-up and Figure 3.6 shows the solution obtained with the GRG Nonlinear method of Solver. As the figure shows, the obtained solution is the point (0.5,0.5) at which $F = 1.0$.

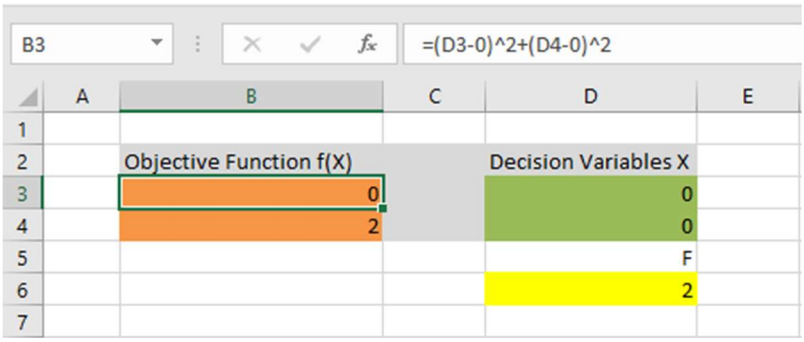

Figure 3.4. Excel sheet for solving the single-objective problem by using Solver

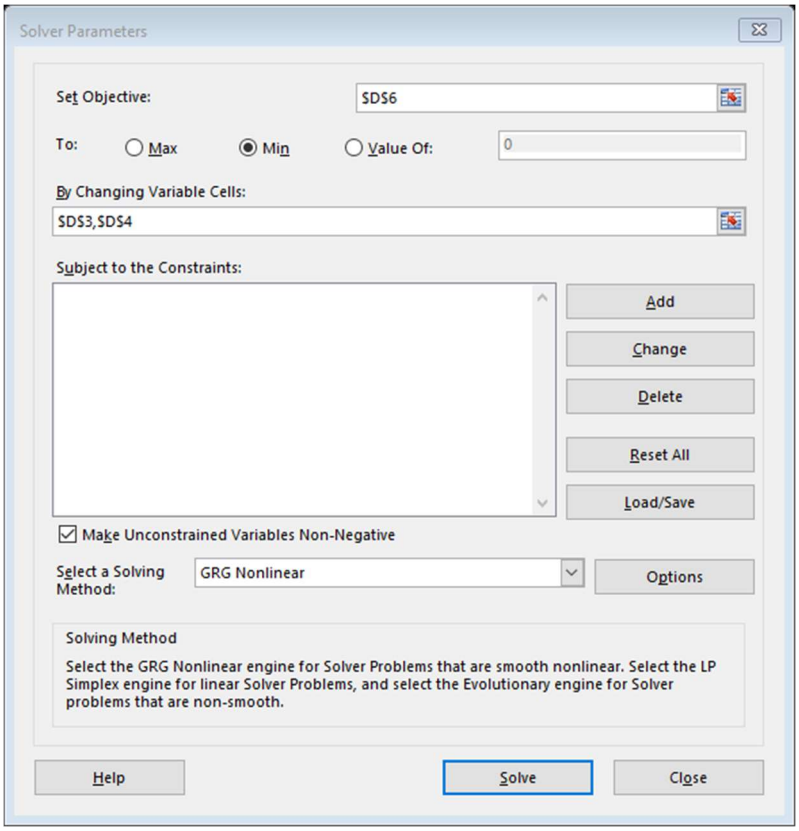

Figure 3.5. Solver's set-up for solving the single-objective problem

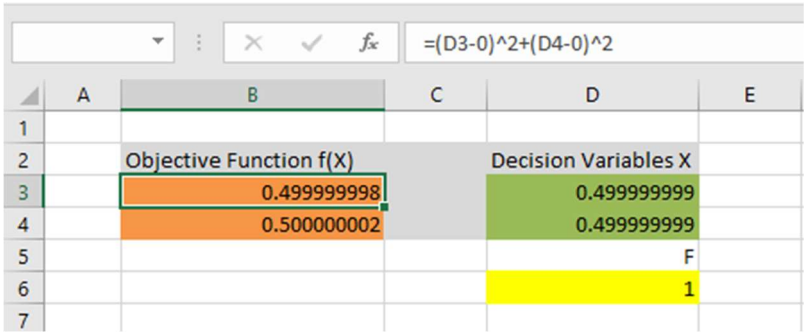

Figure 3.6. Solver's solution of the single-objective problem

A single solution to this problem could be obtained because the problem applies no constraints. Constraints are one of the reasons why MOOPs have multiple solutions. To see the effect of adding a constraint to the present problem let's assume that we are only interested in the solutions for which:

$$F(x,y) \geq 1.2 \tag{3.5}$$

With this condition, the solutions marked red on Figure 3.3 become infeasible. The eight points marked blue on the figure have the lowest value of F. Therefore, any one of these points is an optimum solution. Figure 3.7 shows Solver's set-up for solving the optimisation problem subject to the constraint specified by Equation (3.5) and Figure 3.8 shows the solution obtained. As the figure shows, Solver's solution is the point (0.724,0.724) at which $f_1 = 1.047$, $f_2 = 0.153$, and $F = 1.2$. To find multiple optimal solutions with this method one chooses a different weight vector and solves the resulting single-objective optimisation problem again. Simplicity is the main advantage of this approach, but its disadvantages are that it is difficult to set the weight vectors to obtain an optimal solution in a desired region in the objective space. Moreover, these methods cannot find certain optimal solutions in the case of a nonconvex objective space as shown on Figure 3.9 [1,6].

3.2.2. The Pareto approach

This is the approach that has become commonly used for solving MOO problems particularly in engineering design. The name Pareto refers to the Italian economist who first introduced the "*dominance*" concept which is the central idea of the approach. In the single-objective optimisation problem, the superiority of a solution over other solutions is easily determined by comparing their objective function values. In the Pareto approach there are dominated solutions and non-dominated solutions and the goodness of a solution is measured according to its dominance as determined by the *dominance test* [6]. According to this concept, solution S_1 dominates solution S_2, if:

1. Solution S_1 is no worse than S_2 in all objectives
2. Solution S_1 is strictly better than S_2 in at least one objective

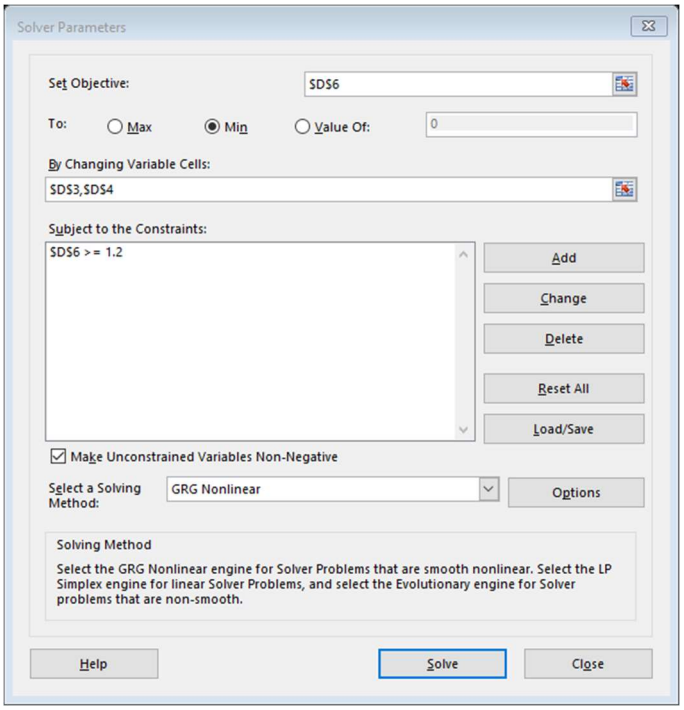

Figure 3.7. Solver's set-up for solving the constrained single-objective problem

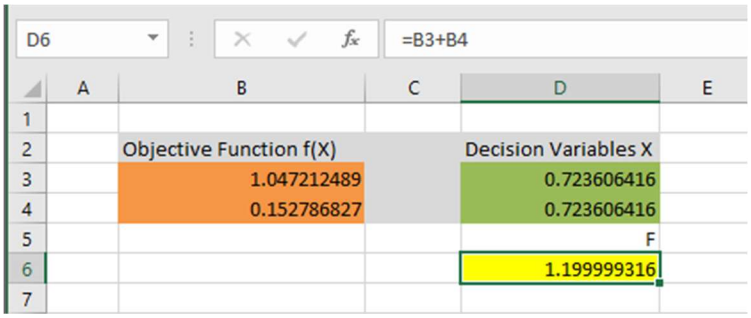

Figure 3.8. Solver's solution of the constrained single-objective problem

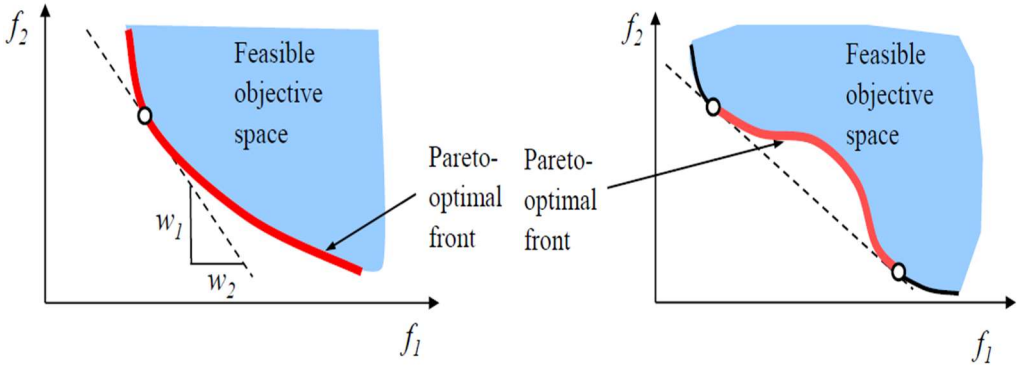

Figure 3.9. The scalarisation approach applied to convex and nonconvex problems [6])

The set of solutions that pass the test are called the *Pareto optimal solutions*, *Pareto-optimal set*, *Pareto efficient set*, or the *non-inferior" solutions*. As an example, consider a problem that involves two objective functions f_1 and f_2 and requires f_1 to be maximised and f_2 to be minimised simultaneously for which five solutions are shown on Figure 3.10. Table 3.1 shows the conclusions that can be made when solution 1 is compared to the other four solutions. Similar comparisons show that solution 3 dominates solutions 2 and 4, but not 5. The three solutions 1, 2, and 4 are dominated solutions, while the other two solutions 3 and 5 are non-dominated solutions. Therefore, the dominance test has reduced the number of solutions that are potential optima from five to two, but the selection of the best solution among these two solutions requires additional information.

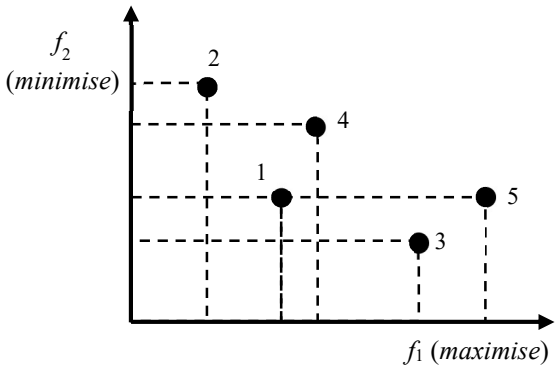

Figure 3.10. Illustration of the dominance test (adopted from [1])

Table 3.1. Application of the dominance test to Solution 1 shown on Figure 3.10

First solution	Second solution	Dominant solution
1	2	1
1	3	3
1	4	Neither
1	5	5

As a real-world example, consider the case of a passenger willing to buy an air ticket to a certain destination with two objectives: to save money and get the shortest flying time. Table 3.2 lists five available options [7]. Two cases are obvious: if the passenger's budget is limited and if he/she has to catch-up with an important appointment. In the first case the passenger will most probably go for Ticket A and in the second case Ticket E is the best option. Otherwise, the passenger will weigh the different options. Ticket A is cheaper than ticket B, but the journey takes a longer time. So, we can't judge which one is better without knowing the relative importance of travel time versus price. However, ticket C is better than ticket B in both objectives and there is no reason for choosing B instead of C. Therefore, we can say that C dominates B. Similarly, E dominates D. Out of the five options, tickets B and D are dominated solutions and need not be considered further. The three remaining options A, C, and E have trade-offs associated with travelling time versus price and none of them is superior over the others without further information.

Table 3.2. A passenger's options for buying an air ticket [7]

Ticket	Travel time (hours)	Price ($)
A	10	1700
B	9	2000
C	8	1800
D	7.5	2300
E	6	2200

Figure 3.11 shows a graphical representation of the two objective functions (Flight time and Price) for the travelling-passenger problem. The figure shows the feasible region, dominated solutions, non-dominated solutions, and the Pareto front.

1. Feasible region: The set of all feasible objective functions (A, B, C, D, and E)
2. Dominated solutions: The solutions that lie inside the line (D and B).
3. Non-dominated solutions: The set of all the solutions that are not dominated by any member of the solution set (A, C, and E).
4. Pareto front: The boundary defined by the set of all non-dominated solutions.

It should be noted that multiple Pareto optimal solutions exist only if the problem objectives are conflicting to each other. In the case of non-conflicting objectives, the Pareto front becomes a single point.

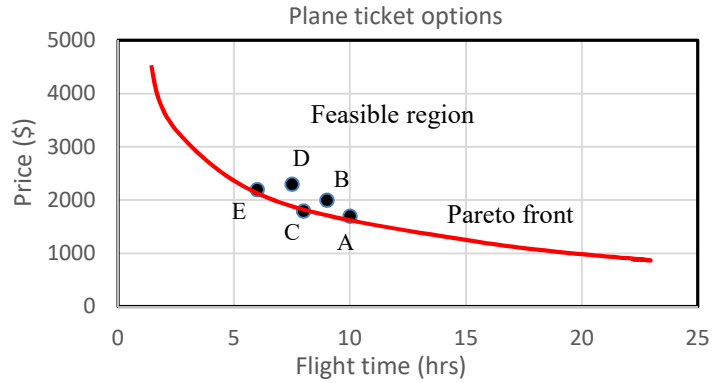

Figure 3.11. The objective space for the travelling-passenger problem

3.3. MOO algorithms based on the Pareto approach

The answer to a MOOP is set of solutions that define the best trade-off between competing objectives [6]. Therefore, the solution method to a MOOP should provide a variety of optimal solutions that trade the various objectives differently. The decision-maker can then decide the best solution among the set of optimal solutions. A multi-objective optimisation algorithm that cannot find a diverse set of solutions to a problem in each simulation run is as good as a single-objective optimisation algorithm that can at best find one solution in one run [1]. A multi-objective optimisation algorithm that adopts the Pareto approach has two tasks:

1. To find a set of solutions as close as possible to the Pareto-optimal front.
2. To find a set of solutions as diverse as possible so as to be assure of having a good set of trade-off solutions among objectives.

The two tasks are somewhat orthogonal to each other and, therefore, the achievement of one goal does not necessarily mean the achievement of the other goal. Therefore, an efficient MOO algorithm must work on satisfying both of them. Explicit or implicit mechanisms to emphasise convergence to the optimal solution while maintaining a diverse set of solutions must be introduced in the MOO algorithm. Because of these dual tasks, MOO algorithms are more difficult to develop than SOO algorithms.

The need to identify as many solutions as possible within the Pareto-optimal range often represents a problem for classical optimisation techniques [8,9]. Therefore, most MOO methods use evolutionary algorithms (EAs). The main advantage of EAs, when applied to solve MOO problems, is their ability to generate sets of solutions (in a single run) that allow computation of an approximation of the entire Pareto front. Among EAs, the most popular algorithms are genetic algorithms (GAs) although some schemes based on particle swarm optimisation and simulated annealing are significant.

3.3.1. Elitist and non-elitist algorithms

By maintaining and continually improving a population of solutions, a GA can search for many non-dominated solutions in every run. However, even for GAs, the two tasks mentioned above cannot be achieved by adopting simple and naive approaches. The simplest possible multi-objective GA is the vector evaluated GA (VEGA) originally suggested by David Schaffer in 1984 [1] which is a straightforward extension of a single-objective GA to suit multi-objective optimisation. A schematic diagram of the VEGA is shown on Figure 3.12.

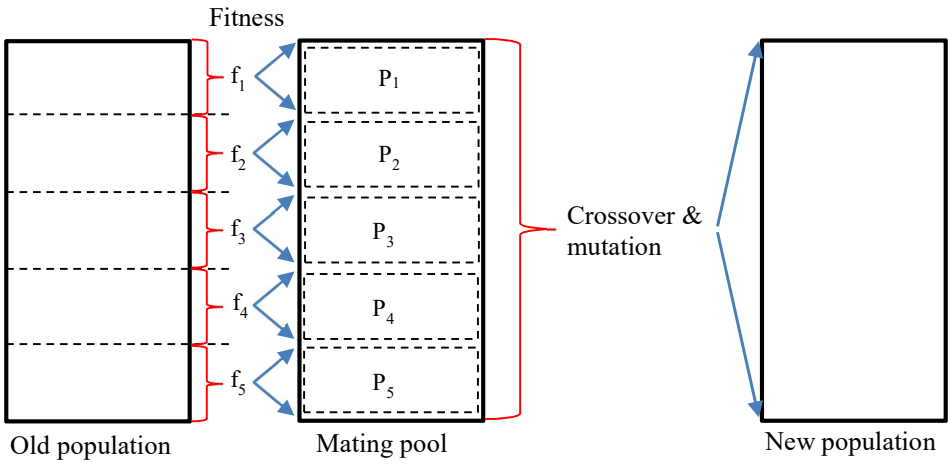

Figure 3.12. Schematic of a VEGA (adopted from [1])

VEGA modified the simple tripartite genetic algorithm by performing independent selection cycles according to each objective. However, the algorithm suffers from its bias towards individual objectives. Although the first task of multi-objective optimisation was fulfilled by VEGA, the second task of maintaining a good spread of solutions in the obtained front was not entirely accomplished.

In order to have the ability to produce diverse non-dominated solutions in each iteration, the more recent multi-objective EAs use an elite-preserving operator for preserving and using previously found best solutions in subsequent generations [1,6]. These algorithms are called elitist MOO solvers. As the name suggests, an elite-preserving operator favours the elites of a population by giving them an opportunity to be directly carried over to the next generation. Elitist multi-objective EAs proved to be faster than the non-elitist algorithms. In addition to an overall increase in performance, there is another advantage of using elitism which is that the statistics of the population-best solutions cannot degrade with generations. Deb [1] describes a number of ways to introduce elitism in multi-objective EAs. Few elitist GA algorithms exist today of which the Non-Dominated Sorting Genetic Algorithm-II (NSGA-II) and its extended version NSGA-III have become standard algorithms [1,10,11,12].

3.3.2. Termination condition and selection of the best solution

The use of GAs in MOO guarantees that none of the generated solutions is dominated by another, but does not guarantee that the Pareto optimal solution has been reached. So, when should an algorithm stop generating new populations? Most GAs commonly terminate when either a maximum number of generations has been produced or a satisfactory fitness level has been reached for the population. If the algorithm has terminated due to a maximum number of generations, a satisfactory solution may or may not have been reached [11]. A typical setting of the solver parameters is shown on Table 3.3 based on the data given by Keshtkar and Talebizadeh [12] who used the NSGA-II algorithm for a MOO of a R744/R134a cascade refrigeration system (CRS) with two objective functions; minimising the total cost rate and maximising the exergy efficiency of the system. Figure 3.13 shows the Pareto front obtained for the CRS system by using the NSGA-II solver.

Table 3.3. A typical setting of the NSGA-II parameters for an optimisation process [12]

Setting parameters	Value
Population size	500
Maximum number of generations	400
Maximum function tolerance	10^{-3}
Probability of crossover	90%
Probability of mutation	1%
Number of crossover points	2
Selection process	Tournament
Tournament size	2

Since the Pareto front contains the best solution family of the problem, selecting the best single point considering the trade-offs is not a trivial task [5]. In fact, without further information, all the solutions are equally acceptable. Therefore, MOO methods need to have some tools to analyse the solution space and make the optimal choice relevant to the problem. In this regard, the methods can use one of the decision-making techniques to select the best optimum solution among the non-dominated solutions [13]. Ganjehkaviri et al. [11] used the concept of equilibrium point, while Keshtkar and Talebizadeh [12] used the TOPSIS method [14].

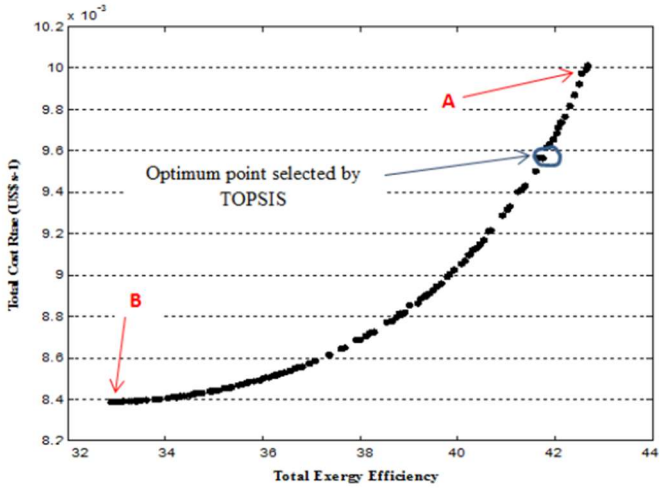

Figure 3.13. Pareto optimal front from multi-objective optimisation of a cascade refrigeration system (adopted from [12])

3.4. Multi-objective optimisation by using the MIDACO solver

MOO solvers are still in the research and development stage and, therefore, not many of them are available for use with general-purpose software like Excel [15]. Fortunately, the developers of MIDACO (Mixed Integer Distributed Ant Colony Optimization) have made a limited version of the software publicly available for Excel and several programming languages including VBA and Fortran [16,17]. The solver, which has been created by the European Space Agency (ESA) in collaboration with EADS Astrium for space applications, implements an evolutionary hybrid algorithm for solving constrained mixed-integer non-linear problems restricted by equality and/or inequality constraints. It treats the problem as a black-box and can be used to solve single and multi-objective optimisation problems with up to thousands of variables and hundreds of objectives. However, the limited version of the solver allows only four changing variables to be considered in the analysis. In spite of this limitation, the solver can still be used for many multi-objective optimisation analyses that are met in general engineering practice.

Excel's free version of the MIDACO Solver is available at [3] as a Zip file called "MIDACO.zip". To illustrate the use of the solver, the zip file also contains a normal Excel file called "example" for solving the bi-objective optimisation problem expressed

by Equation (3.1). Since this problem involves only two changing variables; x and y, the limited version of MIDACO is adequate for solving it. After downloading and unzipping the file, it should be stored in a folder called "MIDACO" directly under "C:\". Open the "MIDACO" folder located at "C:\MIDACO" and open the "example.xlsx" file. The Excel sheet shown on Figure 3.4 is a slightly modified version of the sheet in this file. The steps of using MIDACO to solve the bi-objective optimisation problem are as follows [3]:

Step 1: Within Excel, click **File -> Open** and select "Midaco.xlam"
Step 2: **Enable Macros** if prompted by Excel
Step 3: Open MIDACO-Solver Add-In from the Excel Ribbon. Figure 3.14.a shows the sheet at this step. Clicking the "Add-ins" tap, the MIDACO solver will appear on the left side of the sheet as shown on Figure 3.14.b.
Step 4: Clicking the MIDACO-Solver, the User Form shown on Figure 3.15 will appear.

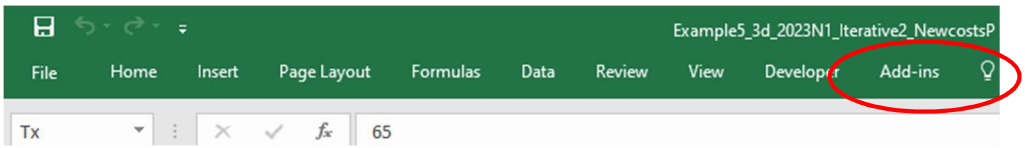

(a)

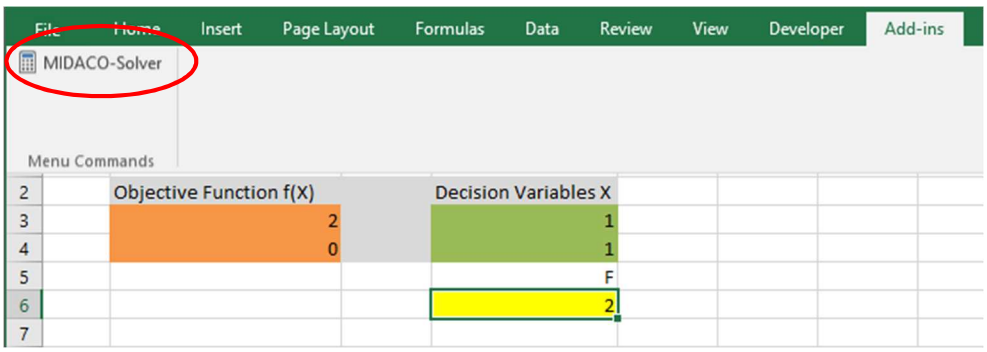

(b)

Figure 3.14. Activation of the MIDACO solver by the example Excel sheet

Figure 3.15 shows the two functions (3.1.a) and (3.1.b) added as objectives to be minimised and the variables x and y specified as "Continuous from 0 to 1". No constraint has been specified for this problem. Clicking on the "**Run MIDACO-Solver**" button will activate the solver to search for the solution and when it meets the termination criterion, the form shown on Figure 3.16 will appear giving some information about the solution. As Figure 3.16 shows, the solution has been terminated after 10,000 evaluations, which is the maximum value set by default, after which 324 Pareto points have been found by the solver. To keep the solution, select the "**Accept**" button. Rejecting the solution will keep the initial values of the functions unchanged. MIDACO automatically stores the

data of the solution's Pareto front in a plain text file called "**MIDACO_PARETOFRONT**".

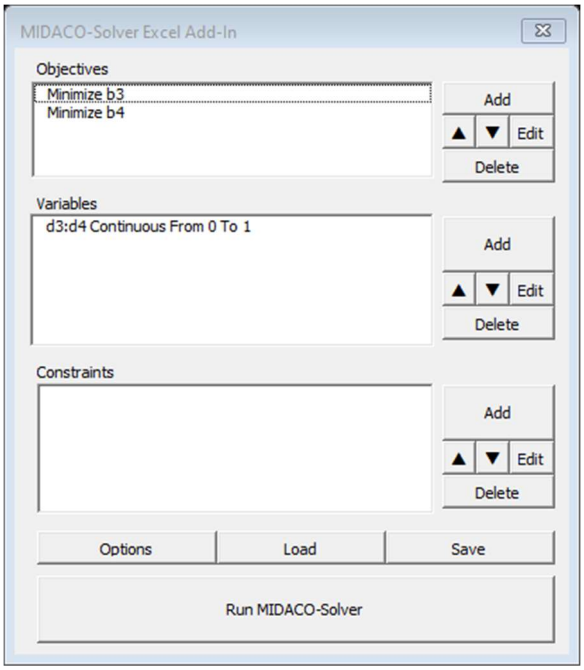

Figure 3.15. MIDACO set-up form for solving Equation (3.1) without a constraint

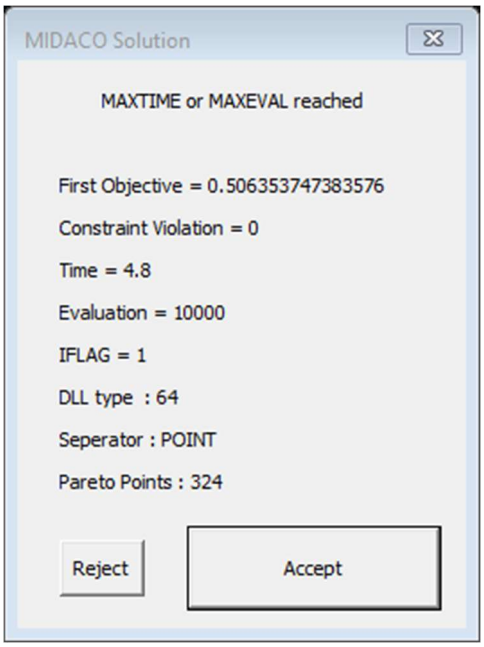

Figure 3.16. The solution termination form of MIDACO

To plot the Pareto front, a plotting tool, called **PlotTool**, can be downloaded from [18]. Figure 3.17 shows the Pareto front generated by this tool for the solution of the problem and the selected optimal solution. Figure 3.18 shows the solution selected by MIDACO out of the 324 Pareto optimal solutions. The solution, which is x = 0.5064, y =0.4939, is very close to the anticipated solution, which is (0.5,0.5).

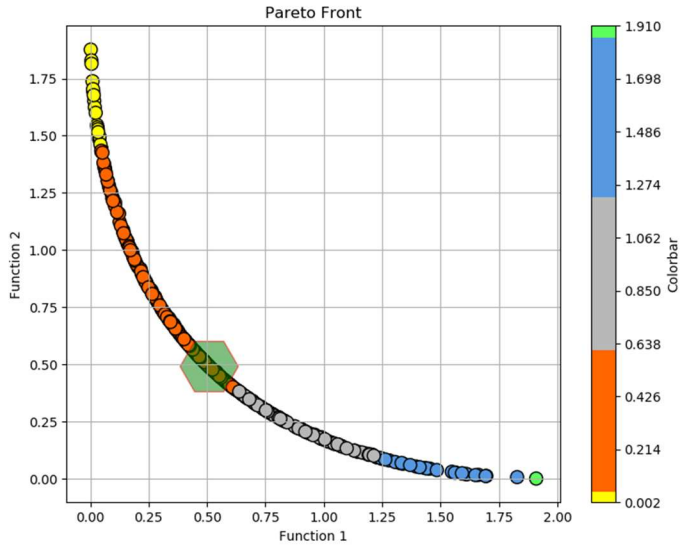

Figure 3.17. The Pareto front generated by MIDACO's plotting tool for the unconstrained Equation (3.1)

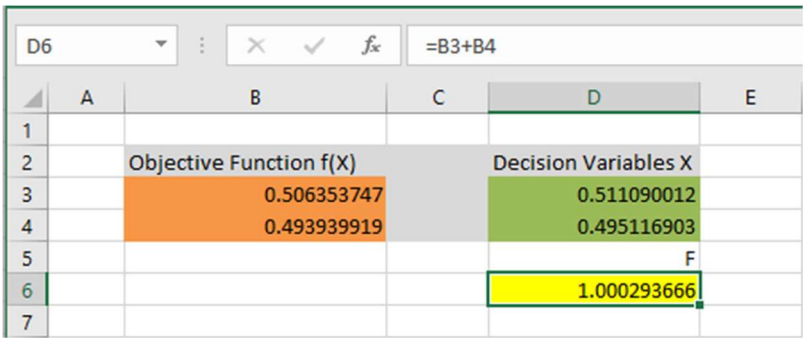

Figure 3.18. The solution selected by MIDACO for the unconstrained Equation (3.1)

Let's now use MIDACO to solve the constrained problem that has multiple solutions. Figure 3.19 shows the modified set-up that adds the constraint specified by the inequality Equation (3.5) to the set-up show on Figure 3.15. Figure 3.20 that shows the termination form of the solver shows that the solution has been terminated also after 10,000 evaluations after which the solver found 184 Pareto optimal solutions. Figure 3.21 shows the Pareto front for the solution of the constrained problem and Figure 3.22 shows the solution selected by MIDACO out of the 184 Pareto optimal solutions, which is: f_1 =

0.612 and $f_2 = 0.588$. Note this solution is different from that obtained earlier by using Solver, which is $f_1 = 1.047$ and $f_2 = 0.153$. Figure 3.21, which also shows the solution obtained by Solver, confirms what has been mentioned earlier regarding the limitation of the scalarisation approach with respect to nonconvex optimisation problems.

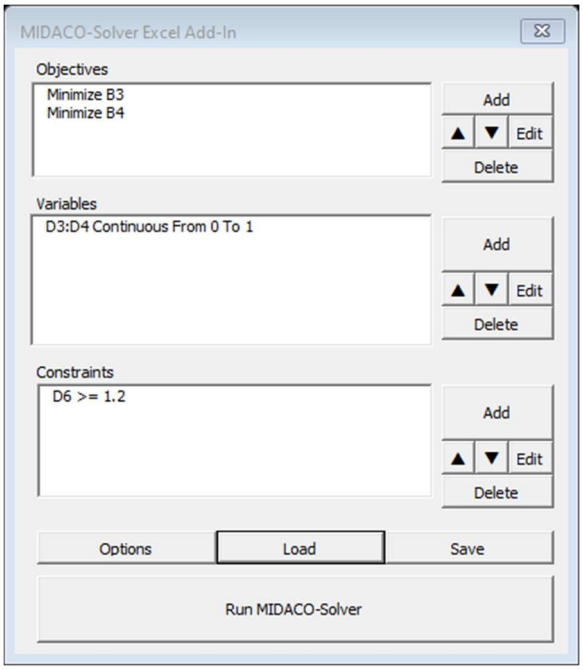

Figure 3.19. MIDACO set-up form for solving the constrained Equation (3.1)

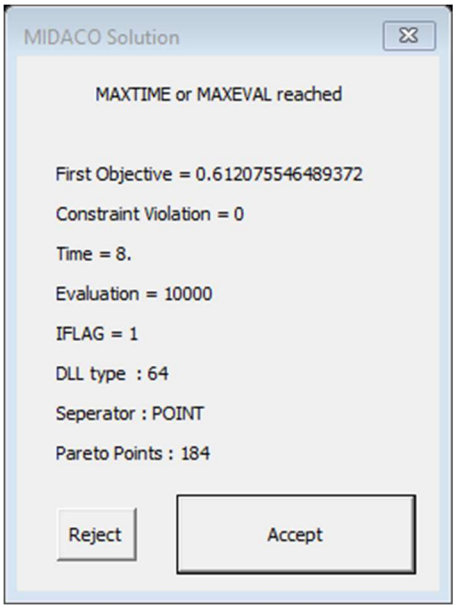

Figure 3.20. Solution termination form of MIDACO for the constrained Equation (3.1)

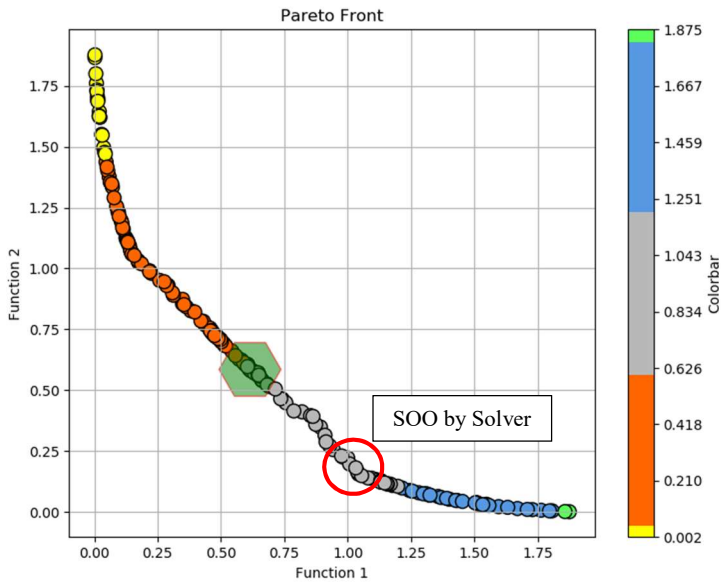

Figure 3.21. The Pareto front generated for the constrained Equation (3.1)

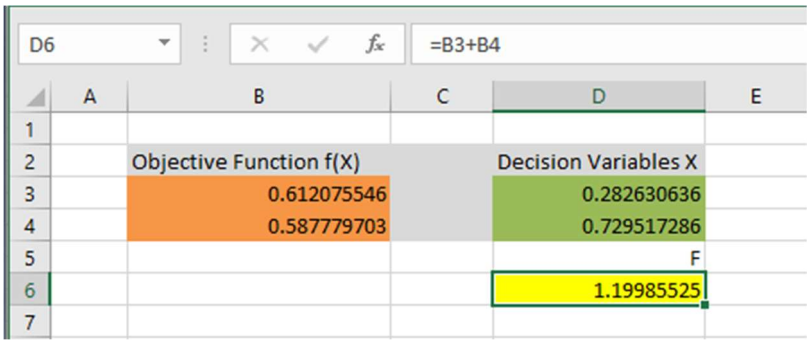

Figure 3.22. The solution selected by MIDACO for the constrained Equation (3.1)

3.5. Single and dual-objective optimisation of a hot-water generation system

Figure 3.23 shows a hot-water generation system described by Li and Priddy [19] that uses a high-pressure (HP) steam heater and a low-pressure (LP) steam heater to raise the temperature of a pressurised stream of water from 65°C to 150°C. Because of the different pressure levels, the two heaters have different initial and steam costs and, therefore, determining the optimum intermediate temperature between the two heaters, T_x, poses a design optimisation problem. Li and Priddy [19] provided the following data:

Water flow rate ($\dot{m}$)	180,000 kg/hr
Steam pressure of low-pressure heater	350 kPa (138.86°C)
Steam pressure of high-pressure heater	550 kPa (155.46°C)
Overall heat transfer coefficient (U)	10220.667 kJ/hr-m^2-°C
Low-pressure heater surface cost	\$108.7/m^2

High-pressure heater surface cost	\$109.8/m^2
Annual fixed charge rate (β)	20%
Total number of operation hours	2000 hours per year

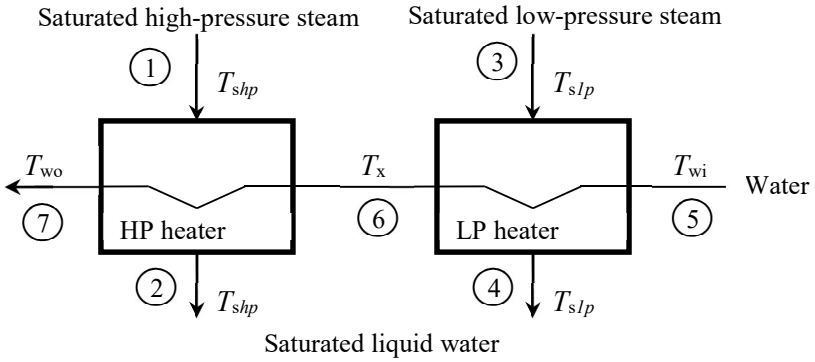

Figure 3.23. Schematic of the hot-water generation system (adapted from Li and Priddy [19])

Li and Priddy [19] performed a conventional energy-based thermoeconomic analysis to determine the value of T_x that minimises the total annualised cost of the system, C_{total}. The present analysis compares the outcome of a single-objective optimisation analysis of the system that minimised C_{total} with that of a dual-objective optimisation analysis that simultaneously minimised the total initial cost, $C_{initial}$, and the total steam cost, C_{steam}. While the SOO analysis adopts the scalarisation approach of multi-objective optimisation, the dual-objective analysis adopts the Pareto approach. The steam costs per unit of energy used by Li and Priddy [19] for the LP steam and the HP steam in \$/Btu have been replaced in the present analysis by the following costs in \$/kJ:

Cost of the LP steam, $c_{lps} = 5.687 \times 10^{-7}$ \$/kJ
Cost of the HP steam, $c_{hps} = 5.725 \times 10^{-7}$ \$/kJ

3.5.1. The analytical model for least-cost and MOO analyses

Using the notation of Figure 3.23, the rates of heat transfer in the two heaters are:

$$\dot{Q}_{lp} = \dot{m} C_p \left(T_x - T_{wi} \right) \tag{3.6.a}$$

$$\dot{Q}_{hp} = \dot{m} C_p \left(T_{wo} - T_x \right) \tag{3.6.b}$$

Where, $\dot{m}$ is the mass flow rate of water and the subscripts *hp* and *lp* refer to the HP heater and the LP heater, respectively.

The total cost of steam (C_{steam}) is the sum of the steam costs in the two heaters and the total annualised initial cost ($C_{initial}$) is the sum of the initial costs of the two heaters:

$$C_{steam} = C_{s,lp} + C_{s,\,hp} \tag{3.7.a}$$

$$C_{initial} = C_{i,lp} + C_{i,\,hp} \tag{3.7.b}$$

Where, C_s is the annual steam cost (\$/year) and C_i is the annualised initial cost (\$/year). The annual steam costs for the two heaters are given by:

$$C_{s,lp} = c_{lps}\,\dot{Q}_{s,lp}\,.3600\;\tau \tag{3.8.a}$$

$$C_{s,hp} = c_{hps}\,\dot{Q}_{s,hp}\,.3600\;\tau \tag{3.8.b}$$

Where, c_{lps} and c_{hps} are the steam costs in the low-pressure heater and the high-pressure heater, respectively, in \$/kJ, and τ is the number of operating hours per year.

The initial cost of each heater (C_i) is the product of its heat transfer surface area (A) and its unit cost per square metre (b). If an annual fixed charge rate β is applied, the annual relative cost of the heater becomes:

$$C_i = b \times A \times \beta \tag{3.9}$$

The heat transfer surface areas of the two heaters are determined by using the log-mean temperature difference method [20]. Accordingly, the surface area of the low-pressure heater (A_{lp}) is given by:

$$A_{lp} = \dot{Q}_{lp} / U_{lp}\Delta T_{lm,lp} \tag{3.10}$$

Where, ΔT_{lm} is the log-mean temperature difference. For the low-pressure heater:

$$\Delta T_{lm,lp} = \frac{\Delta T_{lp,1} - \Delta T_{lp,2}}{\ln\left(\Delta T_{lp,1} / \Delta T_{lp,2}\right)} \tag{3.11}$$

Where,

$$\Delta T_{lp,1} = \left(T_{slp} - T_x\right) \tag{3.12.a}$$

$$\Delta T_{lp,2} = \left(T_{slp} - T_{wi}\right) \tag{3.12.b}$$

Combining Equations (3.9), (3.10), and (3.11) gives:

$$C_{i,lp} = \frac{b_{lp}.\beta.\dot{Q}_{lp}}{U_{lp}} \frac{\ln\left[\Delta T_{lp,1} / \Delta T_{lp,2}\right]}{\Delta T_{lp,1} - \Delta T_{lp,2}} \tag{3.13}$$

Similarly, the annual relative cost for the high-pressure heater is given by:

$$C_{i,hp} = \frac{b_{hp}.\beta.\dot{Q}_{hp}}{U_{hp}} \frac{\ln\left[\Delta T_{hp,1} / \Delta T_{hp,2}\right]}{\Delta T_{hp,1} - \Delta T_{hp,2}} \tag{3.14}$$

Where,

$$\Delta T_{hp,1} = \left(T_{shp} - T_{wo}\right) \tag{3.15.a}$$

$$\Delta T_{hp,2} = \left(T_{shp} - T_{x}\right) \tag{3.15.b}$$

The total annualised cost of the system (C_{total}) is given by:

$$C_{total} = C_{steam} + C_{initial} \tag{3.16}$$

3.5.2. Excel implementation and optimisation analyses

Figure 3.24 shows the Excel sheet developed for applying the above model. The left part of the sheet shows the specified system's data. The sheet determines the saturation temperatures for the low-pressure and high-pressure steams by using Thermax functions in cells **G6** and **J6** and calculates for the specified value of the intermediate temperature in cell **G3** the steam and initial costs of the two heaters and the total relative cost of the system. The initial costs of the two heaters are based on their heat-transfer areas and the formula bar reveals the use of Equation (3.10) to calculate the area of the LP heater. The three cells **J18**, **J19**, and **J20** that store the three costs are the objective cells for the single-objective and dual-objective optimisation analyses. For the specified value of the intermediate temperature, T_x, of 65ºC, Figure 3.24 shows that all the heating load is carried by the HP steam heater. Therefore, both the steam cost and the initial cost are those of the HP heater alone. As T_x increases, the share of the LP heater increases. Figure 3.25 shows the variation of the system's costs with T_x in the range 65ºC < T_x < 135ºC. The figure shows that the lowest steam cost C_{steam} is obtained when the LP heater assumes the maximum possible share of the heating load, but the lowest initial cost $C_{initial}$ is achieved when the HP heater takes the largest share of the load. As the figure shows, C_{steam} decreases steadily with T_x, $C_{initial}$ increases exponentially with T_x, but C_{total} passes through minimum values of T_x in the range 75ºC < T_x < 95ºC.

The conflict between the changes in the total combined steam cost and the total combined initial cost of the system as T_x is increased is clearly shown by Figure 3.25. Therefore, determining the value of T_x that simultaneously minimises both costs is a dual-objective optimisation problem and solving the problem by minimising the total relative cost is

essentially an adoption of the scalarisation approach which can be applied by using Solver or MIDACO. Figure 3.26 shows the set-up of the MIDACO solver for the SOO analysis of the HWG system that minimised its total relative cost by varying T_x between 65 and 135°C. Figure 3.27 shows the solution determined by MIDACO according to which the intermediate temperature is 79.7°C and the total relative cost is 78,122 $/y.

A_I | =Q_I/(Overall_heat_transfer_coefficient*LMTD_I/3600)

	A	B	C	D	E	F	G	H	I	J	K
1			**Hot Water Generation System**								
2		Water flow rate	180000	kg/hr		*Intermediate temperature*					
3		Water inlet temperature	65	oC		Tx	65	oC			
4		Water outlet temperature	150	oC							
5		Cp_water	4.2	kJ/kg-oC		**LP heater**			**HP heater**		
6						ts_l	138.86	oC	ts_h	155.46	oC
7		***Steam pressures***				Q_l	0	kW	Q_h	17850	kW
8		LP heater pressure	350	kPa		ms_l	0	kg/h	ms_h	30650.45	kg/h
9		HP heater pressure	550	kPa		Cs_l	0	$/yr	Cs_h	73577.7	$/yr
10											
11		***Steam costs***				Delt1_l	73.86		Delt1_h	5.46	
12		LP heater steam cost	5.687E-07	$/kJ		Delt2_l	73.86		Delt2_h	90.46	
13		HP heater steam cost	5.725E-07	$/kJ		LMTD_l	73.86		LMTD_h	30.27649	
14						A_l	0	m2	A_h	207.6615	
15		Heater surface costs				Ci_l	0	$/yr	Ci_h	4560.246	$/yr
16		LP heater initial cost	108.7	$/m2		**Subtotal LPH**	**0**	**$/yr**	**Subtotal HPH**	**78137.95**	$/yr
17		HP heater initial cost	109.8	$/m2	124.6						
18									**Steam cost**	**73577.7**	$/yr
19		Overall heat transfer coefficient	10220.67	kJ/hr-m2-oC					**Initial cost**	**4560.246**	$/yr
20		Annual fixed charge rate	20	%					**Total relative**	**78137.95**	$/yr
21		Operation hours	2000	hr/yr							
22											

Figure 3.24. Excel sheet for the hot-water generation system

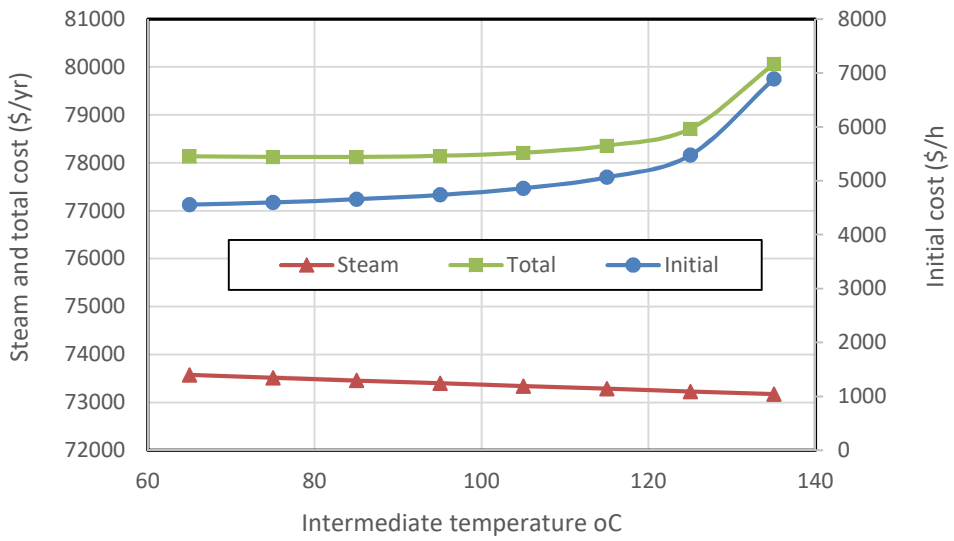

Figure 3.25. Variation of the system's combined steam cost, combined initial cost, and total combined cost with the intermediate temperature T_x

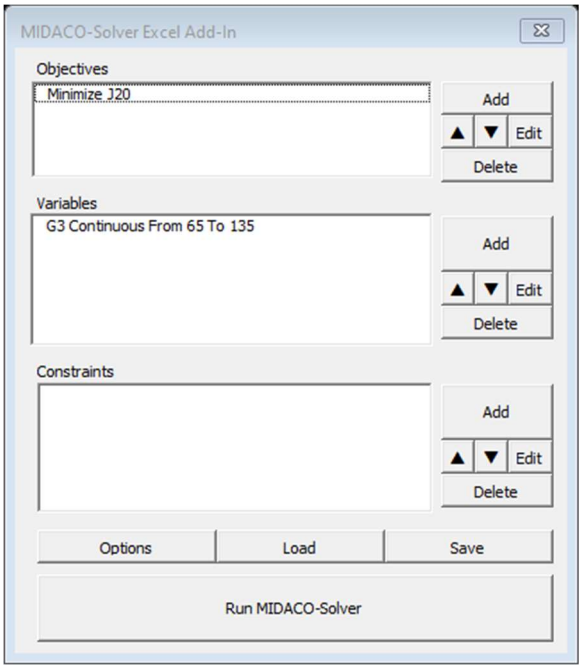

Figure 3.26. MIDACO's set-up for minimising the total cost of the system

Total_cost =Steam_cost+Initial_cost

	A	B	C	D	E	F	G	H	I	J	K
1			Hot Water Generation System								
2		Water flow rate	180000	kg/hr		Intermediate temperature					
3		Water inlet temperature	65	oC		Tx	79.7259	oC			
4		Water outlet temperature	150	oC							
5		Cp_water	4.2	kJ/kg-oC		LP heater			HP heater		
6						ts_l	138.86	oC	ts_h	155.46	oC
7		Steam pressures				Q_l	3092.43	kW	Q_h	14757.57	kW
8		LP heater pressure	350	kPa		ms_l	5183.66	kg/h	ms_h	25340.40	kg/h
9		HP heater pressure	550	kPa		Cs_l	12662.4	$/yr	Cs_h	60830.69	$/yr
10											
11		Steam costs				Delt1_l	59.1341		Delt1_h	5.46	
12		LP heater steam cost	5.687E-07	$/kJ		Delt2_l	73.86		Delt2_h	75.73413	
13		HP heater steam cost	5.725E-07	$/kJ		LMTD_l	66.2244		LMTD_h	26.72243	
14						A_l	16.4477	m2	A_h	194.519	
15		Heater surface costs				Ci_l	357.573	$/yr	Ci_h	4271.637	$/yr
16		LP heater initial cost	108.7	$/m2		Subtotal LPH	13020	$/yr	Subtotal HPH	65102.33	$/yr
17		HP heater initial cost	109.8	$/m2	124.6						
18									Steam cost	73493.09	$/yr
19		Overall heat transfer coefficient	10220.67	kJ/hr-m2-oC					Initial cost	4629.21	$/yr
20		Annual fixed charge rate	20	%					Total cost	78122.3	$/yr
21		Operation hours	2000	hr/yr							
22											

Figure 3.27. MIDACO's solution for minimising the total cost of the system

Figure 3.28 shows MIDACO's set-up for the dual-objective optimisation analysis that simultaneously minimised C_{steam} and $C_{initial}$. Figure 3.29 shows the Pareto front and Figure 3.30 shows the selected solution for this optimisation analysis according to which the intermediate temperature is 117.6°C and the total relative cost is 78,422 $/y. Although the difference in the values obtained by the two solutions for the total relative costs is a

meagre 0.384%, the difference between their T_x values is significant. To confirm that this difference is due to the optimisation approach and not the solver's algorithm, a third solution was obtained by using the GRG Nonlinear method of Solver. Table 3.4 compares the various costs associated with the three optimised solutions.

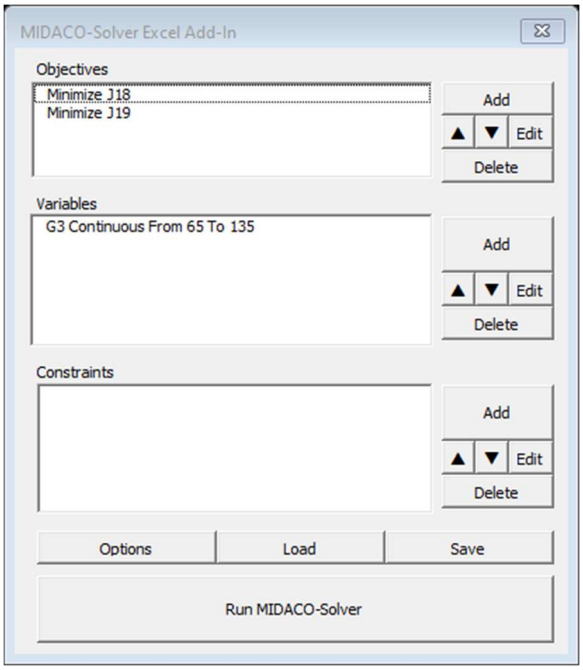

Figure 3.28. MIDACO's set-up for the dual-objective optimisation

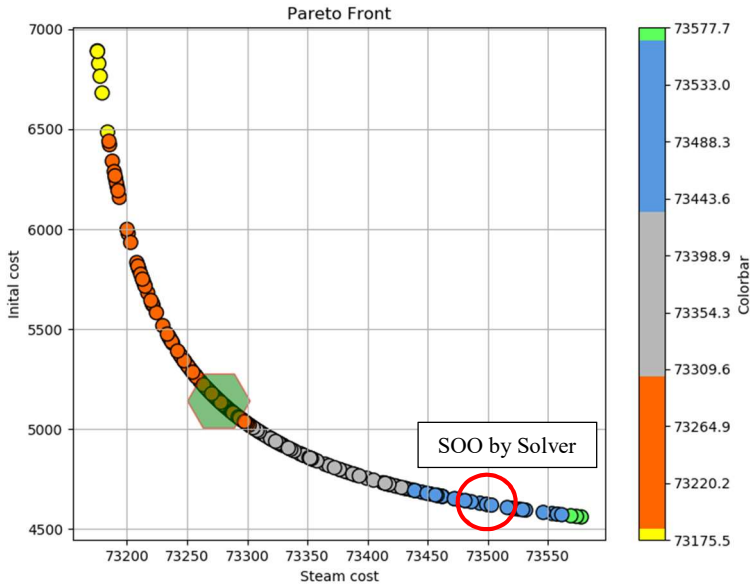

Figure 3.29. Pareto front for MIDACO's dual-objective solution

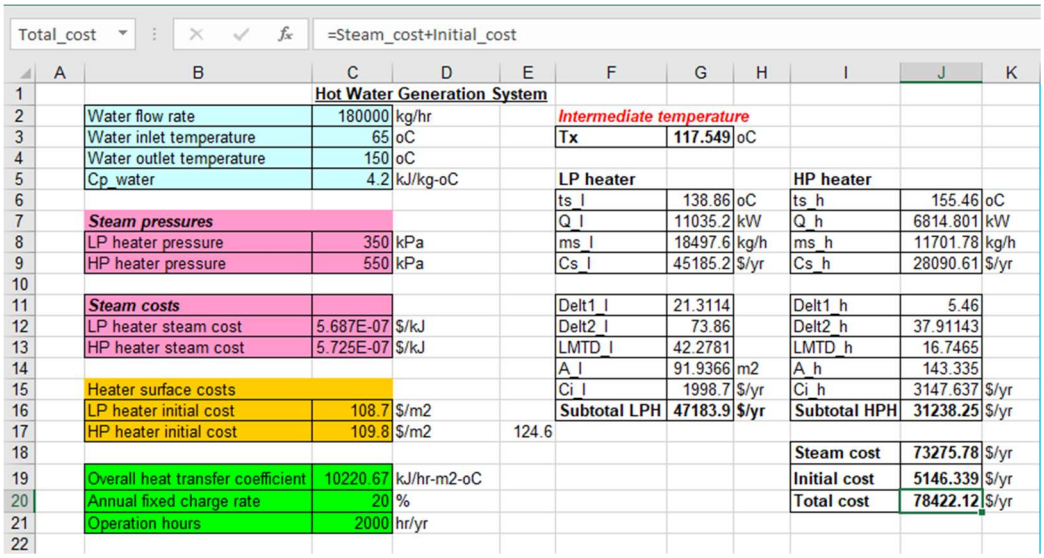

Total_cost =Steam_cost+Initial_cost

	A	B	C	D	E	F	G	H	I	J	K
1			Hot Water Generation System								
2		Water flow rate	180000	kg/hr		Intermediate temperature					
3		Water inlet temperature	65	oC		Tx	117.549	oC			
4		Water outlet temperature	150	oC							
5		Cp_water	4.2	kJ/kg-oC		LP heater			HP heater		
6						ts_l	138.86	oC	ts_h	155.46	oC
7		Steam pressures				Q_l	11035.2	kW	Q_h	6814.801	kW
8		LP heater pressure	350	kPa		ms_l	18497.6	kg/h	ms_h	11701.78	kg/h
9		HP heater pressure	550	kPa		Cs_l	45185.2	$/yr	Cs_h	28090.61	$/yr
10											
11		Steam costs				Delt1_l	21.3114		Delt1_h	5.46	
12		LP heater steam cost	5.687E-07	$/kJ		Delt2_l	73.86		Delt2_h	37.91143	
13		HP heater steam cost	5.725E-07	$/kJ		LMTD_l	42.2781		LMTD_h	16.7465	
14						A_l	91.9366	m2	A_h	143.335	
15		Heater surface costs				Ci_l	1998.7	$/yr	Ci_h	3147.637	$/yr
16		LP heater initial cost	108.7	$/m2		Subtotal LPH	47183.9	$/yr	Subtotal HPH	31238.25	$/yr
17		HP heater initial cost	109.8	$/m2	124.6						
18									Steam cost	73275.78	$/yr
19		Overall heat transfer coefficient	10220.67	kJ/hr-m2-oC					Initial cost	5146.339	$/yr
20		Annual fixed charge rate	20	%					Total cost	78422.12	$/yr
21		Operation hours	2000	hr/yr							
22											

Figure 3.30. MIDACO's solution for the dual-objective optimisation

Table 3.4. The system costs as determined by the two single-objective analyses and the dual-objective optimisation analysis

Cost	SOO Solver	SOO MIDACO	Dual-objective	Deviation %
Steam cost for the LP heater [$/y]	12,662.4	12,662.4	45,185.2	256.8
Steam cost for the HP heater	60,830.69	60,830.69	28,090.61	-53.82
Initial cost for the LP heater	357.573	357.573	1,998.7	459.0
Initial cost for the HP heater	4,271.637	4,271.637	3,147.637	-26.31
The total of steam cost	73,493.09	73,493.09	73,275.78	-0.296
The total initial cost	4,629.21	4,629.21	5,146.339	11.17
The total relative cost	78,122.3	78,122.3	78,422.12	0.384

The figures of Table 3.4 show that the two SOO solutions gave identical results. The higher value of T_x obtained by the dual-objective optimised solution compared to the single-objective optimised solutions indicates that it increased the size of the LP heater at the expense of the HP heater. The table figures show that steam cost and initial cost of the LP heater were increased by 256.8% and 459.0%, respectively, while those of the HP heater were reduced by 53.82% and 26.31%, respectively. Since, the total relative cost of the system produced by single-objective and bi-objective solutions are very close, it can be concluded that the two solutions provide two options for the designer to select from based on other considerations.

3.6. Closure

This chapter discusses multi-objective optimisation and illustrates the application of the scalarisation and Pareto approaches by using the Excel-based modelling platform. The

chapter illustrates the two approaches by considering a simple mathematical problem that involves two objective functions $f_1(x,y)$ and $f_2(x,y)$ and a more practical case of a hot-water generation system that incorporates two steam heaters with different pressure levels and, therefore, different initial and steam costs. Since the two objectives involved in the HWG system are of the same kind, viz. costs, it was possible to cast the optimisation problem as a single-objective optimisation problems and solve it by using Excel's solver. However, the solution of the bi-objective problem by using the Pareto approach required a MOO solver which was achieved by using the free version of MIDACO solver.

In general, MOO analyses do not require their objectives to be of the same kind like the two examples considered here. In fact, MOO methods are more useful when considering objectives of different kinds and different scales such as thermodynamic, economic, and environmental-impact factors. In this case, the use of MOO algorithms that adopt the Pareto approach and apply evolutionary methods becomes necessary. Although the free version of MIDACO allows only four changing variables to be used, it is still adequate for dealing with practical optimisation analyses of various types of energy-conversion systems as shown in the following chapters of the book. Chapter 9 presents a technique that allows MOO analyses with any practical number of design variables to be conducted with Excel's Solver by utilising the TOPSIS decision-making method [14].

References

[1] K. Deb, Multi-Objective Optimization using Evolutionary Algorithms, JOHN WILEY & SONS, LTD, 2001

[2] J. Renuka Kumari, Optimization Techniques – A Review, Int. Journal of Engineering Research and Application, Vol. 6, Issue 11, (Part -4) November 2016, pp.01-05,

[3] MIDACO-Solver, http://www.midaco-solver.com/

[4] Wiki, https://en.wikipedia.org/wiki/Multi-objective_optimization

[5] A. Salian. A Gentle Introduction to Multi-Objective Optimisation https://codemonk.io/blog/a-gentle-introduction-to-multi-objective-optimization/

[6] Lecture 9: Multi-Objective Optimization, https://engineering.purdue.edu/~sudhoff/ee630/Lecture09.pdf

[7] https://www.slideshare.net/slideshow/multi-objective-optimization-and-pareto-multi-objective-optimization-with-case-study/139174517

[8] D. Savic, Single-objective vs. Multiobjective Optimisation for Integrated Decision Support, (2002). International Congress on Environmental Modelling and Software. 119. https://scholarsarchive.byu.edu/iemssconference/2002/all/119

[9] M. Mahrach, G. Miranda, C. León and E. Segredo, Comparison between Single and Multi-Objective Evolutionary Algorithms to Solve the Knapsack Problem and the Travelling Salesman Problem, Mathematics 2020, 8, 2018; doi:10.3390/math8112018

[10] Á. Benet, A. Villalba-Herreros, Ó. Santiago and T.J. Leo Application of genetic algorithms to the design and dimensioning of maritime hybridpower plants fueled

by alternative fuels, Proceedings of ECOS 2023 - the 36th International Conference on Efficiency, Cost, Optimization, Simulation and Environmental Impact of Energy Systems 25-30 June, 2023, Las Palmas de Gran Canaria, Spain

[11] A. Ganjehkaviri, M.N. Mohd Jaafar, P. Ahmadi, H. Barzegaravval, Modelling and optimization of combined cycle power plant based on exergoeconomic and environmental analyses, Applied Thermal Engineering 67 (2014) 566e578

[12] M.M. Keshtkar, P. Talebizadeh, Multi-objective optimization of a R744/R134a cascade refrigeration system: exergetic, economic, environmental, and sensitive analysis (3ES), Journal of Thermal Engineering, Vol. 5, No. 4, pp. 237-250, July, 2019, Yildiz Technical University Press, Istanbul, Turkey M.

[13] I. Dincer, Renewable energy and sustainable development: a crucialreview, Renewable and Sustainable Energy Reviews, Volume 4, Issue 2, June 2000, Pages 157-175

[14] S. Diyaley, P. Shilal, I. Shivakoti, R.K. Ghadai and K. Kalita, (2017) PSI and TOPSIS Based Selection of Process Parameters in WEDM, Periodica Polytechnica. Engineering. Mechanical Engineering, vol. 61, pp. 255

[15] T. Balabanov, Solving multi-objective problems by means of single objective solver, Problems of engineering cybernetics and robotics,Vol. 76, 2021, pp. 63-70 https://doi.org/10.7546/PECR.76.21.05

[16] M. Schlueter (2014). MIDACO software performance on interplanetary trajectory benchmarks. Advances in Space Research. 54 (4): 744–754

[17] M. Schlueter; S. Erb; M. Gerdts; S. Kemble; J.J. Rueckmann (2013). "MIDACO on MINLP Space Applications". Advances in Space Research. 51 (7): 1116–1131

[18] MIDACO plot tool: http://www.midaco-solver.com/index.php/more/multi-objective

[19] K.W. Li and A.P. Priddy, Power Plant System Design, John Wiley and Sons, 1985.

[20] Y.A. Cengel and A.J. Ghajar. *Heat and Mass Transfer: Fundamentals and Applications*. McGraw Hill, 2011